University of Colorado
Department of Aerospace Engineering

ASEN 5018/6028

CANVAS

Climatology of Anthropogenic & Natural VLF Wave Activity in Space

Fall 2021 Final Report

Jett Moore[1], Cooper Gould[2], Andy Starr[3], Marlin Jacobson[4], Andrew Sabovik[5], Paraksh Vankawala[6], Raphael Rodriguez[7], James Cannon[8], Sebastian Wankmueller[9], Aldo Aguilar-Nadalini[10], Jash Bhalavat[11], Nathan Sunnarborg[12,13], Adam Oswald[14], Brittany Nez[15], Zoe Witte[16]

[1]Project Manager, [2]Systems Engineer, [3]Structures Lead, [4]Thermal Lead, [5]Assembly Lead, [6]Instrumentation Lead, [7]COMMS Lead, [8]GSE Lead, [9]Electronics Lead, [10]EPS Lead, [11]Solar Panel Lead, [12]Testing Lead, [13] ADCS Lead, [14]FSW Engineer, [15]B-Field Engineer, [16]E-Field Engineer

Submitted: 12/13/2021

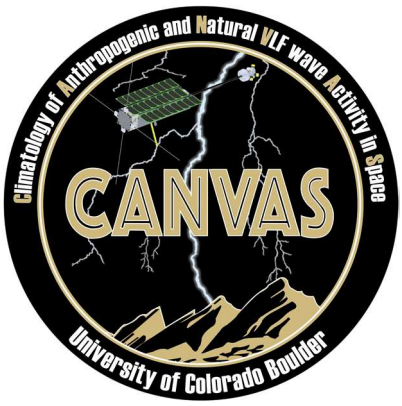

Advisor:
Dr. ROBERT MARSHALL

Table of Contents

1. Introduction

The Climatology of Anthropogenic and Natural VLF Wave Activity (CANVAS) CubeSat mission will make continuous observations of very low frequency (VLF) waves in low-Earth orbit originating from lightning and ground-based transmitters. CANVAS is a 4U CubeSat that was funded in February 2019 by the National Science Foundation. A team of graduate students at CU Boulder began working towards a PIR level design after a successful CDR in Summer of 2020 under the guidance of Principal Investigator Dr. Robert Marshall. The following report is an overview of the work completed during the Fall 2021 semester, with the details of each section placed into their respective documents.

2. Team Roles

CANVAS is led by Principal Investigator (PI) Dr. Robert Marshall of the Aerospace Engineering Department at CU Boulder. Jett Moore is the Project Manager (PM) and Cooper Gould is the Systems Engineer (SE). This fall, the team was broken up in 3 sections - Instrumentation, Avionics, and Mechanical. This decision was made because of the focus on flight development and system testing. For instrumentation there is Paraksh as the lead, Zoe Witte who works on E-field instrument, Sebastian Wankmueller who is working on the Analog and Digital boards, and Brittany Nez who is working on the B-field instrument. For avionics, Aldo Aguilar-Nadalini has been leading Electrical and Power System (EPS) and Jash Bhalavat has been working on the solar panels. CANVAS finally had the personnel to dedicate someone to COMMS and FSW, this fall it was Raphael Rodriguez and Adam Oswald respectively. Nathan Sunnarborg oversaw all testing and documentation as Testing Lead, while also putting in time to necessary ADCS updates with help from Andrew Sabovik. Andy Starr was tasked with CAD and manufacturing as the Structures Lead while Marlin Jacobson took on the thermal model and Andrew Sabovik pushed forward on assembly and integration. Figure TR-1 details the team organization for the semester.

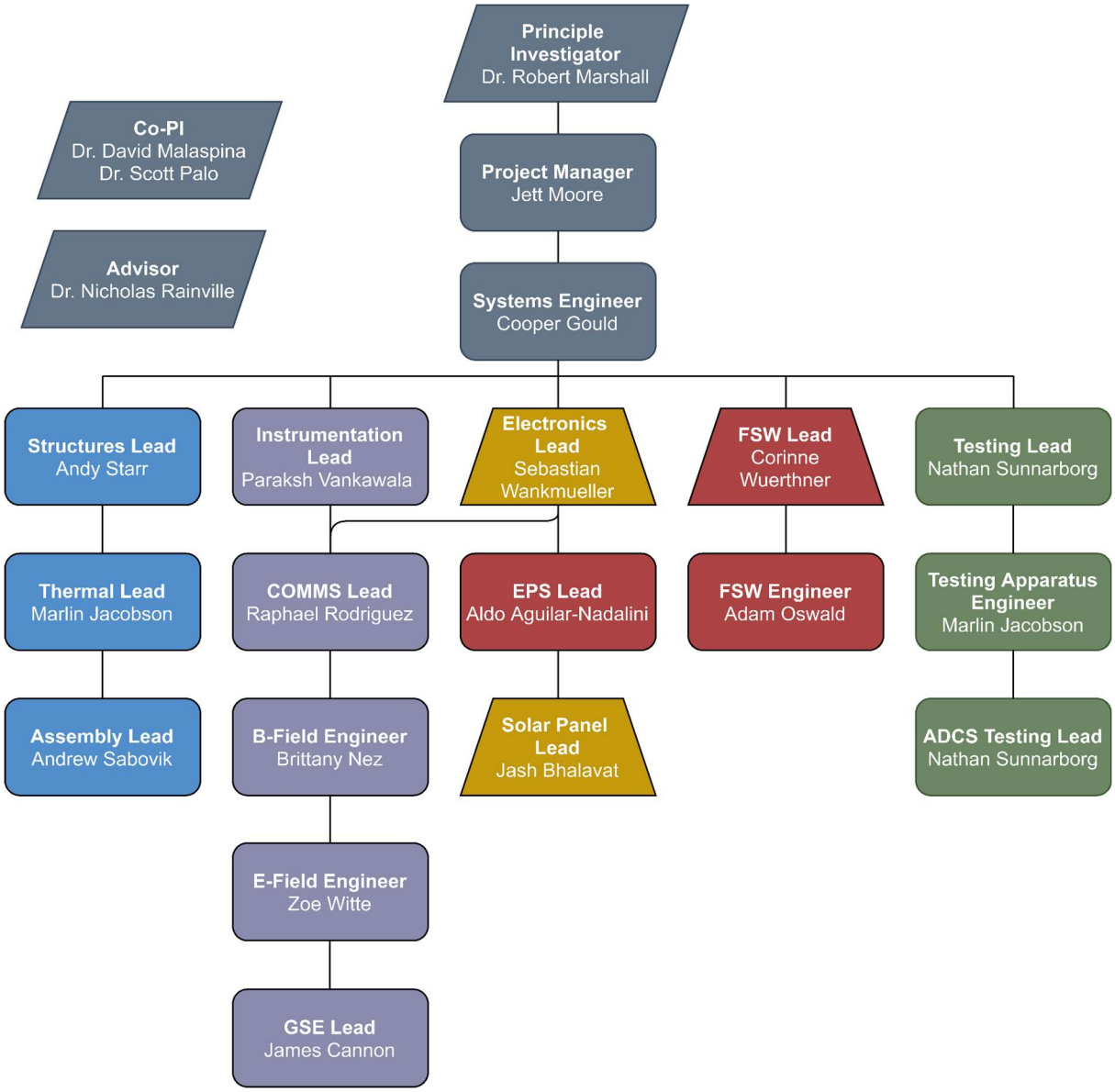

Figure TR-1. CANVAS Fall 2021 Team Organization

3. Science Background

VLF waves play an important role in controlling the evolution of energetic electron distributions in near-Earth space. Whistler-mode waves propagating in the magnetospheric plasma can induce pitch-angle scattering and precipitation of trapped energetic particles, and research has shown that VLF waves radiated from both lightning and ground-based VLF transmitters play a significant role in radiation belt dynamics [1]. An accurate quantification of the amount of VLF energy which penetrates from the ground, through the ionosphere, and into the magnetosphere is critical to the understanding of the effects of ground-based electromagnetic sources in the space environment [2].

CANVAS will make continuous observations of VLF waves in low-Earth orbit originating from lightning and ground-based transmitters with CANVAS instrumentation. The CANVAS instruments will observe VLF waves in the 0.3-40 kHz frequency range using a

three-axis magnetic search coil, deployed on the end of a 1-meter carbon fiber boom, and two electric field dipole antennas. Together, these five wave components will be used to calculate the spectral matrix components at 1 second time resolution using real-time FFTs and spectral matrices calculated in an on-board FPGA. Spectral matrix components will be sent to the ground to determine the full set of wave parameters, including polarization, planarity, and k-vector direction[3]. Using these wave observations, CANVAS will provide trans-ionospheric attenuation profiles as a function of frequency through the observation of broadband VLF waves from lightning, using sferics observed by ground-based VLF receivers as the source function. Figure SB-2[4]shows an average energy density of VLF waves, a function of latitude and longitude for both day and night, a potential data product that CANVAS will be able to provide.

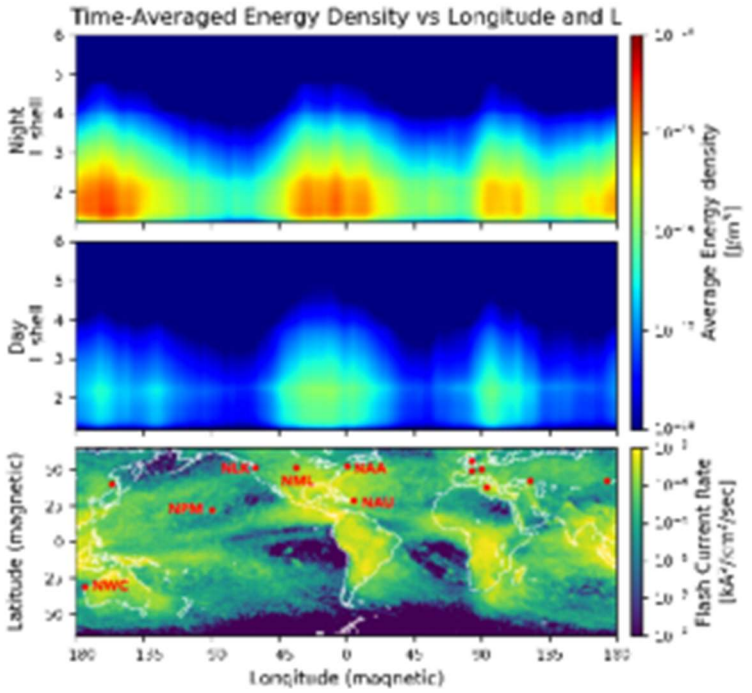

Figure SB-2. Energy Density vs. Longitude and Latitude [4]

Transionospheric attenuation will be estimated as a function of latitude, longitude, time of day, and season. In addition, wave parameters measured above the ionosphere will be used to forward-propagate these waves throughout the magnetosphere, in order to provide a data-driven estimate of the VLF energy distribution in the inner magnetosphere. These measurements are critical for an understanding of the effects of VLF wave energy in the magnetosphere, including its effects on radiation belt electron populations.

3.1. Key Science Requirements

The objective of measuring VLF energy in near-Earth space drives the requirements for the payload, and therefore the rest of the spacecraft, which is supporting the payload. Here, Table SB-1 shows the Science Traceability Matrix and details requirements for the payload to meet science questions as discussed in the previous section.

The desired frequency range is derived from previous missions to observe whistler

spectra; the science satellite DEMETER observed VLF energy up to 20 kHz, but studies have shown that whistler waves can propagate at frequencies as high as 40 kHz, and therefore CANVAS will improve on existing data sets by doubling the range to up to 40 kHz [5]. Sensitivity and spurious-free dynamic range requirements for the instruments are also derived from observed whistler wave amplitudes observed by DEMETER. Finally, the 1 second time resolution is set so only one whistler is contained by each FFT.

Science Goals	Science Objectives	Science Requirements		Instrument Performance				Data Products	Mission Functional Requirements
		Physical Parameters	Observables	Parameter		Requirement	Projected		
Determine the dynamics and coupling of Earth's magnetosphere, ionosphere, and atmosphere and their response to solar and **terrestrial inputs** *NASA 2013 Solar and Space Physics Decadal Survey, Priority #2*	What is the electromagnetic energy input into the space environment by **lightning and ground-based VLF transmitters?**	VLF wave power and k-vectors	VLF wave amplitude in E and B components	E-field	Min. sensitivity	$1\frac{\mu V}{m\sqrt{Hz}}$	$\leq 0.2\frac{\mu V}{m\sqrt{Hz}}$	5-channel spectra and cross-spectra	1 year mission
					SFDR	50 dB	50 dB		Low Earth Orbit
					Freq. range	0.3-40 kHz	0.3-40 kHz		$> 50°$ inclination
					Freq. resolution	10%	$\leq 9\%$		Wave components directions known within 1°
	What is the frequency spectrum of VLF wave energy above the ionosphere in the **0.3–40 kHz range?**	VLF spectral energy density	VLF wave spectra in E and B components		Time resolution	1 sec	1 sec	256 1024-pt FFTs averaged every second	
Explore the physics processes in **the space environment** from the Sun to the **Earth** and throughout the solar system *NASA 2014 Science Plan, Heliophysics Science Goal*				B-field	Min. sensitivity	$10^{-4}\frac{nT}{\sqrt{Hz}}$	$\leq 7 * 10^{-5}\frac{nT}{\sqrt{Hz}}$		Position knowledge better than 10km
					SFDR	50 dB	50 dB		
	What is the **transmission transfer function** of the ionosphere for VLF energy, and how does it vary in space and time?	VLF wave power and spectrum	VLF wave amplitude and spectra		Freq. range	0.3-40 kHz	0.3-40 kHz	57 log spaced freq. bins & 10 high resolution TX bins	
					Freq. resolution	10%	$\leq 9\%$		On-board FFT engine
					Time resolution	1 sec	1 sec		

Table SB-1: Revised Science Traceability matrix

4. Spacecraft Overview

The CANVAS mission will be carried out by a 4x1U CubeSat equipped with two electric dipole field measurements consisting of four 400mm-long antennas to measure the E-field and three orthonormal magnetic search coils to measure the B-Field. The search coils are placed at the distal end of a 1-meter boom to isolate the inputs from any noise given off by the spacecraft main bus. Specific information regarding the payload and instrumentation can be found in the CANVAS Instrumentation Interface Control Document. The CANVAS spacecraft can be seen in Figure SO-1.

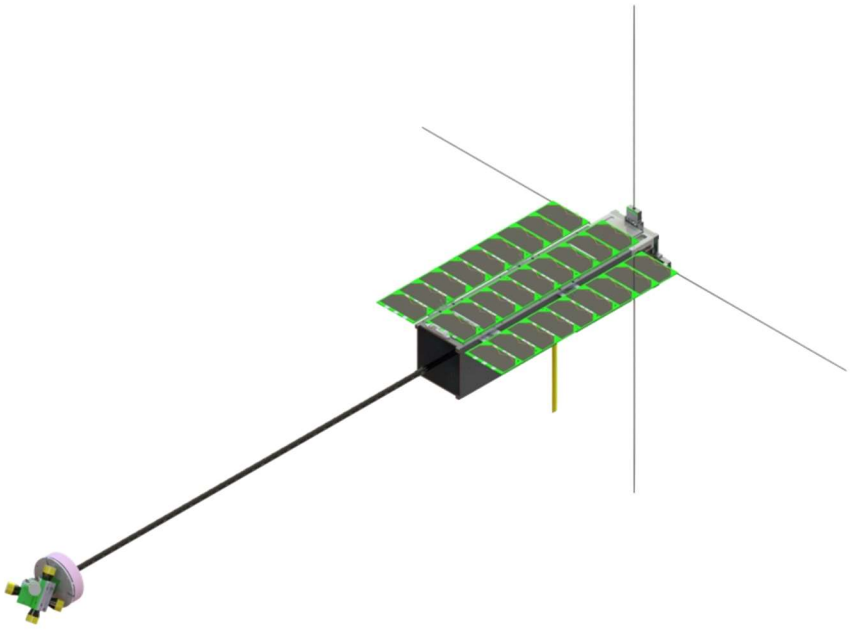

Figure SO-1. CANVAS Spacecraft Overview

The spacecraft's coordinate frames can be seen in Figure SO-2, where the spacecraft frame is aligned with the ADCS solution's XACT-15's coordinate frame. The Coarse Sun Sensor's (CSS) frame, used to determine the sun's direction, can also be seen in this figure. The coordinate frame used by the Search Coil Magnetometer is also shown.

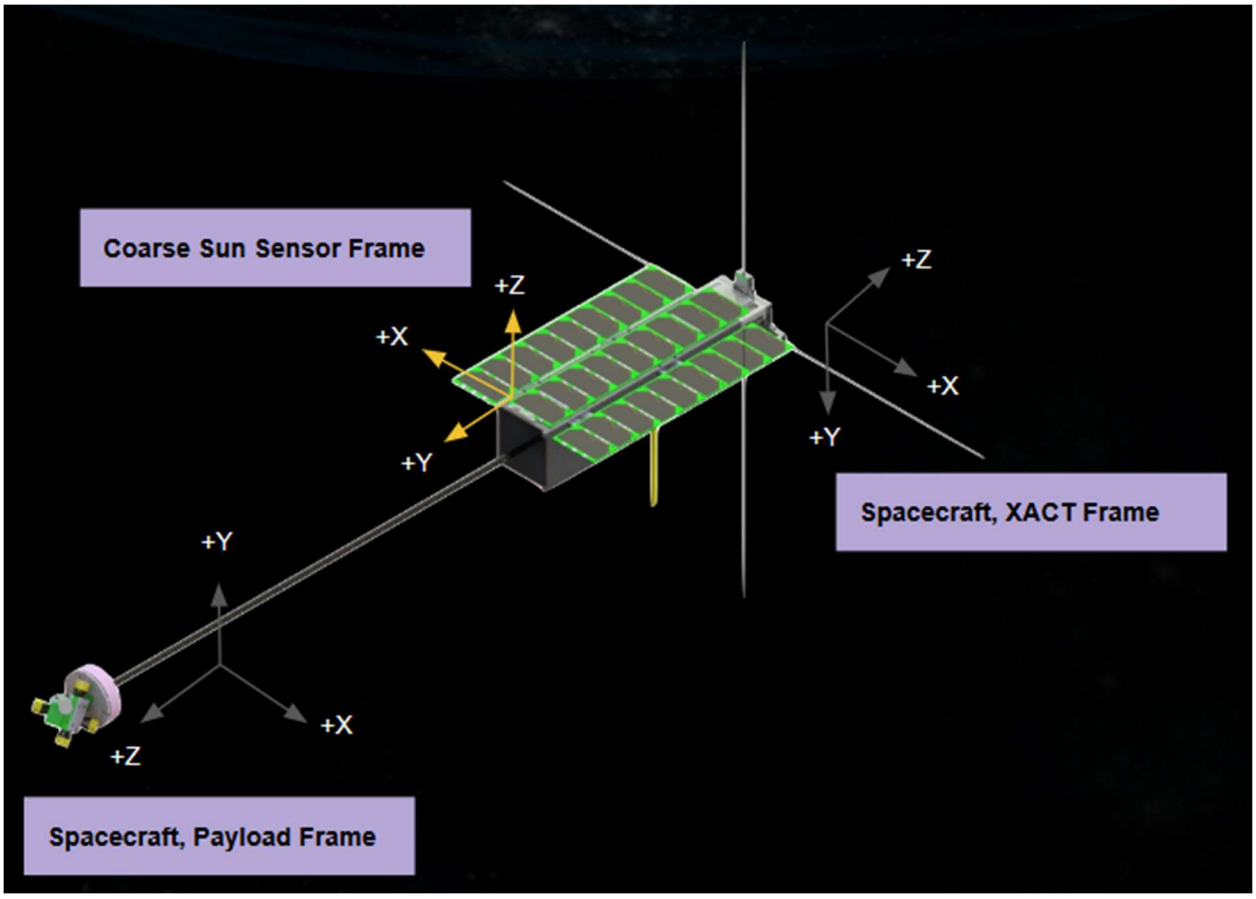

Figure SO-2. CANVAS Coordinate Frames

The figure below provides a functional block diagram of the spacecraft. This captures how different parts of the satellite communicate with each other. An in depth discussion can be found in the CDH section.

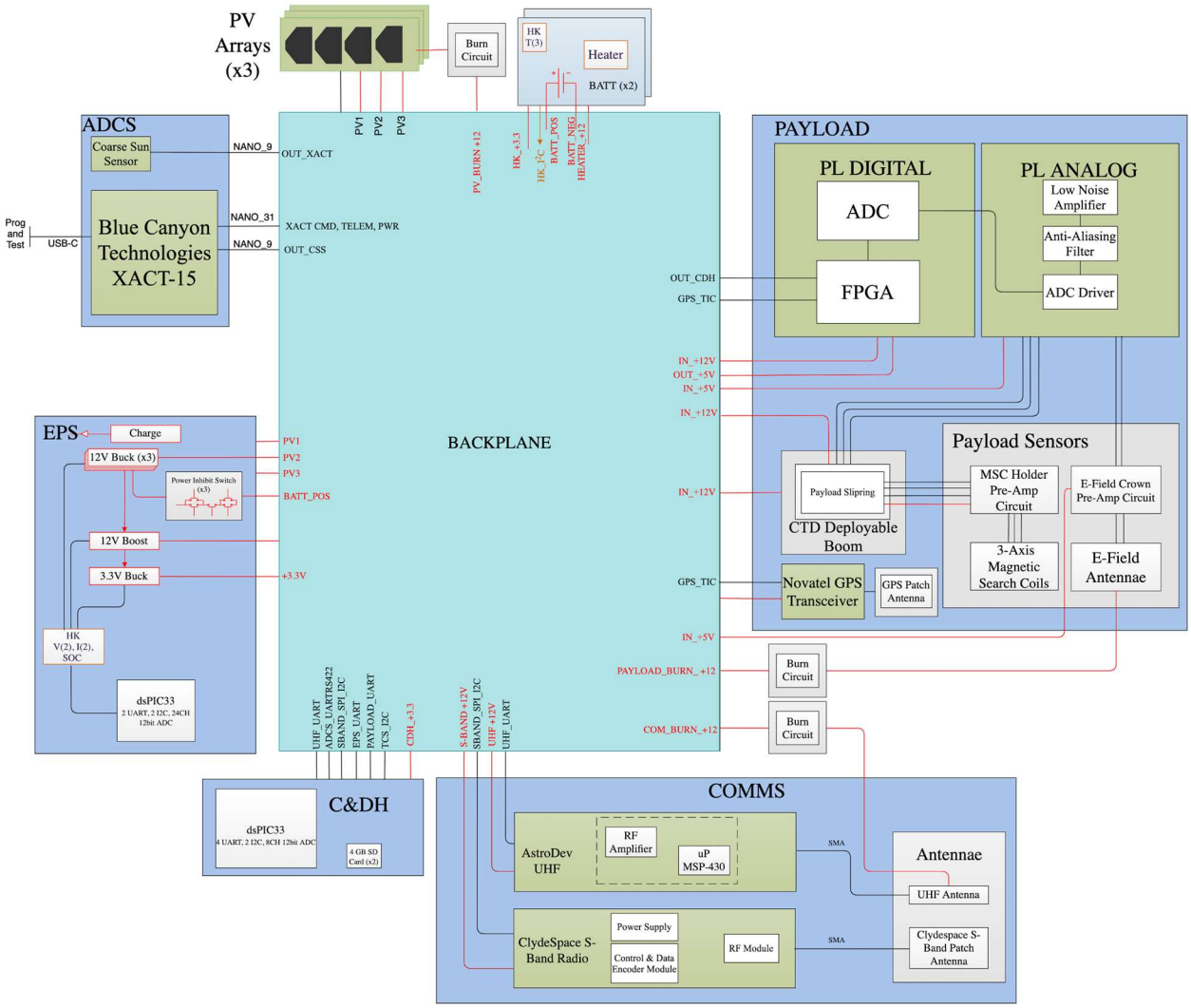

Figure SO-3. Functional system block diagram

5. Concept of Operations and Mission Design

The Systems Engineering documentation can be seen in detail with the CANVAS Concept of Operations (CONOPs) and the CANVAS Test Plan. Instrumentation and SE have contributed jointly to the CANVAS Payload ICD. An overview of the aforementioned documentation is available below. Included in the documents listed are requirements to bring them forward to PIR. The CONOPs and Test Plan will likely require minor updates and alterations. The ICD will continue to grow as fidelity in the instrumentation and structural designs increase.

5.1. Concept of Operations

Below is a diagram of the Concept of Operations from deployment, science, communication and end of mission operations.

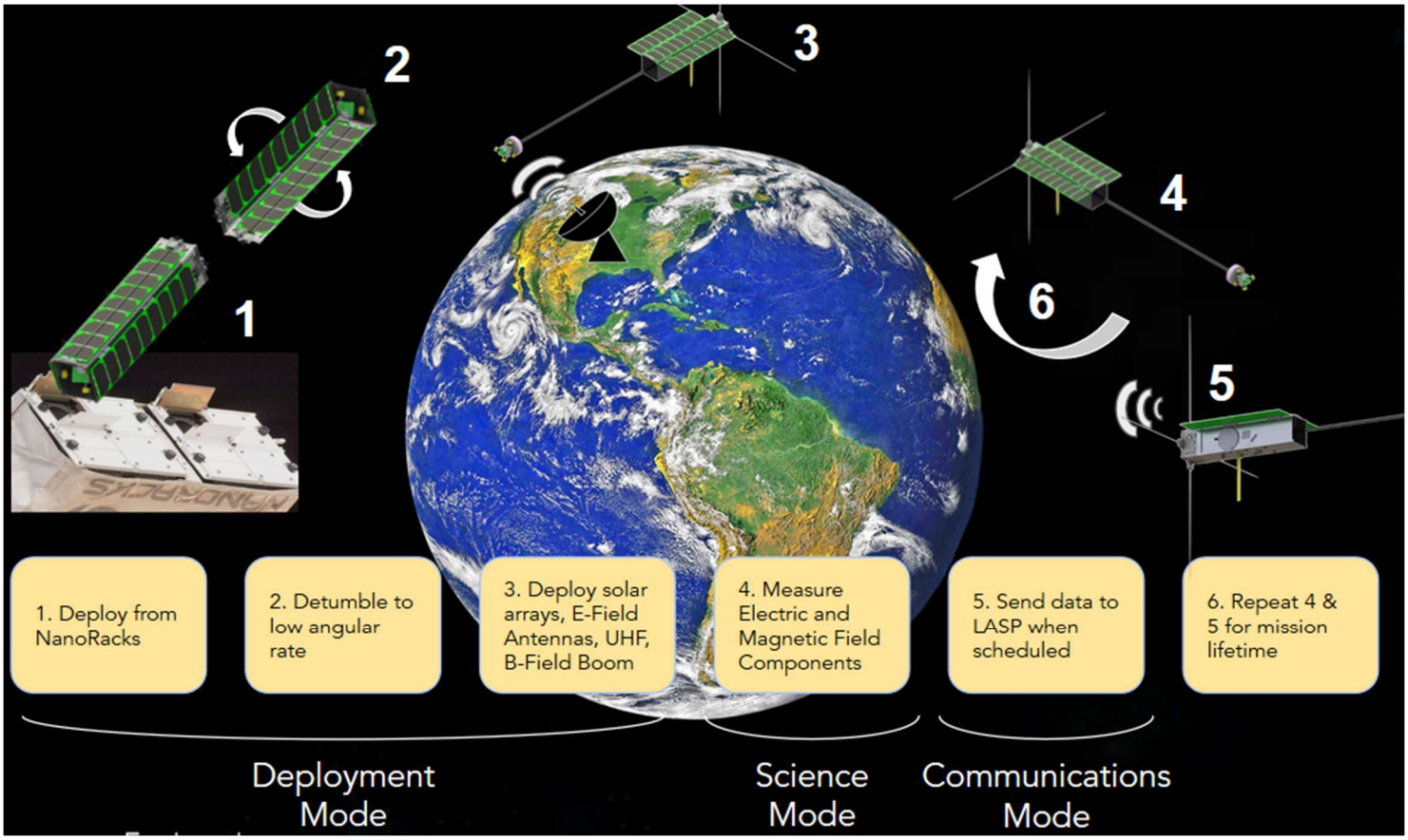

Figure MD-1. Concept of Operations for CANVAS

5.1.1 Deployment

Below is a table describing the current CANVAS deployment sequence. More detail can be found in the CANVAS Deployment Sequence document in the CONOPS folder. The estimated times are subject to change and should be developed with the ADCS team. This table does not include power requirements for using the science instruments to confirm proper deployment. These should be added.

Table MD-1. Sequence, Deployable part, power, time of deployment.

Event	Power Required (W)	Estimated Time (s)	Energy (Wh)
NanoRack Ejection	0	60	Negligible
Release hardware inhibit switch	0	Negligible	Negligible
CDH/EPS Enable	Negligible	Negligible	Negligible
ADCS Enable	Negligible	Negligible	Negligible

Spacecraft Detumble	2.96	300 - 2700	~ 0.25 - 2.22
Sun-pointing maneuver (-y align)	2.96	~ 210	~ 0.17
Solar array burn wire	2.5	30	0.02
E-Field antennas burn wire	2.5	30	0.02
UHF burn wire	1.25	30	0.01
UHF Radio Beacon	3.15	60	0.05
CTD Boom Deploy	2.1	360	0.21
Health and Status check	3.15	120	0.11

5.2. Mission Design

Since CANVAS would like to study the seasonality effects of how VLF energy transmits through the ionosphere, the mission has been designed for a one year on orbit time. The spacecraft design, power budget, link budget, and data budget were all completed assuming a 500 [km] altitude. In order to sample the majority of ground-based VLF sources, including lightning and VLF transmitters, the inclination of the orbit is required to be above 50 degrees. The design point chosen was the 51.6 degree inclination of the International Space Station, as a supply vehicle would dock with the ISS and then boost the cubesat to a higher altitude. Command uplinking and data downlinking will be handled through the LASP ground station. Details and design explanations for the mission design are in the CANVAS CONOPs document. The acceptable ranges and chosen design points are listed in Table MD-2.

Table MD-2. Mission Design Elements

Mission Element		
	Acceptable	Design Point
Altitude	450-550 km	500 km
Inclination	50-70°	51.6°
Duration	≥ 6 months	1 year
COMM	UHF and S-Band	
Ground Station	LASP	

6. Instrumentation

6.1. Overview

The CANVAS spacecraft will carry two on-board scientific instruments for data collection. A set of three orthogonal magnetic search coils (MSC) will be used to detect the magnitude and direction of lightning-generated whistlers and VLF transmissions above the ionosphere. A set of electric-field (E-field) antennas mounted to the main bus will detect electric-field signals from lightning-generated whistlers and anthropogenic sources on Earth's surface.

For detailed descriptions and rationale for all design decisions regarding the CANVAS payload, please refer to the CANVAS Payload Design Document.

6.2. Key Driving Requirements

Instrument requirements are derived from science observables as shown in SB-1 and shown condensed in Table INST-1. Frequency range and uniform gain requirements are derived from the desire to measure VLF waves from whistlers and transmitters. Sensitivity and SFDR requirements are derived from amplitudes of whistler observations made by DEMETER. Direction accuracy and position knowledge requirements derive from the desire to measure the spatial dependence of VLF spectra.

Table INST-1. Instrumentation Key Driving Requirements

Req.	Description
SCI-1, SCI-2	CANVAS shall measure electric and magnetic fields between 0.3 and 40 kHz
SCI-1.1	CANVAS E-field antennas will be designed to have low capacitance (<35pF)
SCI-1.2	CANVAS shall measure electric fields with sensitivity less than 10^{-6} $V/m/Hz^{1/2}$in the band of interest
SCI-2.2	CANVAS shall measure magnetic fields with sensitivity less than 10^{-4} $nT/Hz^{1/2}$in the band of interest
SCI-1.3, SCI-2.3	CANVAS shall measure electric fields and magnetic fields with a minimum SFDR of 50 dB above the sensitivity requirement
SCI-1.4, SCI-2.4	CANVAS shall have a uniform gain within 3 dB across the frequency band of interest
SCI-1.5, SCI-2.5	CANVAS shall measure electric and magnetic field components orthogonal to within 5 degrees E-field sensitivity

6.3 E-field instrument

The E-field instrument is composed of the E-field antennas assembly and the E-field preamplifier. The E-field antennas are a set of four antennas deployed on one end of the spacecraft (opposite the B-field instrument). The antennas are oriented with two antennas per axis, forming a two-axis dipole antenna.

Status

As of 5/6/21, the status of the individual components are as follows

- E-field antenna assembly Revision 2 has been manufactured and assembled in AERO machine shop
- E-field crown Revision 1 has been 3D printed and fit check with the manufactured Revision 2 antenna assembly and flight version XACT
- E-field crown Revision 2 has been updated with the appropriate changes and is ready for manufacturing
- E-field preamplifier Version 2 has been ordered, populated, and tested

Revision 2 of the E-field antennas were designed to be easier to manufacture. The changes included having threaded antenna rods that connect to the brass piece. The brass piece diameter was also made smaller in order to lower the capacitance of the E-field assembly (SCI-1.1). Version 2 of the E-field preamplifier was redesigned with an improved layout and routing to reduce the chances of crosstalk between signals. The preamplifier design was also changed to mechanically interface with the E-field crown.

This Spring 2021 semester, there was a primary focus on the testing of the instrument. A storage test, capacitance test, fit check test, and signal test (this time including the analog board unlike the prior semester) were performed. The storage test consisted of a wooden stand to hold the Revision 2 antenna assembly in the stowed position. The entire set up was left untouched for a one month period to simulate the shipping and pre launch period the satellite will endure. After one month, the antenna was released to check its deployment remained as designed (fully extended and a full 90 degrees from the stowed position). The test was successful and satisfied SCI-1.5.

The capacitance test included a research component in order to solve for an acceptable maximum capacitance value for the assembly (35 pF). This estimation was performed based on the LEO plasma environment parameters and RAPS plasma sheath resistance analysis. Our tests indicated the assembly remained near 30 pF and satisfied the requirement SCI-1.1 for the E-field instrument.

The fit check test was performed with the manufactured Revision 2 antenna assembly and preamplifier along with a 3D printed E-field crown Revision 1 and flight version XACT. This test indicated the dimensions of the components are correct. However, the crown would need to be modified in order to accommodate the screws that would attach it to the XACT. These changes have been made already to the crown design.

The signal test this semester had two significant changes to the setup compared to Fall 2020. The first being that the analog board was included in the test. We input a gain of 50dB on the analog board and confirmed the gain on the data output. Secondly, we utilized one Revision 2

antenna and one Revision 1 antenna to create a dipole, improving upon using just the single antenna in previous tests. The dipole configuration resulted in a ~10dB drop in the noise floor. Moving forward, an outdoor signal test will be performed in an attempt to detect US Navy VLF transmitter signals. Refer to the CANVAS Payload Design Document for more detail about the E-field instrumentation and testing.

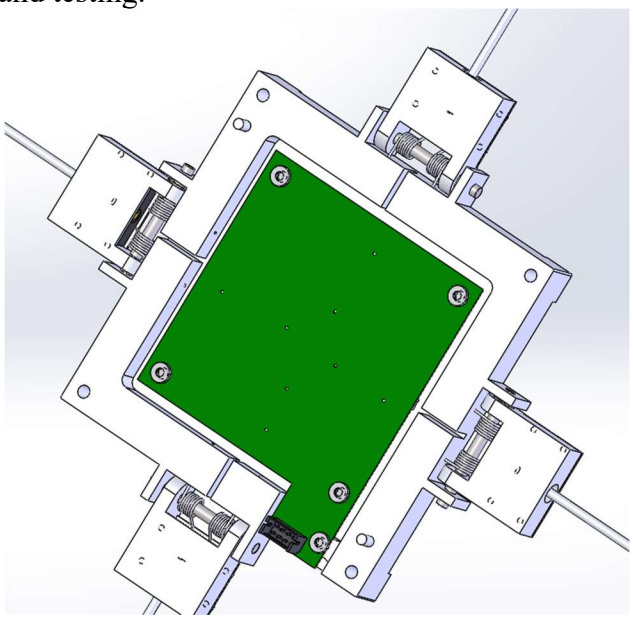

Figure INST-1: Updated E-field Crown with preamplifier board and antennas

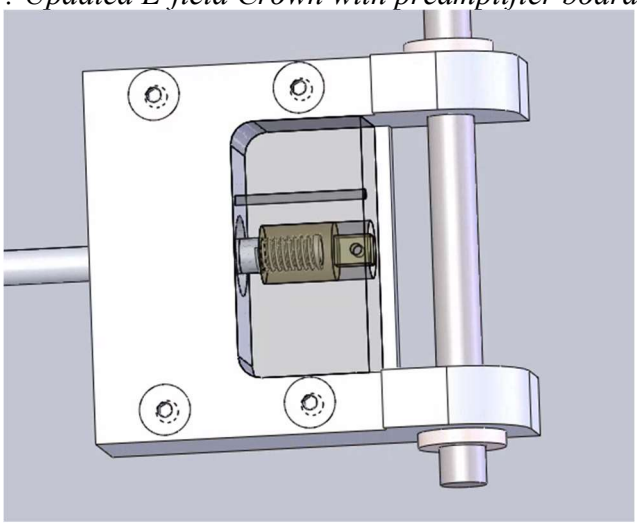

Figure INST-2:E-Field Antenna assembly

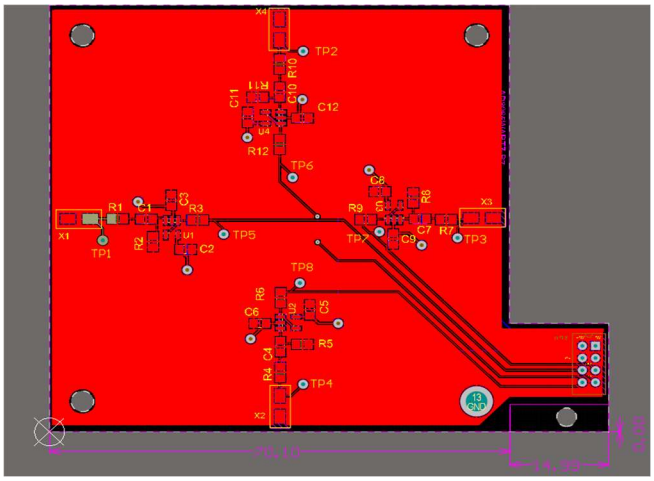

Figure INST-3: Figure for E-field instrument (CAD and schematic)

Fall 2021:

The statuses of each of the components are as follows.

- The E-Field Preamp has its flight design completed and the next step is to order the flight board.
- An aluminum model of the E-Field Crown has been manufactured. Fit checks need to be performed in order to know if this will be the flight version.
- The E-Field Antenna Assemblies third revision have been manufactured/assembled and the flight version is currently being machined and will be assembled Spring 2022.

The current E-Field Preamp (Revision 3) underwent bring up testing as well as frequency response testing and passed both successfully. The flight version of the board will be manufactured and populated coming Spring 2022.

The E-Field crown's current version has been machined from Aluminum 6061. Fit checks will be performed by Spring 2022 to determine whether or not a new flight version needs to be machined. The fit check includes (1) ensuring all 4 of the "feet" are coplanar within 0.1mm and (2) ensuring that once the whole spacecraft is assembled, the faces between each foot on the crown and the corresponding foot on the bus panels on the other side are separated by 454+/-0.1mm.

The E-Field Antenna Assemblies flight versions are currently being machined and will be ready for assembly in January 2022. The Brass Connector has been redesigned to protrude from the Delrin Sleeve in order to avoid breaking the wire connecting the assemblies to the preamp board. In Fall 2021, the engineering models have successfully undergone Signal Testing and Noise Floor Testing, and SFDR Testing is in progress. All of these tests were performed in a Faraday Cage, which was built up in the Fall 2021 semester as well.

Future Steps

Revision 3 of the E-field crown has been updated to correct for proper integration with the XACT as well as to mitigate plasma exposure to the preamplifier board resting within the crown. The new design will be submitted to the AERO machine shop and manufactured. As previously mentioned, the signal testing will continue with an outdoor test in an attempt to detect VLF transmitters. Additionally, connectors have been ordered to provide a better test setup and eliminate wire connection interference. The antenna assembly was successful in its deployment

so four assemblies will also be manufactured in the AERO machine shop. A capacitance test will be repeated with the manufactured crown and antenna assembly to ensure the value remained below 35 pF per requirement SCI-1.1. Pending the successful results of the outdoor signal test, the flight version preamplifier can be manufactured and populated this summer with no further changes. With all the components manufactured, the instrument will be fully assembled to check for appropriate integration.

Fall 2021:

Next semester the focus will be on flight assemblies and integration. Each component of the Antenna Assemblies will be machined for flight and fully assembled. SFDR testing will finish up on the engineering models Antenna Assemblies. The crown will undergo fitchecks with the potential of being remachined. The preamp board's flight version will be manufactured and populated. The entire instrument subassembly components will be integrated with each other and testing will be performed on the flight version's capacitance and signal detection. Fit checks will be performed with the E-Field instrument and the XACT ADCS component before full integration with the CANVAS cubesat. Once the instrument is integrated, capacitance will be measured again and a deployment test will be conducted to verify the burn wires and spring mechanism can deploy the antennas to the correct dipole position.

6.4 B-field instrument

The B-field instrument consists of 3 mutually-orthogonal magnetic search coils and a preamplifier board, as well as their associated holder structures. The instrument is located at the end of a 1 meter boom for magnetic cleanliness and noise reduction purposes.

Status

As of 05/06/21, the status of the individual components are as follows:

- Search Coils (x3) - Received engineering models, expecting flight models September 2021
- Preamp Board - Circuit Rev3 complete, currently populating PCB layout
- B-field holders - Rev2 complete and Prototype 2 being manufactured

This semester the updates to the mechanical design of the B-field instrument include updating the design for Revision 2 and ordering Revision 2 to be manufactured. If additional updates are not required, Rev2 of the holder will be the flight version. The design has been updated to only allow for a single assembly configuration, as well as easier assembly. For updated assembly details, please refer to the B-Field Assembly Document.

Figure INST-4. B-field Holder Prototype Rev1

The preamplifier board underwent a revision at the beginning of the semester adjusting the voltage filter to better apply a uniform gain over the frequencies of interest. Since then, several tests have been performed to verify the success of this change as well as to verify the breadboard preamplifier circuit design. The layout of the preamplifier board is being revised to reflect the new circuit design and Rev3 is expected to be complete and ready for manufacture in January 2021.

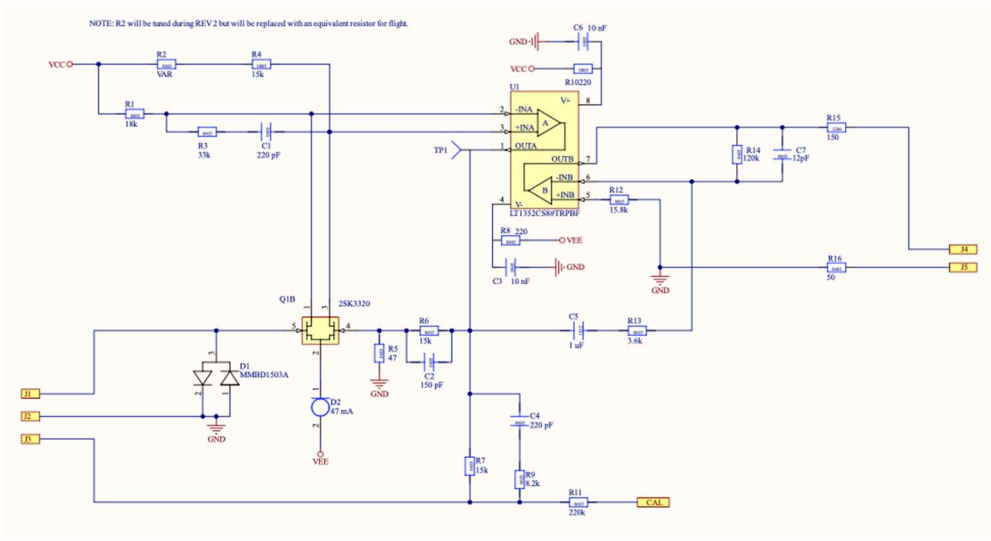

Figure INST-5. B-field Preamplifier Design Rev3

Table INST-2: B-field Bill of Materials

Name of Part	#	Description	Image
Search Coils	3	Cylindrical/Barbell-shaped parts with a wire exiting one end	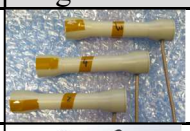
SC holder and preamp lid	1	Large block on a circular plate	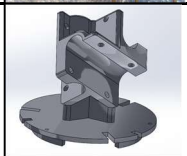
SC hold-down	3	Rectangular with cylindrical bore	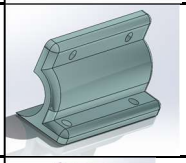
Preamp Can	1	Shaped like tuna can with extra edges	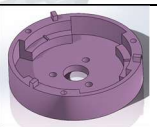
Preamplifier	1	Circular circuit board	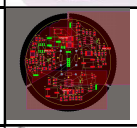
Screws - Long	14	High-Strength A286 Stainless Steel Socket Head Screw 4-40 Thread Size, 3/8" Long	
Helicoil Taps	14	Brass Tapping Inserts for Plastic 4-40 Thread Size, 0.172" Installed Length	
Screws - Short	3	High-Strength A286 Stainless Steel Socket Head Screw 10-32 Thread Size, 3/8" Long	

As of 12/13/2021, the status of the independent components are as follows:

- Search Coils (x3) - Tested the engineering models in a full signal chain test, received flight models in November 2021
- Preamp Board - Tested Rev. 3 engineering model B-Field preamp board in a full signal chain test and design of the flight model preamp board is complete and ready for PCB manufacture and population.
- B-Field Search Coil Holders - Flight model search coil holder being reprinted by Roboze to reduce warping of the lid.

This semester full chain signal testing was conducted using the payload test board, the analog board, the slip ring cable, the preamp board, and the three mutually orthogonal search coils. There were four tests conducted to verify the key driving requirements. These tests included frequency response testing, sensitivity testing, crosstalk testing, and SFDR testing. After conducting several iterations of this test, the instrumentation team was able to verify that the SCI-2.1 and SCI-2.4 were validated.

The search coil holder underwent a redesign to reduce warping in the lid. The material used for the print was changed from PEEK to Carbon PEEK with a 10% C addition for better printability. Three ribs were also added underneath the lid to restrict residual stresses built up in

the part during printing to curl the lip upward. Additionally, three screw connections were added to the lid and can to create more fastening points. In order to add the extra screw connection points, the internal preamp shelf was expanded to create a full circular shelf. There were several minor modifications made to the part including increasing the size of the boom connection thru holes and increasing the length of the search coil cable slots. These modifications show an anticipated increase in mass by ~27g. This increase in mass stayed below the mass budget for B-Field subassembly and did not bring up any concerns.

Future Steps

The B-field instrument is currently undergoing testing, including noise floor, frequency response, and crosstalk tests. As of 5/6/21 testing has been delayed due to wiring and soldering issues on the preamplifier board. A new preamplifier board has been designed and manufactured to mitigate these issues. Testing is scheduled to begin mid-May 2021. For a more detailed timeline to the July 15 2021 Pre-Integration Review, please refer to the Instrumentation Path to PIR document.

As of 12/13/2021 the future steps of the B-Field instrument are as follows:

Sensitivity, crosstalk, and SFDR testing will continue until the key driving requirements are met. Unverified requirements include SCI-2.2, SCI-2.3, SCI-2.5, and SCI-2.6. Upon verification of KDRs, the flight model preamp board design can be sent out for PCB manufacture and the board can be populated. A final full signal test will be conducted on the flight model preamp board to verify that all components within the B-Field subsystem functions properly. A fit-check of the flight model search coil holder will need to be conducted prior to subsystem assembly. Boom deployment testing will need to be conducted in mid-February. Assembly of the B-Field subsystem will commence and once all fit-checks are complete, the subsystem will be integrated into the full CANVAS satellite system. Once the B-Field instrument is incorporated into the full system, environmental testing, full electrical signal chain testing, and B-Field instrument deployment testing will need to be performed.

6.5. Analog Receiver Board

6.5.1 Functional description

The analog receiver board is in charge of the analog signal handling, and for the digital conversion coming from the preamp boards. The analog signal chain includes amplifier, filter, differential buffer and overvoltage protection. The digital conversion is handled by a 16-bit ADC, which is controlled by the FPGA on the Digital Receiver Board. The supplied power includes a 12V and a 3.3V rail. The necessary $\pm$ 5V and the 2.5V are converted on the analog board. There are housekeeping devices for voltage, current (12V, 3.3V and 2.5V) and temperature monitoring which are controlled via I2C through the PIC on the CDH board.

6.5.2 Development status

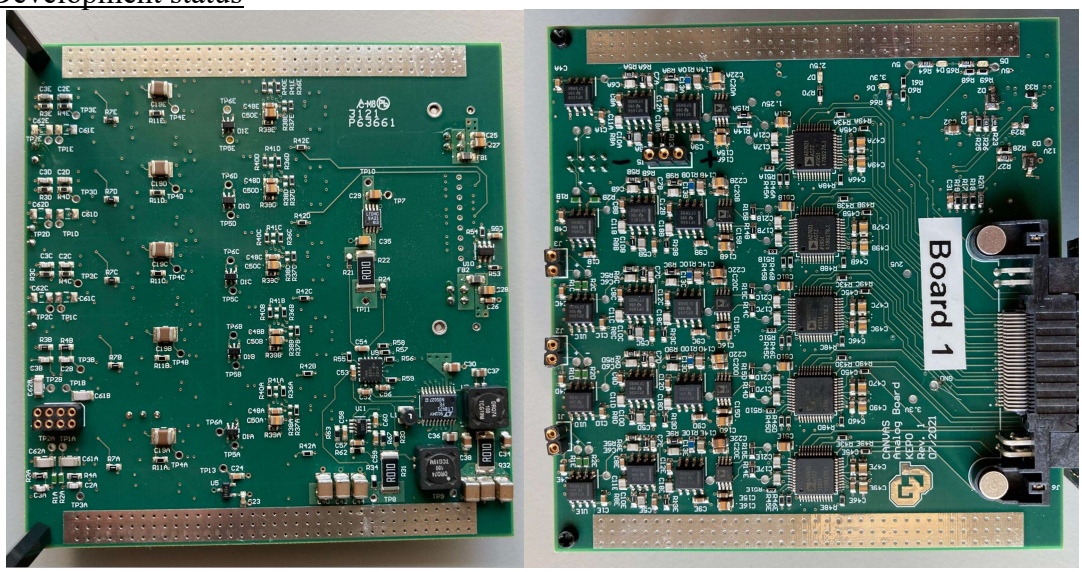

Figure INSTR-6: Current Revision of the Analog Board

The second revision (Rev 1) has been developed and assembled over spring and summer of 2021 as shown on Figure INSTR-6. The board bring up testing has been successfully accomplished and the analog section of the board has been fully tested. Amplification, filtering (Figure INST-6) and overvoltage protection (Figure INST-7) are working as intended. Unfortunately, the digital section could not be tested yet, due to missing FPGA firmware for the digital board. The altium project and further documentation is available on the LAIR gitlab server with additional information about design decisions and changes.

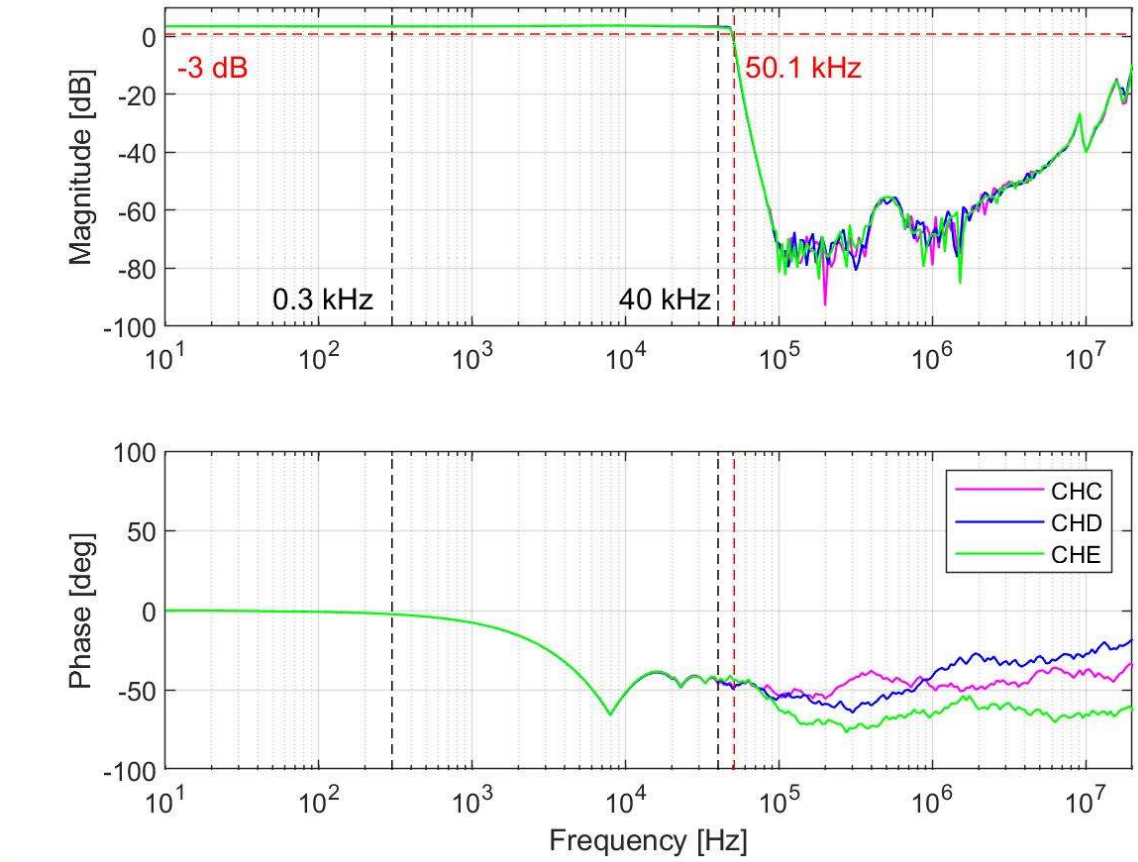

Figure INST-7: Frequency response of the analog B-field channels

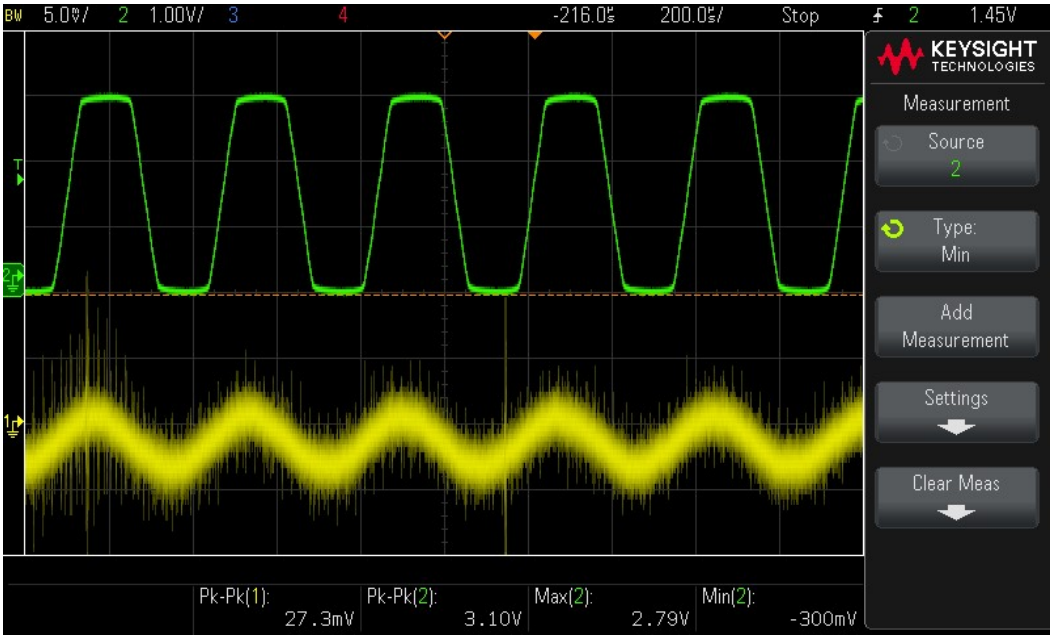

Figure INST-7: Overvoltage protection for ADC input. Clipping under -0.3V and 2.8 V (GND, 2.5V ± 0.3V)

6.5.3 Next steps

Before the flight board can be manufactured, the digital section of Rev 1 needs to be verified. This includes housekeeping testing with FSW as well as the digital conversion with the FPGA on the digital board. During the board bring up, minor changes to the schematic have been determined and during the assembly, some wrong footprints on the PCB have been identified. These require a redesign of the analog board which will lead to the flight version. The design changes will be implemented towards the end of December 21 and manufacturing and assembling is scheduled for January 22.

6.6. Digital Receiver Board

6.6.1 Digital Board functional description

The Digital Board has an input voltage of 12 V and generates its needed supply voltages of 1.0 V, 1.8 V and 3.3 V with three buck converters. The switching frequency is actually set to 400 kHz but can be changed up to 2 MHz if it is necessary. The FPGA is driven by a 224 Hz (16.7 MHz) oscillator and has an external 8 Mbit SRAM connected with a 16 Bit parallel interface. The firmware is stored in three NOR Flashes that are controlled by a voting logic (majority function) to settle the loss of at least one of the devices. For communication there is an RS-422 interface and an I2C to the CDH board and 5 single (read-only) SPI buses to the ADCs on the Analog Board. The FPGA receives a pulse-per-second (PPS) signal from the XACT. For debug purposes, there are additional interfaces that are described in the interface section. The RS-422 bus is connected to a UART-RS422 converter which is connected to the FPGA. The PPS signal is routed to a buffer to protect the FPGA from any over voltage. For housekeeping there

are three I2C secondary devices for voltage, current, and temperature monitoring. The altium project and further documentation is available on the LAIR gitlab server with additional information about design decisions and changes.

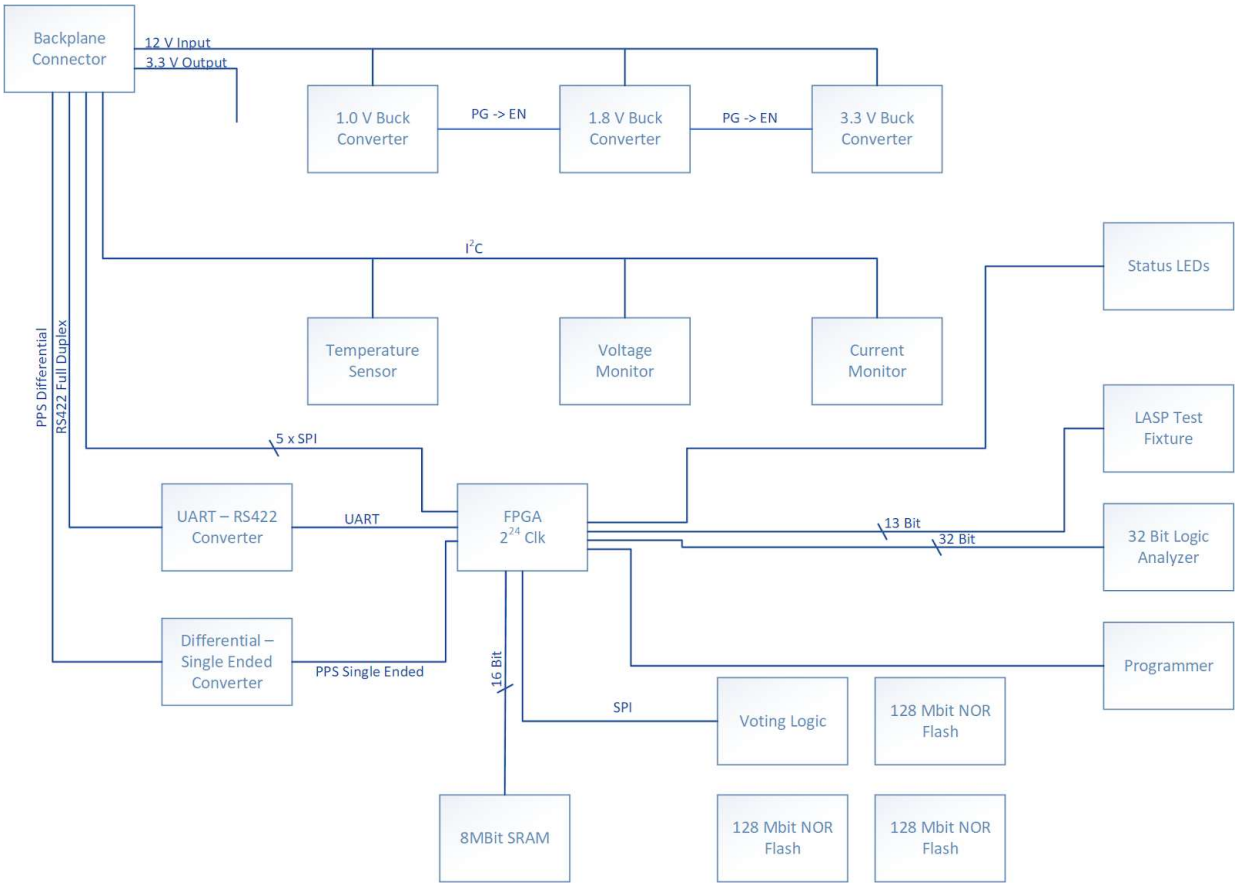

Figure INST-8: The ICD of the Digital Board.

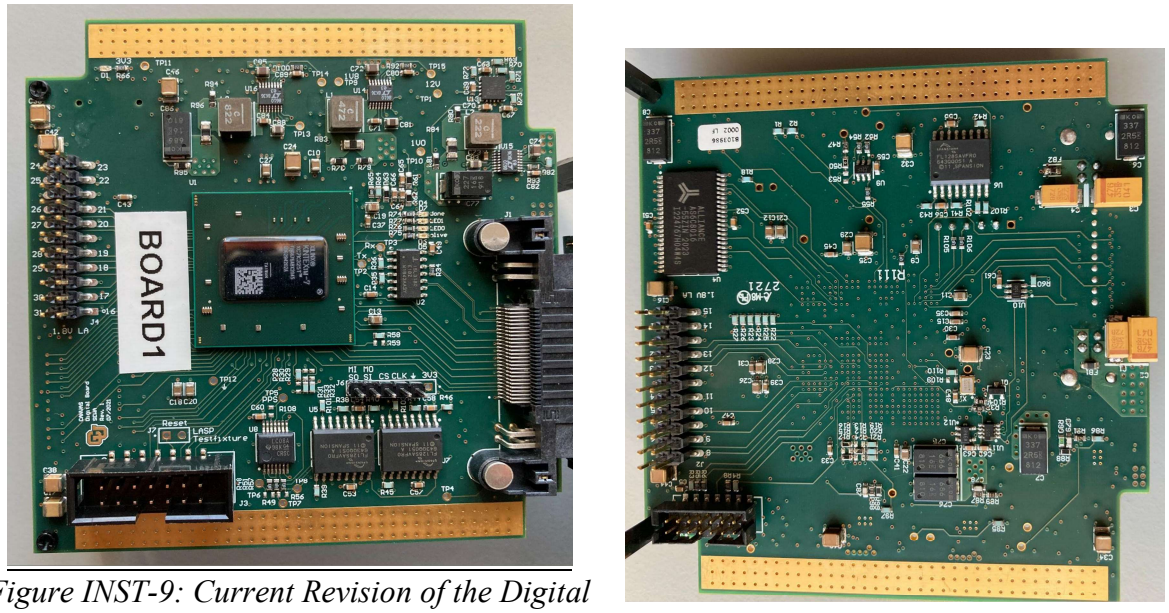

Figure INST-9: Current Revision of the Digital Board.

6.6.2. Semester progress and next steps

During the spring semester, the first version (Rev 0) of the Digital Board was populated with a smaller FPGA. During board bring up and initial testing, some design errors have been identified. Nonetheless, initial firmware testing could be performed and the pin configuration and the SPI interface module for the ADCs is verified. Further testing to verify the remaining modulus of the firmware needs to be done. The second revision (Rev 1) of the board has been developed and manufactured as shown on Figure INST-9. The initial board bring up was successfully accomplished and the boot and pin configuration of the FPGA is verified. The two remaining tests include I2C-housekeeping with FSW and digital conversion on the analog board. If these tests run without errors, the current design will become the flight version.

6.6.3. FPGA-firmware

The FPGA is required to further process and reduce the data. The data products from the ADC cannot be directly processed from downlink, as it would greatly exceed the data budget. Each ADC samples at 2^17 Hz with 16 bit depth leading to 113.2 GB of raw data produced per day. Instead, the FPGA performs 1024-pt FFTs with a 50% window, converting the data from the time domain to the spectral domain. Next, the FFT output is handled as either 1) spectra or 2) cross spectra, according to the required entries from the 5x5 spectral matrix, as described in the Payload Design Document. Spectra power and cross spectra power are then accumulated every second, so that 128 FFTs are averaged together. The 512 resulting FFT bins are also averaged in 67-log spaced bins (with 10 of those being special VLF transmitter bins). The final bin and time averaged data is then compressed and packeted according to CCSDS packets (each data packet will have 67 'bins' with 5 spectra and 20 cross spectra averaged per second) and sent to CDH. For more information, see Payload ICD.

LASP engineer Magnus Karlsson, has been developing the FPGA algorithm. Last semester the

team initiated efforts to unit test steps in the FPGA beginning with Python/IDL models. As of May 2021, the FPGA had been unit tested against Python/IDL in FFT for all FPGA modules. Now that software validation is complete, we are working towards verifying test FPGA versions in hardware. As of December 2021, 22 individual functional tests have been identified for validation testing, the details of which can be found in the FPGA Hardware Validation Test Document. These tests step through validating every individual function of the FPGA algorithm and conclude by validating that 5 channels of raw input are processed and compressed in the expected ways. More information about the algorithm in general, rotation, and decisions on the science packets can be found in the Payload Design Document.

7. Spacecraft Design

7.1. Command and Data Handling Subsystem & Backplane Board

7.1.1. CDH OVERVIEW

The Command and Data Handling (CDH) subsystem is responsible for storing payload data, communicating with all other spacecraft subsystems, and running the Flight Software (FSW). Figure CDH-1 shows some of these interfaces in a block diagram format. It is entirely composed of the CDH Printed Circuit Board (PCB) and its components. The main components include the Microchip PIC32MZ2048EFM100 Microcontroller and three Single Layer Cell (SLC) microSD cards. Additional background information about the CDH Board components and design can be found in the CANMO_Core_Avionics_ICD . This design has heritage on MAXWELL and MinXSS, but has been significantly modified for COSMO and CANVAS interfacing. This semester saw very few hardware updates due to ongoing FSW discussions and developments with LASP, so the CDH board is similar to how it was at the end of Fall 2020.

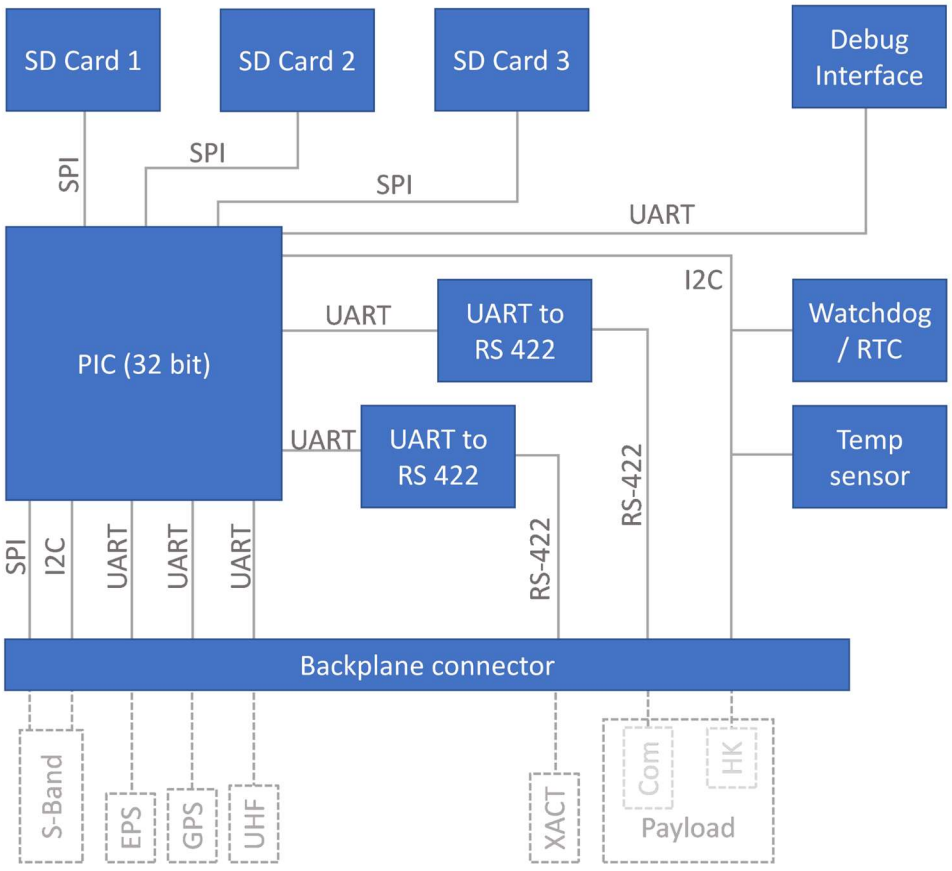

Figure CDH-1: COSMO CDH Block Diagram

7.1.2. Backplane OVERVIEW

The backplane is the main electrical interface between all of the subsystems in CANVAS. It features connectors for each of the main boards in the electronics card stack (EPS, CDH, S-Band DB, Analog, and Digital) and peripherals necessary for the mission (UHF radio, solar panels, XACT ADCS, deployment switches, RBF pin, and batteries). The backplane is currently in pre-revision redesign, with pin assignments and component locations still being finalized. The board shape dimensions, and connector locations are finalized. Figure BP-1 below shows a FBD for the backplane and its connections to main boards and peripherals.

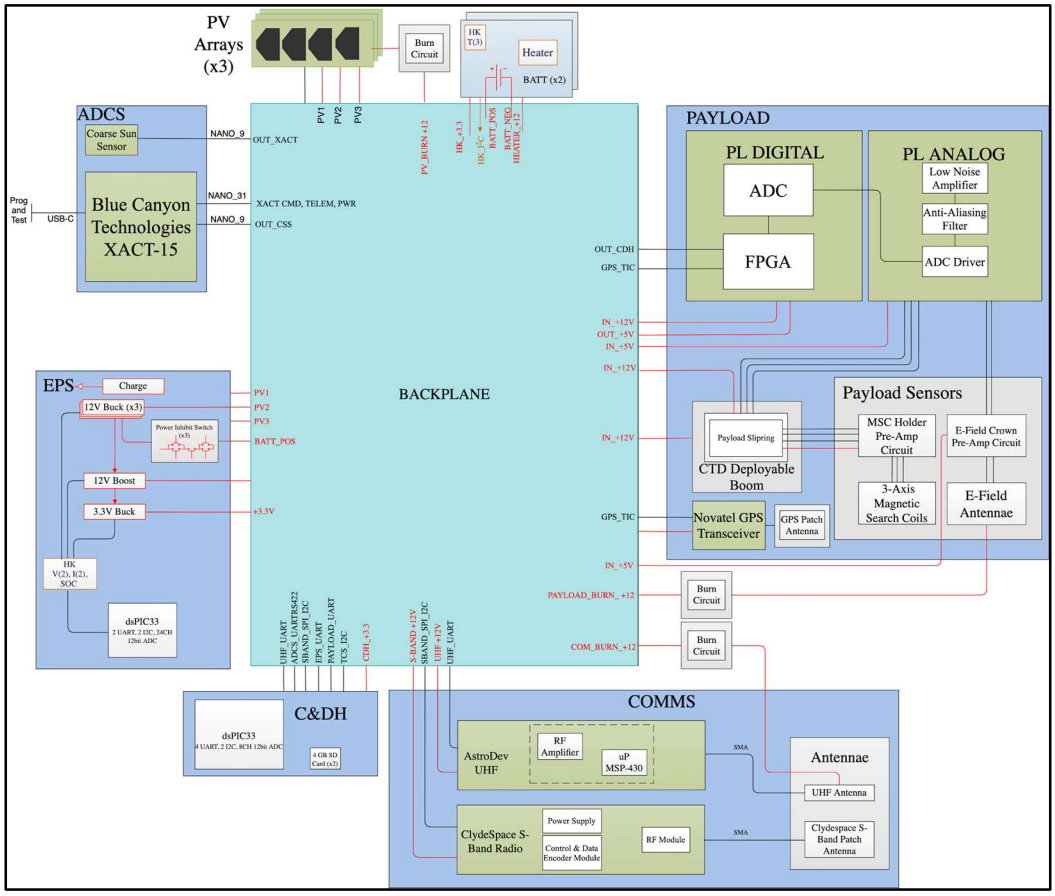

Figure BP-1: Backplane FBD for connections and signal lines to CANVAS Electronics

7.1.3. CDH KEY DRIVING REQUIREMENTS

Table CDH-1 lists a few of the mission requirements that drive the CDH design. The full list of requirements can be found in the CANVAS RVM.

Table CDH-1. CDH Key Driving Requirements

Req.	Description
CDH-8, 9,10,11,12,	The CANVAS CDH shall be capable of interfacing with all spacecraft subsystems and components (including STR)

13, 15,16	
CDH-14, SAT-5	The CDH shall be capable of operating in the radiation environment of Earth.
CDH-3	The CDH shall include a minimum of 2 weeks worth of onboard data storage.

7.1.4. Backplane KEY DRIVING REQUIREMENTS

Table BP-1 shows the key driving requirements for the backplane PCB. The requirements shown are not the entire list of backplane requirements, but they represent the key drivers behind the backplane design. The key driving requirements for the backplane mostly come from NanoRacks requirements for inhibit circuitry and switches to ensure CANVAS does not power on before deployment.

Table BP-1. Backplane Key Driving Requirements

Req.	Description
EPS-11	The subsystem shall adhere to all Electrical System Design and Inhibits outlined by NRCSD.
EPS-11.3	The subsystem design shall incorporate a minimum of three (3) independent inhibit switches "actuated by physical deployment switches as shown in Figure 4.2-1.
EPS-11.6	The RBF/ABF feature shall preclude any power from any source operating any satellite functions except for pre-integration battery charging.

7.1.5.1 CDH DESIGN STATUS

The CDH board has been redesigned to meet COSMO and CANVAS interfacing requirements and has undergone two layout revisions based on the changing project needs. The current revision is in a pre-reviewed state. The main schematic design has remained mostly unchanged since Fall 2020, but a few small changes have been made this semester. The layout of the board has not changed since Fall 2020.

Many general electronics updates have been carried out since CDR with the assistance of CANVAS' Electrical Engineer. These include the implementation of Altium project version control, unified board design principles, common board shape and templates, and library control. Additional information on these principles can be found in the Electrical Engineering Principles document in the LAIR-Altium Shared Drive.

The following schematic changes occurred in Fall 2020, but are reiterated here due to a lack of schematic changes in Spring 2021. The schematic changes mainly include the addition of internal signal debug connectors and removal of the large Debug connector that can be found on previous CDH revisions and that of MAXWELL and MinXSS in favor of a new GSE design. Another schematic change was the significant re-assignment of pins on the PIC and backplane connector to promote routing ease. These pin assignment updates can be seen in this document: CDH_PIC_Redesign_Notes.

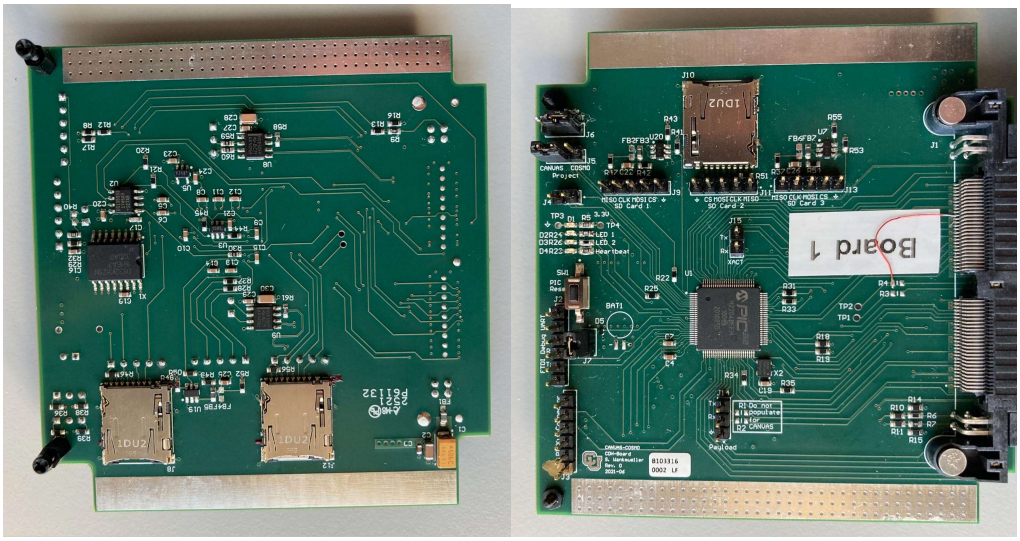

Figure CDH-2: Current CDH Revision

Layout changes were unchanged in Spring 2021, but in Fall 2020 they included the move from a 4-layer to a 6-layer board. This allowed for an internal signal routing layer which increases the cost of the board, but allows for significantly easier routing and wider spacing between traces. This wider spacing was required upon implementing new unified Design Rules for CANVAS and COSMO PCB Layout, which include increased spacing between data signals, clock signals, and differential pairs.

A number of internal signal debugging headers were also added to the CDH board, as were an FTDI connector, PICKit connector, reset button, and external 3.3V power jack. These connectors allow integrated and non-integrated debugging and programming directly connected to the PIC. With the removal of the Debug connector, full CDH debugging and testing will now be done using the GSE board through the backplane connector in a "FlatSat" configuration. This frees up significant amounts of space on the CDH board, and does not require that signals be split from the PIC to the backplane and the Debug connector - as was required in the previous design.

The board shape was modified to adhere to the common board design and the board was re-routed with the above changes in mind. The current layout can be seen in Figure CDH-2. Additionally, suppliers were investigated for the parts on the CDH board using Altium's ActiveBOM feature, so that the CDH board is ready for manufacturing as soon as possible.

In preparing for the semester Reviews, a number of unit testing protocols were also

considered in slightly more detail for the first time, and these can be found in Table CDH-2.

Table CDH-2: Unit Testing Overview

Test Name	Description	Resources needed
Acceptance - Continuity	Check continuity between pins and their locations on the backplane, power, GND, etc.	Multimeter (GSE preferred), power supply
Acceptance - Basic Functionality	Ensure connection to required components, check output of OSC2, I/Os should be high-Z	Multimeter, oscilloscope, power supply (GSE preferred)
Acceptance - Programmable (LED)	Plug in PIC programmer to GSE connector, attempt to program device and make LED blink	PICKit4 Programmer, power supply, LED blink program
Functional- Digital Interfaces	Load tested program to toggle at least all digital interfaces (possible all pins), check high/low	PICKit4 Programmer, power supply, toggle I/Os program, multimeter (GSE preferred)
Functional - Peripheral Interfaces	Test UART, SPI, I2C lines for basic functionality, heavily test RS422 converters	PICKit4 Programmer, power supply, simple interface driver program, oscilloscope (GSE *strongly* preferred)
Functional - SD Card Memory Test	Read/write SD Card with dummy data, ensure access to specific areas of memory	PICKit4 Programmer, power supply, simple SD card read/write program, (GSE *strongly* preferred)
Functional - RTC Watchdog Reset	Test the watchdog's ability to reset the CDH in the event of a latchup	PICKit4 Programmer, power supply, program to cause reset, (GSE *strongly* preferred)

The first revision of the CDH board was developed with a four layer design and two boards were manufactured. The bring up test was successfully accomplished. From originally two boards, only one is still functioning whereas the PIC on the second one is dead. If needed a replacement is possible.The altium project and further documentation is available on the LAIR gitlab server with additional information about design decisions and changes.

7.1.5.2 Backplane DESIGN STATUS

The backplane shall be based on the design of the current GSE board shown in Figure BP-2 . The GSE board acts as an interface for all avionics during testing and enables a "Flat Sat" configuration. The functionality of the backplane is identical to the GSE, therefore the only major change needed is to the layout. Once all interfaces have been verified with the GSE, backplane development will begin on the flight revision.

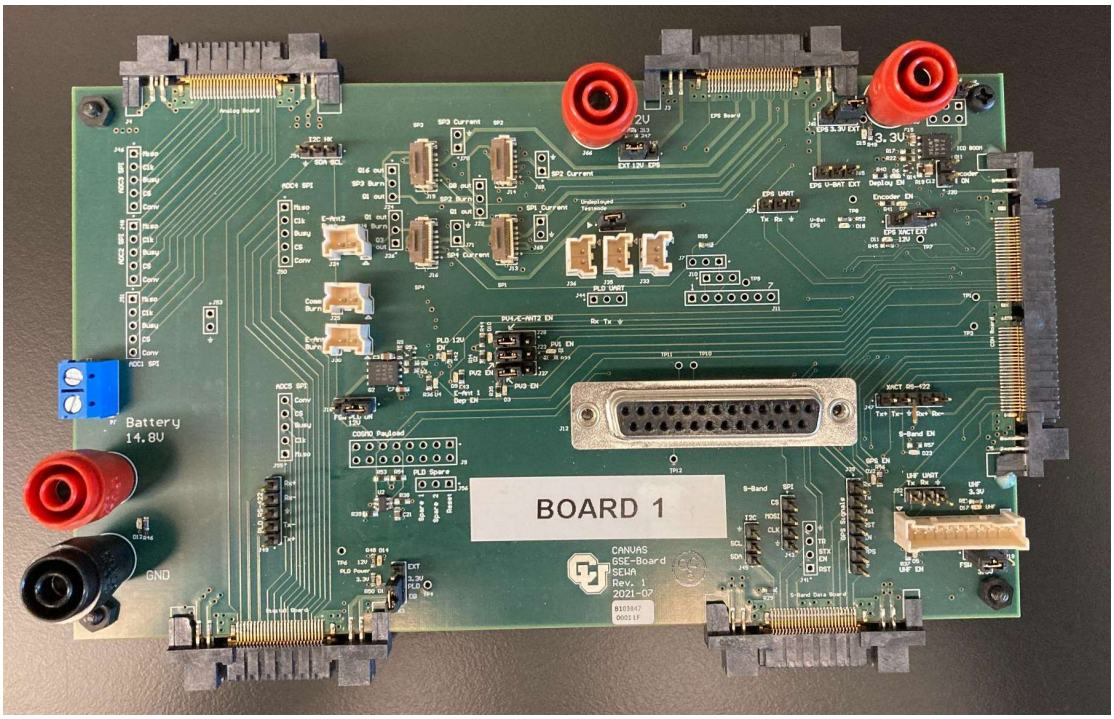

Figure BP-2: Current GSE Board

7.1.6.1 CDH MOVING FORWARD

Pre-Integration Review readiness is defined here as having a fully manufactured and unit-tested CDH board that is functional and ready to begin integration and integrated testing. The steps to reach this point, in chronological order, are:

1. CDH Board Layout Review with CANVAS EE and make final revisions
    a. Planned to be done beginning of Summer 2021 (end of May or early June)
2. CDH Board Revision 1 manufacturing preparation
3. Procure CDH board and components
4. Board manufacture by assembly of components onto PCB (internally or externally)
5. CDH Unit Testing (see table CDH-2)
    a. Requires additional resources like FSW scripts and a fully populated GSE board
    b. Test procedures should also be written if possible

At this point, the first revision of the CDH board should be ready for PIR. After PIR, the CDH component ratings should be checked to ensure their maximum limits meet at least twice the expected operating conditions (Parts Ratings Template). Additionally a hard reset concept should be considered and implemented on Revision 2 of the CDH board. This reset method would help the CDH recover itself and the rest of the spacecraft from failures caused by Single Event Effect (SEE) radiation events. It is crucial, however, that this reset concept perform a full power removal from the CDH (as opposed to the current watchdog and reset button performing a "soft" reset by toggling the PIC's MCLR pin). It is tentatively recommended to use the CDH

RTC Watchdog (TBD - see CANMO Avionics ICD) as the master device and to edit its circuitry to be able to activate an enable line on the backplane or CDH board which completely severs the connection from the backplane power to the CDH power plane. The CDH, effectively reset, may then operate and work to individually reset additional subsystems (including the EPS PIC) as needed to attempt to recover from a SEE failure.

The current CDH design (Rev 0) is waiting to be fully verified. This is done during the FSW development. Once the design is verified the necessary changes can be implemented and the flight version (Rev 1) of the board can be manufactured.

7.1.6.2 Backplane MOVING FORWARD

- Rework connector order & re-route board - 6/14/21
- Layout Review - 6/24/21
- Procure Rev0 - 7/1/21
- Populate Rev0 - 7/8/21
- Test Rev0 - 7/8/21 to 7/15/21

7.2. Electrical and Power Subsystem

7.2.1. EPS OVERVIEW

The Electrical and Power Subsystem (EPS) is responsible for generation, storage, and distribution of power to all subsystems. The subsystem consists of three primary components: two 14.8 V 2600 mAh Tenergy Li Ion batteries, three solar panels and a power management board. The EPS board takes in a 17-24V solar panel voltage and converts it to a 13.2 - 16.8 V bus voltage to charge the batteries. Further, the EPS board bucks the bus voltage into three regulated voltage rails. One of the voltage rails is 3.3V and powers most spacecraft electronics and ICs. The other two rails output 12V, with one of the 12V rails dedicated to the XACT due to its 3A inrush current. In addition to distributing power, the EPS monitors the battery state of charge and is tasked with efficiently optimizing solar panel power using the dsPIC33 microcontroller. The chip also packages data for UART communication with the CDH. For ground testing and powering, the EPS contains pin headers for programming and a DC jack for ground charging. The EPS also contains part of the inhibit circuitry required by Nano Racks. The physical deployment switches for this circuitry can be found on the backplane, or GSE board. Figure EPS-1 depicts the block diagram for EPS.

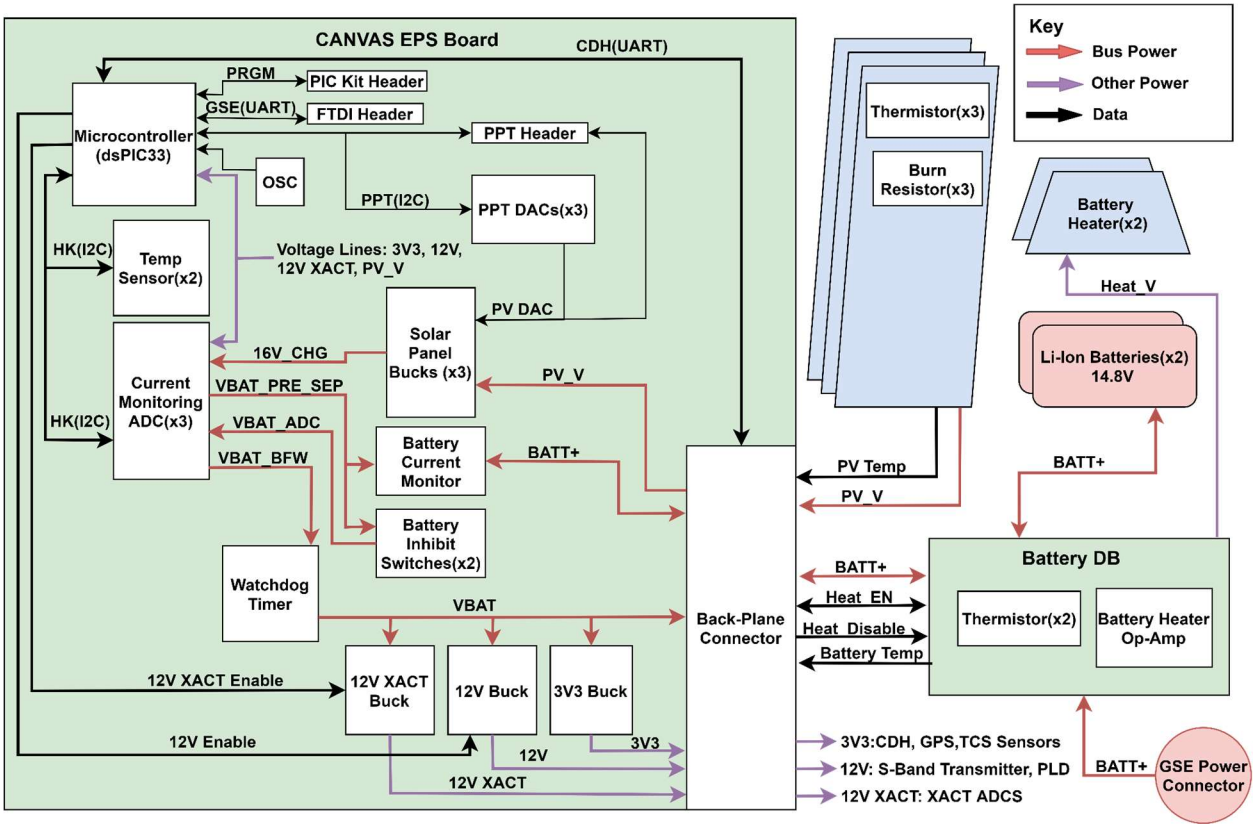

Figure EPS-1. Block diagram for EPS. (updated)

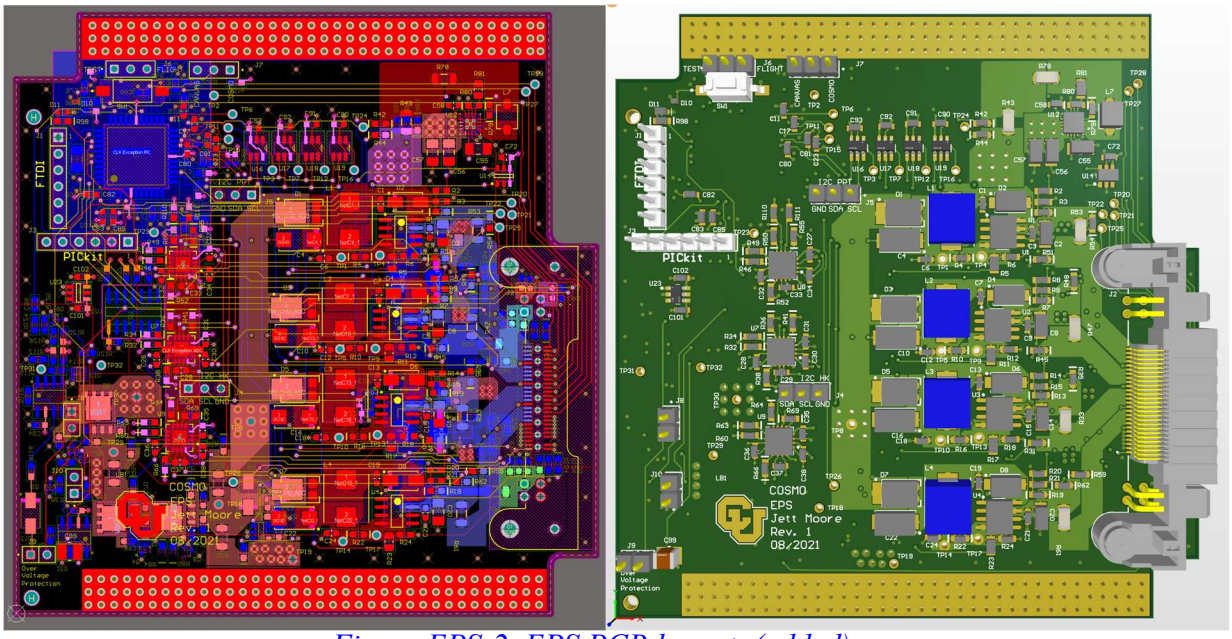

Figure EPS-2. EPS PCB layout. (added)

7.2.2. EPS KEY DRIVING REQUIREMENTS

Table EPS-1 displays the key driving requirements behind the Electrical and Power Subsystem. The requirements listed are not an exhaustive list of the requirements behind EPS, but they do capture what led to the design described in the EPS overview. Requirement EPS-2.1 is motivated by advice from LASP. Due to the large number of battery discharge cycles expected over the course of a three year mission, the depth of discharge is limited to at most 40% per cycle.

Table EPS-1. EPS Key Driving Requirements

Req.	Description
EPS-1	CANVAS shall be power positive on average over the course of an orbit.
EPS-2.1	The EPS battery shall not fall below a state of charge of 60%
EPS-6	The EPS shall provide power to every subsystem at the appropriate voltage
EPS-11	The EPS subsystem shall follow all electrical system requirements of the dispenser.

7.2.3. EPS STATUS

7.2.3.1 Power Management Board

7.2.3.1.1 Design

1. Spring 2021 Status: (does not reflect current status as of 12/2021 - see Fall 2021 Status below)

Revision 0A of the EPS board has been procured from Advanced Circuits and populated in house. To get to this point, the EPS board has been significantly modified from the MAXWELL design. In order to meet structural requirements the board was constricted to a 90x94 mm footprint. To accommodate the limited surface area 2 more layers were added to the PCB including an additional signal layer and an additional ground layer. With the extra signal layer the board was rerouted. The board also contains the necessary components for mounting in the cardstack including copper pours for the rails, a notch and removal holes. The copper pours are the primary interface with the rails. The rails provide thermal relief and prevent abrasions to the surface of the PCB. The notch enables external wire routing through boards on the cardstack. The removal holes allow the EPS board to evenly be pulled out of the backplane using allen wrenches. In addition to structural changes, several electrical changes were made from MAXWELL's design. Instead of 12V regulated rails, MAXWELL's EPS board contained two 5V rails. To accommodate 12V, the peripheral components for the 5V buck converters were modified to alter the output voltage. Similarly the peripheral components for the Solar Panel buck converters were exchanged to account for CANVAS input and output voltage requirements. Additionally, voltage dividers surrounding the dsPIC 33 were adjusted for 12V rail monitoring. In order to ease ground testing a physical program reset switch was added to the board in order to reset the dsPIC. Further, pin headers were added to the board for signal testing and microchip programming.

The current design follows the MAXWELL pseudo peak power tracking methodology for power conversion. The current peak power tracking(PPT) is not implemented through flight software and is instead replaced by a less efficient current limiting resistor. The hardware should be capable of PPT, but there are concerns about the lag time and compatibility of peak power tracking with the current EPS buck converters. The current limiting resistors should be sufficient as described in the testing below, but PPT may be worth developing to build better heritage and produce the highest efficiency possible.

In order to populate the board, a stencil was used to apply solder paste and an assisted pic-n-place in the Smead electronics shop was used to place components. Once components were placed the EPS was placed in a reflow oven to melt and harden the solder paste. The board with components attached can be seen on the Figures below:

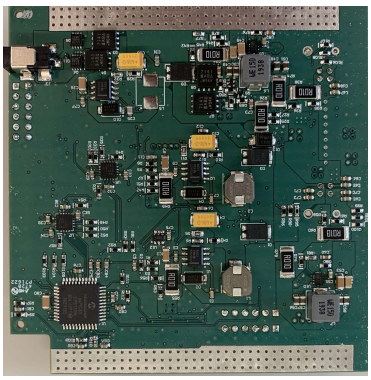

Figure EPS-3: EPS Rev. 0A: Top

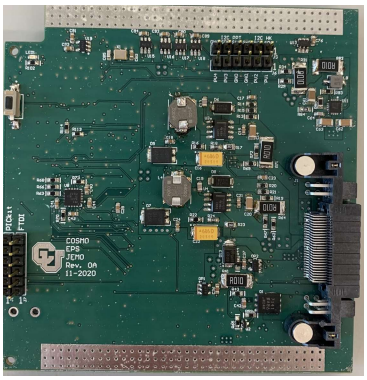

Figure EPS-4: EPS Rev. 0A: Bottom

2. Fall 2021 Status: (reflects current status of the board as of 12/2021)

Revision 1 of the EPS board has been manufactured, populated, and successfully tested. Bring-up tests (continuity tests, visual inspection, smoke tests), power distribution tests, and

software tests have validated the correct assembly of the EPS PCB. Two boards of the EPS Rev.1 design have been assembled in order to hand over one of the boards to LASP for software testing. Figures EPS-5 and EPS-6 show an EPS PCB fully assembled. More information regarding the current design of the EPS PCB can be found in the EPS ICD.

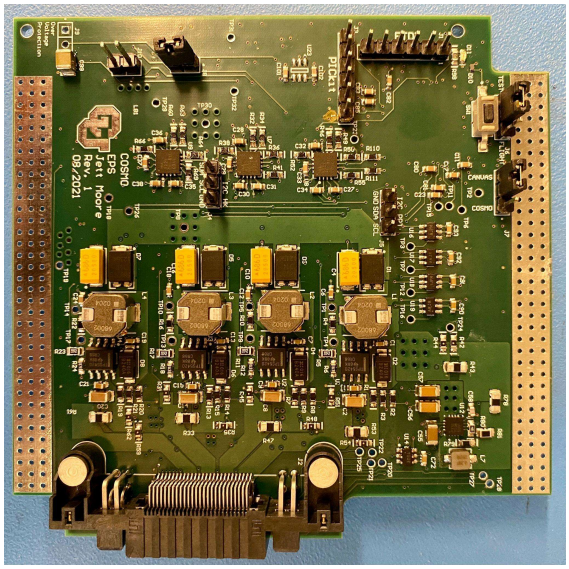

Figure EPS-5: EPS Rev. 1: Top

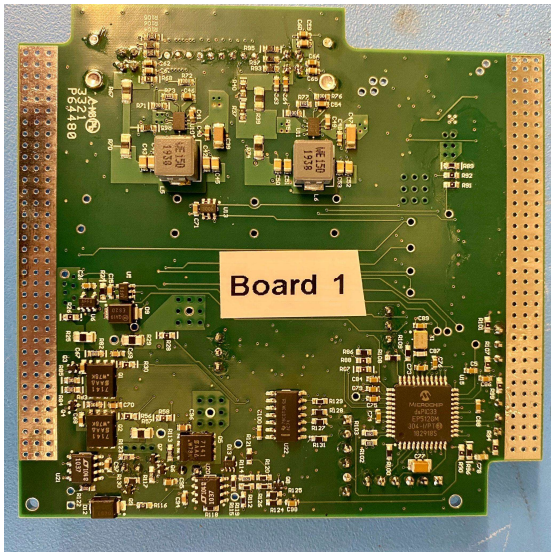

Figure EPS-6: EPS Rev. 1: Bottom

7.2.3.1.2 Testing

As mentioned above, power distribution tests were performed to verify the output of the voltage converters used to power up each of the satellite's rails. The EPS board was powered up through the GSE board, as seen in Figure EPS-7. The tests confirmed that all converters were regulating each rail adequately to power up the components connected to each one of them. Thus, the EPS is currently fulfilling the EPS-5 requirement: *"The subsystem shall provide required electrical interfaces to each subsystem"*. Inhibit switch tests confirmed that the subsystem powered

down when any of the switches was activated. Thus, the EPS is currently fulfilling the EPS-11.3 requirement: *"The subsystem design shall incorporate a minimum of three independent inhibit switches"*.

Software upload tests confirmed that the EPS microcontroller could be programmed successfully using an FTDI cable in preparation for upcoming FSW testing. Further software tests were carried out to validate the communication with the EPS housekeeping sensors and to validate the enabling/disabling of both 12 V rails that power up other subsystems. The tests confirmed correct power monitoring and distribution throughout the satellite's power grid. Therefore, the EPS is currently fulfilling the EPS-9 requirement: *"The subsystem shall provide power toggling for components as commanded by CDH"*, and the EPS-10 requirement: *"The subsystem power measurements shall be tracked for independent solar panels, batteries, power distribution buses, and critical components"*.

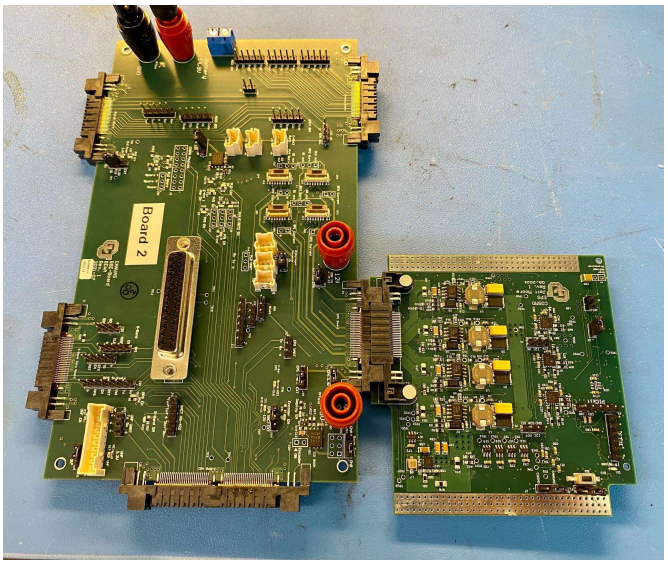

Figure EPS-7: EPS board connected to the GSE board

7.2.3.2 Solar Panels

The solar panel board has the solar cells attached to it along with the burn wires and houses on the outside of the satellite. The solar cells provide power to the spacecraft such that it can sustain flight operations even during eclipses. When the spacecraft is not in an eclipse, the board collects the power and charges the battery that will be used during the eclipses. The burn wire resistors are hooked up to the wires and they will burn in order to cut the wire and deploy the solar panels. For Canvas, the solar panels have 9 cells on each board totalling 27 cells for the satellite. The primary difference between CANVAS and COSMO is that the COSMO PCB is the same for all of its solar panels. However, CANVAS has different configurations for its hinge and body mounted solar panels. Therefore, as seen in the schematic below, there are slots for multiple connectors, burnwire resistors and thermistors. Thus, only one PCB is needed and the various components are populated depending on the configuration required.

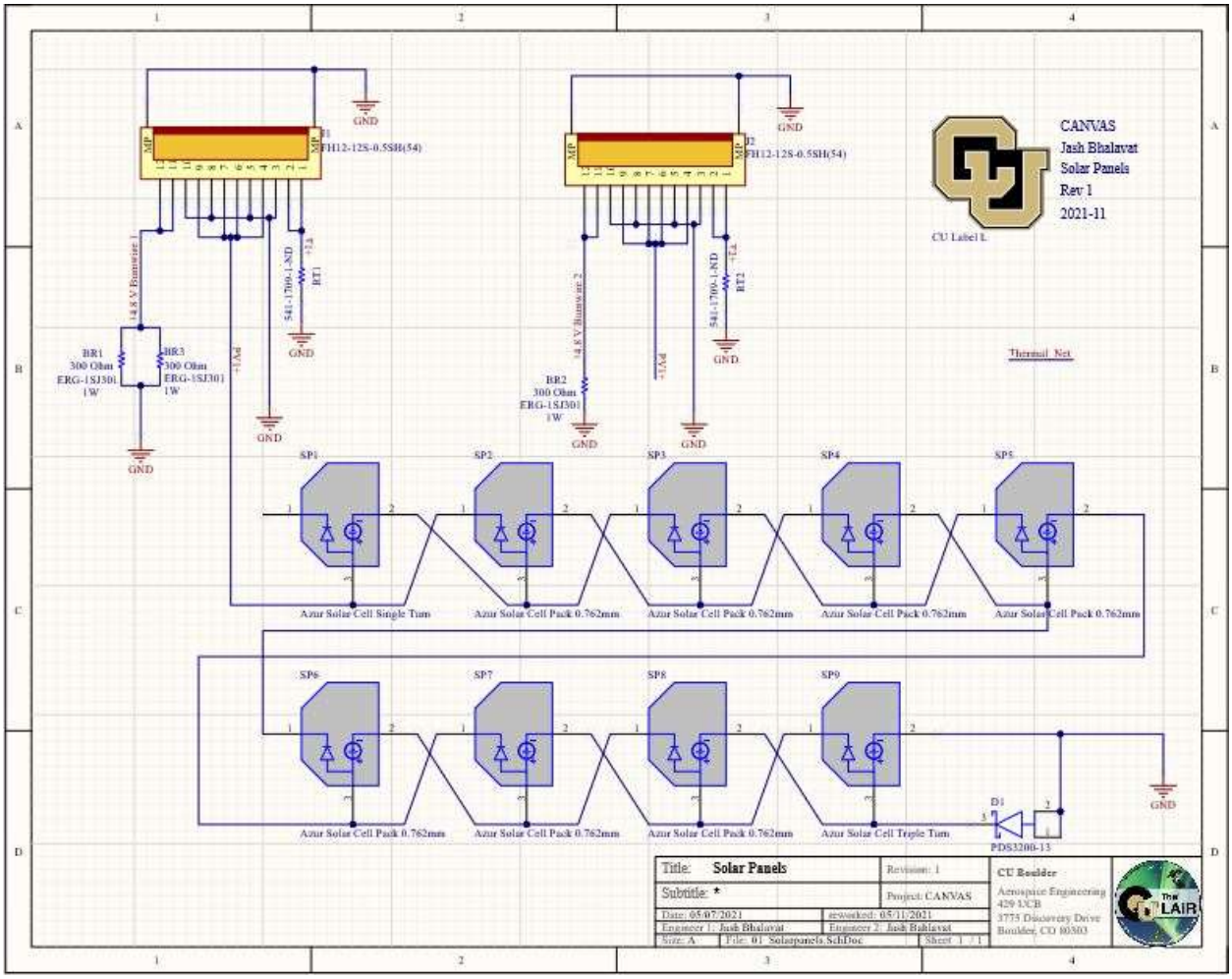

Figure EPS-8: Schematic of the Solar panels

7.2.3.3 Power Budget

The CANVAS power budget was updated during the Fall 2021 semester using power consumption data obtained through direct testing of the components. There are currently four main modes of operations established: Phoenix Mode, Safe Mode, Nominal Mode (Science Ops.), Nominal Mode (Downlink). Under Phoenix Mode, it is estimated that the spacecraft will demand 6.72 W. Given that the solar panels are able to produce 31 W at maximum power point (already accounting for solar buck converter power loss), the batteries will be able to comfortably recharge after any battery depletion events that cause an autonomous transition to Phoenix Mode. The spacecraft is expected to demand 8.03 W under Safe Mode, 13.08 W under Nominal Mode (Science Ops.), and 17.79 W under Nominal Mode (Downlink).

If we were to assume that the solar panels will generate 31 W in sunlight, that the satellite will be 62% of the orbit in sunlight (59 minutes of a 95-min orbit), and that the satellite will be downlinking data during 100% of the orbit (unreal worst-case power consumption scenario) and thus demanding 17.79 W for 95 minutes, the satellite would have a positive energy margin of 2.31 Wh per orbit. Note that this is under an unreal max power consumption scenario. In conclusion, the EPS currently fulfills the EPS-1 requirement: *"CANVAS shall be power positive on average over the course of an orbit"*.

7.2.4 EPS Flight Software Improvements

The EPS FSW was improved in preparation for EPS-CDH communication tests to be carried out in coordination with LASP. Firstly, the CDH command reception and execution functionality was implemented in the code. Secondly, the functionality to send a housekeeping packet containing variables such as voltages, currents, and temperatures of the subsystem back to the CDH when requested was added to the FSW as part of the spacecraft's health monitoring process. Thirdly, an EPS parameters table containing operational limits was added to the software. This table can be modified via CDH commands to change variables that affect the EPS mode of operation.

Furthermore, new algorithms implemented in the EPS FSW to improve it. A battery state of charge estimation algorithm was added to the EPS FSW to be able to indirectly measure battery SOC using battery voltage and current measurements. Additionally, the functionality to control the solar buck converters through the EPS microcontroller was added to the EPS FSW in preparation for Peak-power point tracking (PPT) algorithm implementation. Further details on these two new algorithms can be found in the EPS ICD.

7.2.4. EPS MOVING FORWARD

EPS Board

Rev 1 was found to be completely functional. However, some improvements can still be made to the board to guarantee mission success in space. The solar buck converters were found to be functional and their output voltage could be controlled via a Digital-to-Analog converter connected to the EPS microcontroller. However, the minimum output voltage that the buck converters could reach when controlled by the DAC's was found to be still too high to guarantee that the solar panels are not going to be browned out in a worst-case power consumption scenario (battery fully discharged and the spacecraft demanding peak power. Therefore, new resistors have been ordered to tweak the control loops of the solar buck converters on the EPS PCB to modify the voltage range of the solar buck converters. Another improvement that will be performed on the EPS PCB in Spring 2022 will be the improvement of the current battery thermal sensors which have a non-ideal resolution of 4°C/bit addition. A 1-kΩ pullup resistor will be added to the signal line coming from each battery thermistor to drive them at 3.3 V instead of 16.8 V (battery voltage). This will improve sensor resolution to 0.22°C/bit.

For testing, there are several steps that should be conducted before ordering the EPS flight revision. Flight software tests need to be executed to validate that all sensors and actuators were designed correctly. These tests include the following: EPS-CDH communication tests at LASP to evaluate retrieval of EPS housekeeping data, tests to verify correct modification of the EPS parameters table via CDH command, and fault tolerance tests to evaluate watchdog timer performance when detecting software hangs. Furthermore, PPT algorithm tests need to be performed to validate the solar panel buck converter design. As a first step, PPT algorithm evaluation using the EPS board, a battery, an electronic load, and the solar panel simulator from STIg Lab will be carried out. Subsequently, the PPT algorithm will be evaluated with the flat-sat assembly and a solar panel with flight solar cells.

In addition, battery tests and SOC estimation algorithm tests need to be carried out to verify that the EPS fulfills the EPS-11.8 requirement: *"All flight battery packs shall be subjected to an approved set of acceptance screening tests"*. Firstly, flight batteries need to be selected via TVAC

and charge/discharge tests. Secondly, the selected batteries need to be characterized (measurement of internal resistance and charge/discharge) to adapt the SOC algorithm to the selected batteries. The accuracy of the aforementioned algorithm needs to be evaluated at low battery temperatures (1 - 5°C). This test will be performed during the Battery and Heater Operational Test scheduled for February 15th, 2022.

Solar Panels

This semester, the PCB went through a lot of changes. Firstly, in order to accommodate the E-Field antennas atop the solar panel, spacers were added to the PCB. This was possible because the solar cell interconnect tabs were tucked under the next cell as seen in the figure below. This creates additional room within the PCB where spacers can be placed to hold the E-Field antenna. Additionally, the solar panel PCB was changed to a 4-layer board instead of just 2 layers. This was done to prevent overheating the body mounted solar panels that received heat from the battery pack. Hence, the internal layers were assigned as thermal layers. Also, additional mounting holes were added between solar cell 1 and 2 in order to decrease the cantilever distance to prevent flutter during launch.

Moving forward, the PCB is ready to be procured. A test PCB will be procured and populated. Then, the test panel will go through a glow test and the Power Point Tracking test. In the glow test, a voltage will be applied across the panel and the cells will be observed in the infrared spectrum. This test should point out the cracks and deformities on the cells. The PPT test will be conducted with the EPS board to confirm the PPT algorithm and to point out errors. Subsequently, revisions will be made to the solar panel PCB and after that, flight panels will be procured. Those shall be populated with solar cells, burn wire resistors, thermistors, and the corresponding connector. Similar tests shall also be conducted on the flight PCB as the test PCB.

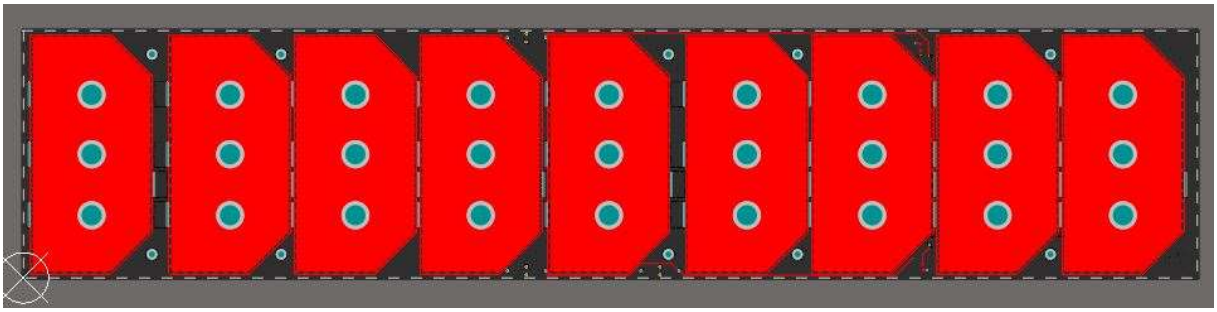

Figure EPS-8: Solar Panel PCB

7.3. Communication Subsystem

7.3.1. COMMS OVERVIEW

The COMMs subsystem will transmit payload data via amateur S-band (2402.5 MHz), transmit beacon and housekeeping data via amateur UHF (437.25 MHz), and receive uplinked commands via amateur UHF. This mission will use LASP's ground station for all communications. All link budget calculations are based on a 20° elevation mask due to LASP's current capabilities. The current 20° elevation mask is based on empirical data collected from one cubesat mission, LASP is aiming at collecting more data from two current cubesat missions to further characterize the elevation mask. This mission could use

a 10° elevation mask in the future. LASP is helping develop the flight software that will be used for test and operational commanding. Specs for radios can be seen below in the Status section.

The UHF system on CANVAS uses the AstroDev Li-2 radio with a tape-measure antenna. Commands and telemetry are sent over this system at a transmission rate of 9600 bits per second. The S-band system uses the Clydespace HSTX transmitter with a SANT patch antenna. This system has the capability to transmit up to 5 Mbps (megabits per second) of science data (10 Mbps total with a 1:1 convolutional encoding overhead). Due to licensing limitations, a transmission rate of 2 Mbps is most likely to be used.

7.3.2. COMMS KEY DRIVING REQUIREMENTS

Table COMM-1 shows some of the COMMs subsystem's key driving requirements. The requirements shown here are based on the choice of LASP as a ground station. Table COMM-2 shows the subsystem radio specifications.

Table COMM-1: COMMs Key Driving Requirements

Req.	Description
COMM-3	The subsystem shall have a minimum link margin of +6 dB on uplink and downlink at 20-degree elevation mask
COMM-4	The subsystem shall downlink payload data in S-band frequency band
COMM-5	The subsystem shall be capable of receiving uplink commands and downlinking telemetry and system status in the UHF frequency band

Table COMM-2: UHF and S-band Radio Specifications (weight, size,range(Hz), etc)

	Radio	Manufacturer	Freq. (MHz)	RX?	TX?	Weight (g)	L (mm)	W (mm)	H (mm)
UHF	Li-2	Astrodev	130-450	✓	✓	30-52	64-65	32-33	0-10
S-band	HSTX	ClydeSpace	2402.5	X	✓	<100	86.06	91.72	14.55

7.3.3. COMMS STATUS

The goal of the COMMs subsystem this semester was to complete all non-transmitting testing, once all non-transmitting testing is complete, the radio licensing procedure is to be undertaken. On the FSW side of COMMs the goal of LASP was to complete the UHF and S-band radio interfaces as well as work on the GPS interface.

In Fall 2021, all non-transmitting UHF testing barring the UHF antenna tuning test was completed. The non-transmitting UHF tests that were completed were the UHF configuration

test, the UHF Spectrum test, and the UHF Power Test. The UHF Configuration test was performed to ensure the functionality of the Lithium-2 radio as well determine the configuration settings of the radio. The results of the UHF configuration test are shown below in figure COMM-1.

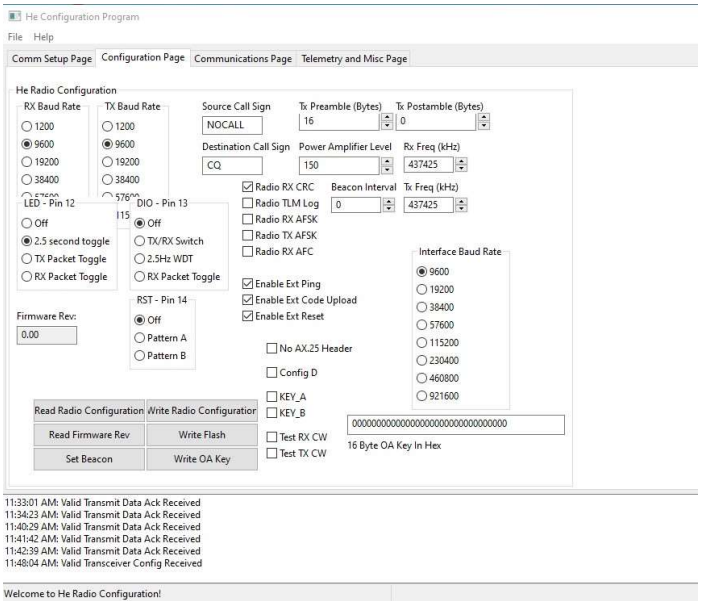

Figure COMM-1: UHF Configuration settings

The UHF power test was conducted to ensure that the manufacturer's stated rf output power was accurate. In verifying the accuracy of the UHF rf power output, the UHF power test also acted as a validation of the current UHF link budget. The test setup included the UHF radio, two 10 dB attenuators, the GSE board, a computer running the Astrodev shared configuration program, and a signal hound USB-SA124B. The test setup is shown below in figure COMM-3.

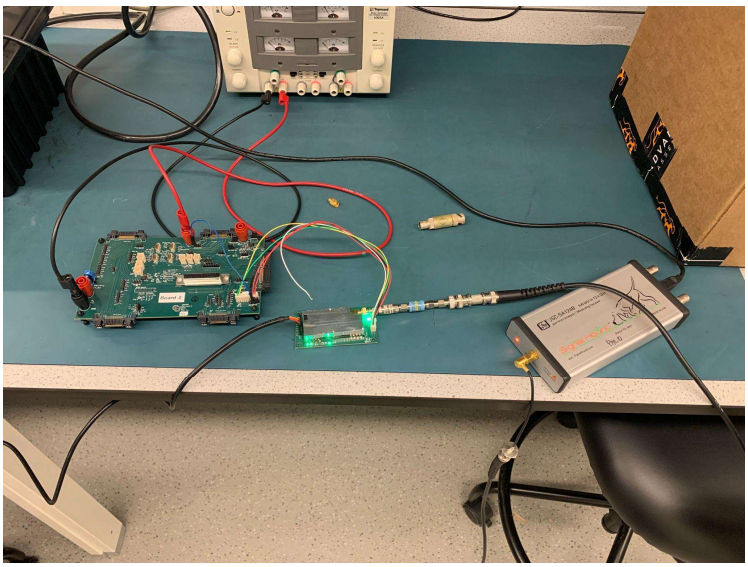

Figure COMM-2: UHF Power Test Setup

The results of the test showed that the UHF rf output power as stated by the manufacturer was

accurate. In figure COMM-3, the results of the power test are shown.

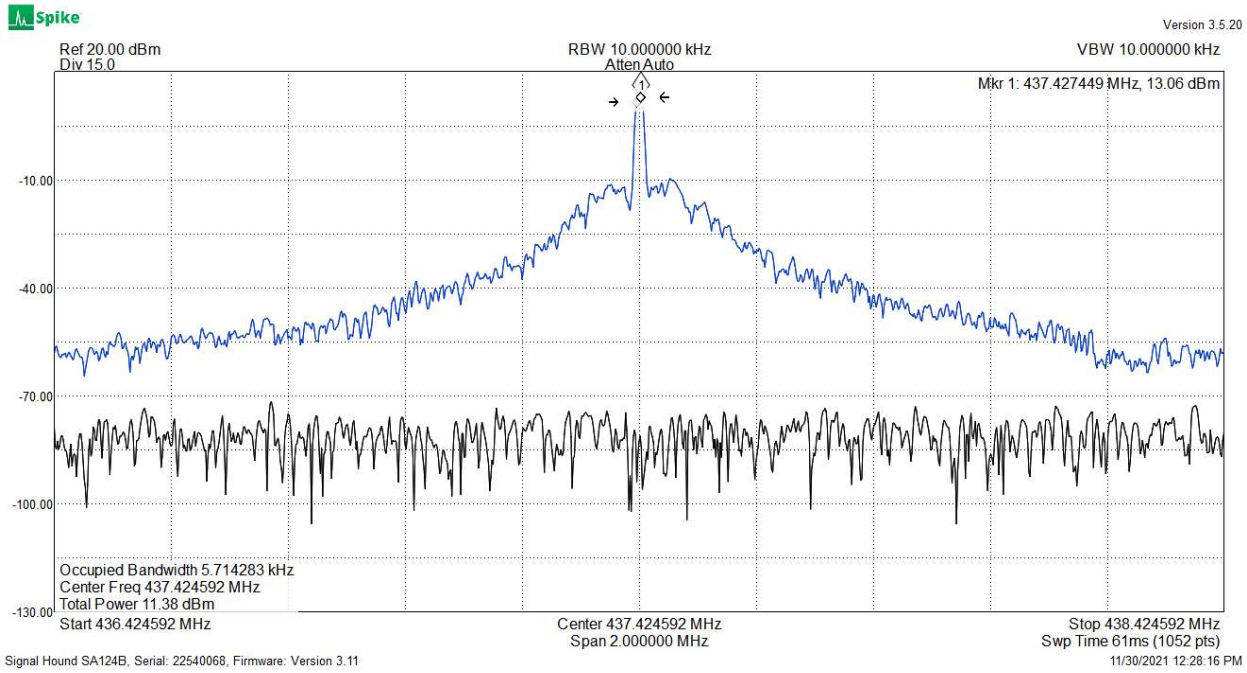

Figure COMM-3: UHF Power Test results

From the results shown above, marker 1 was set to peak tracking, during transmission the marker registered an rf power of 13.06 dBm. This power output was achieved with the addition of two 10 dB attenuators, the attenuators actual attenuation was roughly estimated and their measured values were ~9.07 dB. This shows that the raw, attenuated output power was ~ 30 dBm, verifying the manufacturer specifications as well as the UHF link budget.

The final UHF non-transmitting test that was conducted this semester was the UHF Spectrum test. The UHF spectrum test was conducted with the same test setup as the UHF power test. Again looking at the results from COMM-3, the marker shows that the center frequency is 437.427 MHz, comparing this to the UHF configuration setting of 437.425 MHz shows that the Lithium-2 spectrum measurements were representative of the configuration settings. This test also acted as a verification of KDR COMM-5, demonstrating that the UHF radio is capable of downlinking and uplinking in the UHF band.

During the course of the semester, the UHF radio was integrated with revision 1 of the UHF backplane. After conducting nominal mode current measurements, it was decided a RLC low pass filter would be added to the UHF backplane. This RLC low pass filter was added to filter out signals generated by the operation of the UHF radio. The UHF radio integrated into revision 1 of the UHF backplane is shown below in figure COMM-4, figure COMM-5 shows the 3D rendering of the new UHF backplane design that incorporates the RLC low pass filter. The UHF impedance board also underwent changes as a direct result of the change in the UHF antenna housing. The current design has switched to an MCX connector to match the UHF transceiver connector, currently the impedance board's inductance is unknown. A value for the inductance will be obtained through the UHF antenna tuning test.

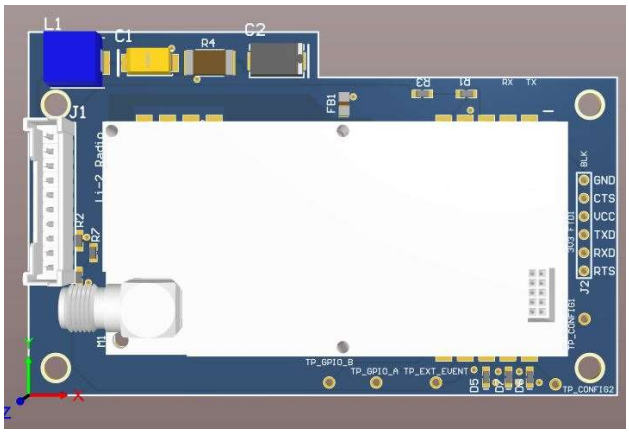

Figure COMM-4: UHF Backplane rendering

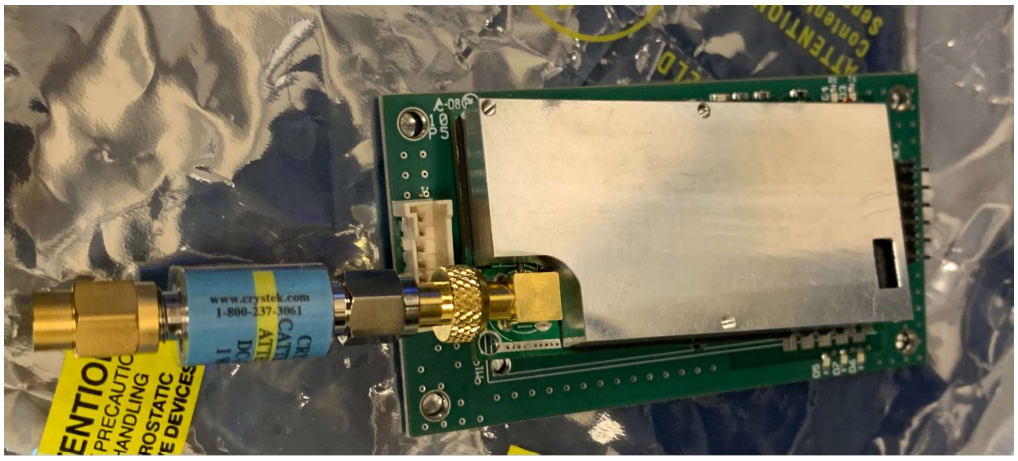

Figure COMM-5: UHF Backplane revision 1 integration

The S-band radio as well as the GPS were also integrated with the S-band Daughter board revision 1. During the course of the semester the FSW modules for the UHF and S-band radios were completed by the LASP personnel. The integrated S-band and GPS with the S-band daughter board are shown below in figure COMM-6

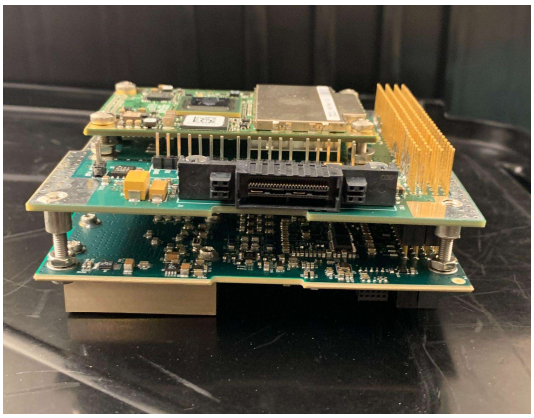

Figure COMM-6: S-band Daughterboard revision 1 integration

Due to unexpected issues with the UHF antenna housing functionality and fit, the design was revised and completed this semester by the structures team. After the redesign was deemed

functional, the new design was machined, fit checked, and is awaiting assembly. The rendering below shown in figure COMM-7 shows the new UHF antenna housing assembly and design.

Figure COMM-7: UHF antenna housing rendering

7.3.4. COMMS MAJOR CHANGES

The major changes to the COMMs subsystem have been in adjusting the potential downlink rate in the link and data budgets. The downlink rate of 2 Mbps is assumed with an elevation mask of 20 degrees. Better capabilities (10 degree elevation mask and 2Mbps) need to be confirmed with LASP in summer. The HSTX can theoretically transmit at up to 5 Mbps, but until this can be confirmed via testing the lower downlink rate is being used. This lower rate results in a margin which is just positive on downlink capability, shown in table COMM-4. This margin is almost guaranteed to change, however, due to increased knowledge of the radio capability through testing, new choice of ground station, and/or through LASP improving their elevation mask. The other changes to the COMMs subsystem were in the UHF antenna housing.

In addition, there have been changes to the estimated S-band data production, as we've further defined the size and structure of the science packets through discussions with LASP and the science team. The current (as of May 2021) structure and size for science packets is outlined in the Payload ICD, and results in 211 MB/day of data production. There are 3 potential ways to mitigate risk as a result of such low positive margin.

- Dropping every other packet
- Find another ground station
- Change integration time from 1 sec to 2 sec

The option that results in least loss of data is dropping every other packet.

Table COMM-3 shows the current S-band and UHF data budgets. Table COMM-4 summarizes the effect different downlink data rates and supported elevation masks have on the S-Band data budget.

Table COMM-3: Data Budget

S-band	UHF

Data production rate	4930.6	bytes/sec	Data production rate	51	bits/sec
Total data produced	426	MB/day	Total data produced	0.5253	MB/day
Ground station coverage	15.16	min/day	Ground station coverage	15.16	min/day
Downlink rate	2000000	bits/sec	Downlink rate	9600	bits/sec
Data downlink capability	**216.4**	**MB/day**	**Data downlink capability**	**1.041**	**MB/day**
Margin	**-209.6**	**MB/day**	**Margin**	**98.15**	**%**

Table COMM-4: S-Band Data Summary for different situations downlink rates and elevation masks. Δ data presented as (downlink capacity - data produced) in MB per day. Minimum operational data budgets highlighted in gold.

Data Budget Summary						
Δ Data (MB/day)		Data Rate (Mbps)				
		5	4	3	2	1
Mask (°)	10	929.6	658.5	387.3	116.2	-155.0
	15	437.5	264.8	92.1	-80.7	-253.4
	17.5	246.2	111.7	-22.7	-157.2	-291.7
	20	115.3	7.0	-101.3	-209.6	-317.9

Full Data Budget:

Table COMM-5 shows the S-band downlink budget. Table COMM-6 shows the uplink and downlink budgets for the UHF system. Note that the values in both link budgets for the ground station are not entirely accurate and must be updated in Summer.

Table COMM-5: S-band Downlink Budget

S-band (Downlink)		
Spacecraft:		
Spacecraft Transmitter Power Output:	1.0	watts
Spacecraft Antenna Gain:	8.3	dBiC
Spacecraft EIRP:	7.3	dBW
Downlink Path:		
Spacecraft Antenna Pointing Loss:	-0.5	dB
Antenna Polarization Loss:	-1.0	dB
Isotropic Signal Level at Ground Station:	-158.3	dBW
Ground Station:		
Ground Station Antenna Pointing Loss:	-0.5	dB
Ground Station Antenna Gain:	40.1	dBiC
Ground Station Transmission Line Losses:	-0.5	dB
Ground Station LNA Noise Temperature:	289	K

Ground Station Transmission Line Temp.:	290	K
Ground Station Effective Noise Temperature:	355	K
Ground Station Figure of Merit (G/T):	14.1	dB/K
G.S. Signal-to-Noise Power Density (S/No):	83.9	dBHz
Telemetry System Eb/No:	23.9	dB
Telemetry System Required Eb/No:	9	dB
System Link Margin:	**14.9**	**dB**

Full downlink budget

Table COMM-6: UHF Uplink and Downlink Budgets

UHF			
	Downlink	**Uplink**	
	Spacecraft	*Ground Station*	
Transmitter Power Output:	2.0	500.0	W
Antenna Gain:	-6.0	10.5	dBiC
EIRP:	-4.0	33.5	dBW
	Downlink Path:	*Uplink Path:*	
Antenna Pointing Loss:	-0.5	-1.0	dB
Antenna Polarization Loss:	-1.0	-4.0	dB
Isotropic Signal Level at Ground Station:	-154.7	-122.2	dBW
	Ground Station	*Spacecraft*	
Antenna Pointing Loss:	-0.03	0.0	dB
Antenna Gain:	40.1	-6.0	dBiC
Transmission Line Losses:	-0.5	-1.0	dB
LNA Noise Temperature:	398	1163	K
Transmission Line Temp.:	290	270	K
Effective Noise Temperature:	563	1449	K
Figure of Merit (G/T):	12.1	-38.6	dB/K
Signal-to-Noise Power Density (S/No):	86.0	67.8	dBHz
Telemetry System Eb/No:	46.2	28.0	dB
Telemetry System Required Eb/No:	9	15.0	dB
System Link Margin:	**37.2**	**13.0**	**dB**

Link to full budget:

7.3.5. COMMS MOVING FORWARD

With the completion of all non-transmitting UHF testing, the immediate next steps of the COMMs subsystem is to complete all S-band non-transmitting testing. The most important of these tests being the S-band maximum bandwidth testing. This test concludes the amount of

bandwidth required by the S-band transmitter at different data rates. The results from this test allow the CANVAS team to accurately state the bandwidth required for the S-band radio in the radio licensing process. Once all Non-transmitting testing is complete, the next step of the COMMs subsystem is acquiring radio licensing for both the UHF and S-band radios. The radio licensing procedure will be conducted as an amateur station under the rules of FCC part 5. The current goal is to complete all licensing procedures by the end of the winter break and apply for the license at the beginning of the spring semester. Upon completion of the radio licensing process, the COMMs subsystem will be in a state of limbo with only the UHF antenna tuning test left to be completed, after the completion of this test, no more COMMs subsystem testing can be performed until the radio license has been obtained. Once the radio license has been obtained, all transmitting tests can be completed. This includes UHF and S-band functional transmitting and receiving testing. Upon completion of these tests, the radios can be integrated into the flatsat configuration and full chain system testing can be done. Table Comm-7 below shows the COMMs subsystem upcoming schedule.

Table COMM-7: UHF Testing Schedule

Names	Description	Start	End	Status
S-Band Non-transmitting tests	S-band configuration, Power, Spectrum Testing	12/13/21	TBD	In Progress
S-Band Max Bandwidth test	Maximum S-band bandwidth required for different transmission rates	12/15/21	TBD	In progress
CANVAS Radio licensing procedure	Process for obtaining radio licensing	12/18/21	TBD-(1/9/22)	Not started
UHF Antenna tuning test	Match the UHF impedance, tune the antenna for max radiation, determine inductance value	1/15/22	TBD	Not started
UHF functional Receive/Transmit test	Using the LASP ground station to ensure the UHF's ability to functionally transmit and receive commands over the air	3/15/22	3/18/22	Not started
S-Band functional Transmit test	Using the LASP ground station to ensure the S-Bands ability to functionally transmit to the ground station over the air	3/15/22	3/18/22	Not started
Flatsat full chain testing	Ensure the radios can interface with the CDH and can each respectively transmit and/or receive data over the air.	3/21/22	3/25/22	Not started

7.4. Attitude Determination and Control Subsystem

7.4.1. ADCS OVERVIEW

The attitude determination and control subsystem (ADCS) will employ the Blue Canyon Technologies (BCT) XACT-15 COTS package, which has heritage on LASP's MinXSS CubeSat. The XACT-15 contains three reaction wheels, three orthogonal torque rods, a coarse sun sensor, star tracker, internal magnetometer, and an inertial measurement unit (IMU). The CANVAS-specific XACT-15 flight-unit has been delivered, and an Interface Control Document (ICD) Addendum and Configuration document has been included. This ICD defines the spacecraft coordinate frames, inertias, appendages, and other information. This is located on Dr. Marshall's export controlled server, so a request for access will be needed.

The ADCS subsystem is responsible for maintaining 3-axis stabilization of the CANVAS CubeSat, maneuvering the spacecraft to the different pointing modes, and other requirements as outlined in the RVM. Testing on the CANVAS ADCS subsystem began in the Spring 2021 semester using the CANVAS flight unit and a Real-time Dynamics Processor (RDP), then was updated in the Fall 2021 semester to accommodate design changes such as swapping the spacecraft axes of the UHF and S-band antennas, as well as the spacecraft undergoing significant changes to its mass and inertias. The RDP receives commands from Ball Aerospace's COSMOS interface software, which then provides real-time sensor stimulus to the flight-unit. Ball Aerospace's COSMOS displays telemetry from the XACT-15, which we also can extract and import to MATLAB to verify the requirements.

7.4.2. ADCS KEY DRIVING REQUIREMENTS

The key driving requirements for the CANVAS ADCS are shown below in Table ADCS-1.

Table ADCS-1: Key Driving Requirements

KDR	Requirement	Description
KDR 1	ADC-2.1	The subsystem shall be capable of desaturating the reaction wheels
KDR 2	ADC-5.1	The subsystem shall be capable of controlling attitude from a maximum tip-off rate of 5 deg/sec/axis
KDR 3	ADC-5.2	The subsystem shall be able to point the solar arrays within ± 15 deg of the sun vector during normal operations
KDR 4	ADC-5.3	The subsystem shall have a magnetic field pointing accuracy during eclipse equal to ± 10 degrees (TBR)
KDR 5	ADC-5.4	The subsystem shall have a pointing accuracy during downlink equal to ±10 (TBR) degrees
KDR 6	ADC-5.5	The subsystem shall be capable of applying a minimum slew rate of 0.45 (TBR) deg/sec that is required to maintain ground station pointing at an altitude of 500 km

7.4.2. ADCS STATUS

This semester was primarily dedicated to re-verifying the CANVAS KDRs that were initially verified back in the Spring 2021 semester. During the summer, mechanical design changes were made which resulted in the UHF antenna moving from the spacecraft -Y face to the -X face, as well as moving the S-band antenna from the spacecraft -X face to the -Y face. The overall spacecraft mass and inertia tensors also changed significantly from design changes throughout the last 6 months or so. All of these alterations directly affected the simulations run by the ADCS team last spring because a few of the pointing command constraints (both primary and secondary) utilized the axes featuring these mentioned antennas, and all testing scripts require a defined spacecraft inertia to accurate model CANVAS' attitude dynamics.

The COSMOS software runs scripts written in Ruby to send commands to the UUT/RDP test setup, where the UUT (unit under test) refers to the CANVAS XACT-15 flight-unit. This semester, testing scripts were updated and run to re-verify the KDRs in Table ADCS-1 and other performance requirements of the ADCS. These scripts contain the general simulation setup commands as well as the commands for maneuvers to the different attitude pointing modes. The changes made to the testing script commands in the Fall 2021 semester include using the "SET_SAT_INERTIA" command to set the inertia tensor to that matching the current CAD assembly, changing the primary constraint for the spacecraft axis pointing at LASP during downlink, changing the secondary constraint during B-field pointing so the GPS antenna has improved visibility of the constellation in MEO, and updating the required torques to tip-off from the Nanoracks dispenser at the desired angular rates. The method for timing the various maneuvers was defined based on the CANVAS STK simulation. The CANVAS ADCS Testing Procedures and Results document [1] describes this testing procedure, the implemented changes, and the results in great detail.

In summary, all CANVAS KDRs were re-verified, although KDR 2 may require a later revision depending on the final launch service provider. Furthermore, a power analysis and maneuver duration characterization are discussed in this report. Document [2] and [3] shows how to implement the test setup and extract the data for analysis.

The command structure in Ruby for the COSMOS software is only applicable for this test setup. These commands were therefore also translated into FSW in the ADCS Software Commands and Telemetry document [4]. This document also contains our recommended telemetry to be passed from the XACT-15 to CDH via FSW. Further FSW development as it pertains to ADCS is discussed in the next section.

7.4.3. ADCS MOVING FORWARD

Table ADCS-2 defines a few action items that are currently ongoing, a few that shall be completed prior to integration, and a multitude of post-integration flight unit tests. It should be noted that these ongoing processes will not necessarily have an exact completion date, and that FSW is completely dependent on the work being done at LASP.

Table ADCS-2: Action Items

Action Item	Timeline	Description
FSW	Ongoing	Develop process for communicating between FSW and the XACT including commands, structure definitions, telemetry/packet definitions, and minimum required telemetry and housekeeping.

Mission Design	Ongoing	Continue to run simulations to obtain more data on maneuver times and variances to increase confidence in these statistics.
CDH Interfacing	January 2022	Test interface and communication between XACT and CDH subsystem.
Flight unit testing	January 2022	CSS Diodes test to make sure they can track light vector.
Flight unit testing	Post-integration	Air Bearing test
Flight unit testing	Post-integration	Sun Sensor Phasing test and Polarity test
Flight unit testing	Post-integration	Torque Rod Phasing test and Polarity test
Flight unit testing	Post-integration	Reaction Wheel Polarity test
Flight unit testing	Post-integration	Star Tracker Communication test and Polarity test
Flight unit testing	Post-integration	Noise Verification
Flight unit testing	Post-integration	IMU Rates test and Polarity test
Flight unit testing	Post-integration	CSS Operation test and Polarity test
Flight unit testing	Post-integration	Magnetometer Bias test and Polarity test
Flight unit testing	Post-integration	GPS Capability test

The post-integration flight unit testing in Table ADCS-2 was compiled with input from Rick Kohnert at LASP and from section 14 of the XACT User Guide (document [8]). BCT strongly recommends that these post-integration tests are completed to ensure the defined software parameters match the as-built CANVAS spacecraft. These tests will help catch any integration-level problems before launch. Detailed procedures on how to complete these tests can be found in section 14 of the XACT Users Guide (document [8], pages 83 - 89.).

Table ADCS-3 contains important documentation for ADCS. The documentation that was created internally contains links to their location on Google Drive.

Table ADCS-3: Reference Documents

Document	Title	Author(s)

Number		
1	CANVAS ADCS Testing Procedures and Results [1]	Conner Neilsen, Dillon Waxman, Nathan Sunnarborg, and Andrew Sabovik
2	UUT/RDP/COSMOS Installation and Setup Guide [2]	Conner Neilsen and Dillon Waxman
3	COSMOS Telemetry Extraction Guide [3]	Conner Neilsen and Dillon Waxman
4	ADCS Software Commands and Telemetry [4]	Lea Chandler, Ryan Stewart, Conner Neilsen, and Dillon Waxman
5	Real-time Dynamics Processor (RDP) Users Guide (Rev: D)	Blue Canyon Technologies
6	XACT Gen3 Interface Control Document (Rev: C)	Blue Canyon Technologies
7	GN&C Users Guide	Blue Canyon Technologies
8	XACT Users Guide (Rev: E)	Blue Canyon Technologies

7.5. Flight Software Subsystem

7.5.1 FSW OVERVIEW

Flight Software is the "intelligence" that efficiently directs onboard operations, orchestrates the functionality of flight hardware to perform specific tasks, and protects against anomalies. The flight software subsystem is composed of the embedded code running on the CDH and EPS computers. The embedded software on the CDH is being developed by the Laboratory for Atmospheric and Space Physics (LASP) flight software group and will be built on the Common Code framework.

In general, the CDH code is responsible for managing the spacecraft modes and subsystems, executing commands from the ground, and handling downlinking data. The EPS code is responsible for peak power tracking, determining the State of Charge (SOC) of the batteries, and collecting EPS telemetry. Since the EPS code is being developed in house and will be treated by the CDH as a peripheral subsystem, its architecture and functionality will not be described here, but can be referenced in the EPS section of this document.

7.5.2 FSW REQUIREMENTS

The key driving requirements for flight software are shown in Table FSW-1. These requirements were selected because they manage mission-critical systems, functionality, and tasks. The complete current list of flight software requirements can be found here.

Table FSW-1. FSW Key Driving Requirements.

Req.	Description
FSW-5	The software shall autonomously manage a set of spacecraft modes defined by ConOps
FSW-8	The software shall be capable of packaging payload data, timing, and the spacecraft state for storage.
FSW-10	The software shall be capable of routing payload data, telemetry, and H&S to the COMMs subsystem for downlink.
FSW-11	The software shall control the deployment of all satellite extensions.
FSW-12	The software shall monitor and provide power cycling of mission-critical subsystems.

7.5.3 FSW ARCHITECTURE DEFINITION

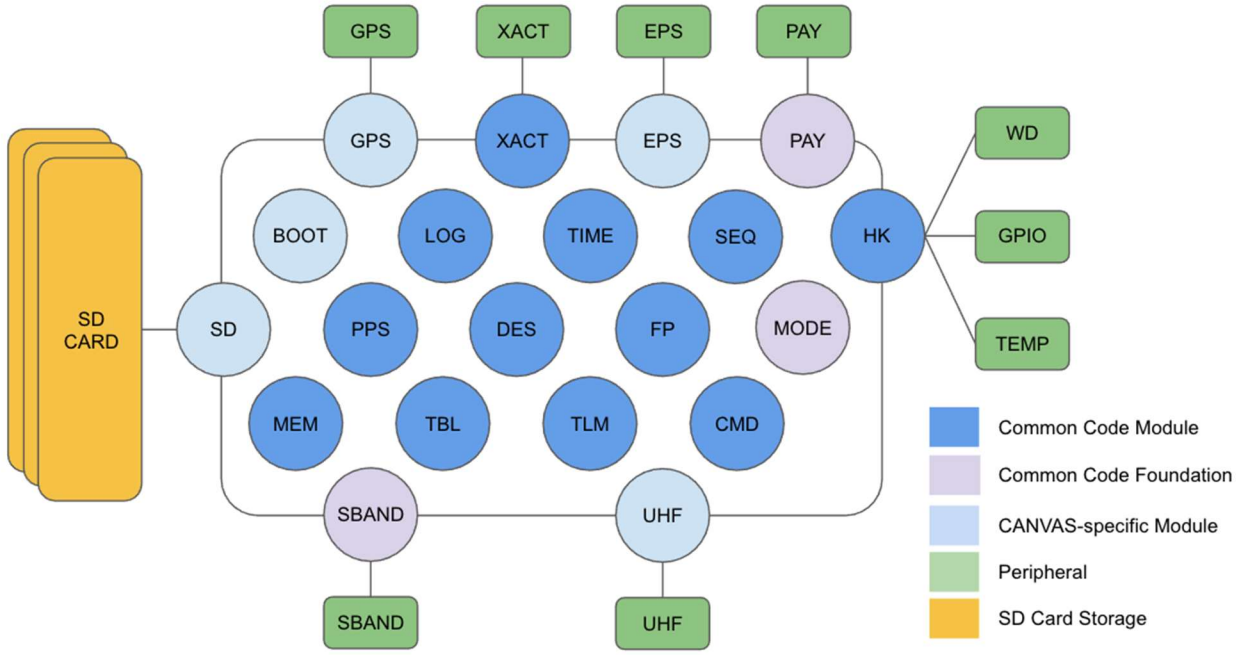

Figure FSW-1. System Architecture

Common Code is a modular framework developed by LASP to provide basic FSW tasks for CubeSat and Small Sat missions. It has been implemented across a number of different CubeSat missions, including CTIM, CIRBE, and INSPIRESAT. The system provides support for command and telemetry handling, event logging, memory management, telemetry monitoring, stored command sequencing, and task scheduling. Different modules for these core functions can be seen in Figure FSW-1 in dark blue. Some modules have heritage in Common Code, but require significant adaptation to CANVAS-specific subsystems and components. These appear in light purple above and include the s-band, payload, and mode manager modules. Finally the light blue modules are entirely CANVAS-specific, requiring the most development and longest lead time. These include the UHF, EPS, SD card storage, and GPS modules. The peripheral components, in green, connect to their respective modules in the diagram, showing the software to hardware interface. Some key aspects of the system include:

- **Deterministic Executive Scheduler.** A key distinction between Common Code and other typical FSW systems is that the Real-Time Operating System (RTOS) is replaced with a Deterministic Executive Scheduler (DES). The DES main loop, seen in Figure FSW-2, executes in one second, which is split up into 200, 5 ms slots and governed by a timing

Figure FSW-2. Current CANVAS Deterministic Executive Scheduler (DES) Main Loop

Slot	Task	Slot	Task	Slot	Task	Slot	Task	Slot	Task	Slot	Task	Slot	Task	Slot	Task	Slot	Task	Slot	Task
0	HK	20	ADCS	40		60		80	ADCS	100		120		140	ADCS	160	ADCS	180	
1		21	ADCS	41		61		81	ADCS	101		121		141	ADCS	161	ADCS	181	
2	MEM	22	ADCS	42		62		82	ADCS	102		122		142	ADCS	162	ADCS	182	
3	LOG	23		43		63		83		103		123		143		163		183	
4	UHF_HK	24		44		64		84		104		124		144		164		184	
5		25		45		65		85		105		125		145		165		185	
6	TLM_DBG	26		46	TLM_DBG	66		86	TLM_DBG	106		126	TLM_DBG	146		166	TLM_DBG	186	
7	TLM_UHF	27		47	TLM_UHF	67		87	TLM_UHF	107		127	TLM_UHF	147		167	TLM_UHF	187	
8	TLM_SBAND	28		48	TLM_SBAND	68		88	TLM_SBAND	108		128	TLM_SBAND	148		168	TLM_SBAND	188	
9		29		49		69		89		109		129		149		169		189	
10		30		50		70		90		110		130		150		170		190	
11		31		51		71		91		111		131		151		171		191	
12		32		52		72		92		112		132		152		172		192	
13	CMD_DBG	33		53	CMD_DBG	73		93	CMD_DBG	113		133	CMD_DBG	153		173	CMD_DBG	193	
14	CMD_UHF	34		54	CMD_UHF	74		94	CMD_UHF	114		134	CMD_UHF	154		174	CMD_UHF	194	
15		35		55		75		95		115		135		155		175		195	
16	SBAND_HK	36		56		76		96		116		136		156		176		196	
17	SBAND_HK	37		57		77		97		117		137		157		177		197	
18	SBAND_HK	38		58		78		98		118		138		158		178		198	
19	SBAND_HK	39		59		79		99		119		139		159		179		199	

interrupt to guarantee each slot is given exactly 5 ms to execute. Tasks are assigned to one or more slots and are a collection of Common Code and CANVAS-specific tasks.

- **SD Card Storage and Voting.** CANVAS's on-board storage is composed of three SD cards for redundancy against single-event effects. Carrying three cards enables not only triplicate data storage, but a voting system for science data as added protection against bit flips. The voting system functions by comparing packets at the bit level and, in the event of a discrepancy, selects the best 2 of 3 for downlink. This approach was implemented due to the risk of an SEU causing a bit flip in an SD card controller, which would cause a significant storage anomaly, such as exchanging rows or columns in tabular data. This is a concern because the SD cards are not radiation hardened. The SD cards store command sequences, tables, telemetry monitoring thresholds, and science data.
- **Mode Manager.** CANVAS modes, defined by ConOps, are managed by calling stored command sequences in response to ground commands or autonomous responses to telemetry monitoring. Beyond the three primary mission modes, listed in Table FSW-2, the mode manager will control switching into comms pointing for s-band downlink during ground station passes, as well as the "canting" mode to reduce heat gain during the rare multi-day periods with no eclipses. The Mode Manager is able to switch into and out of most modes both autonomously and as the result of a ground command.

The Command and Telemetry Handling Task and Mode Manager Module verify FSW-5, 8 and 10 from Table FSW-1. The Initialization Task, which calls the command sequence at system reset to manage initial deployments, verifies FSW-11, but needs to be modified for CANVAS's specific deployables. The Fault Protection module, which checks telemetry item values against programmable thresholds and calls preloaded sequences in response, verifies FSW-12 (and 12.1). Since we do not have NAND Flash Memory, we will not use the NAND Flash Bad Block Memory Management module and instead LASP will develop an SD card interface for the cards already procured. The payload interface module will undergo significant revision to interact with the payload electronics. This process is expected to occur late in the spring 2021 term, as the FPGA code and instrument suite come online.

Table FSW-2. CANVAS Modes

Mode	Description
Phoenix	• Initial mode after startup • UHF and CDH on • Enter autonomously from any mode based on battery SOC • Bare minimum power • Beacon packet transmitted
Safe	• ADCS turned on; Coarse Sun Point • Enter autonomously from Phoenix on good SOC or command • Beacon packet transmitted • Limited command set
Nominal	• All subsystems on as needed, ADCS Fine Point • Enter only via ground command • All commands and telemetry packets available

7.5.4 FSW PACKET STRUCTURE

Both science data and spacecraft telemetry are structured into packets for downlink. This structure helps the ground station understand what is being downlinked and increases the robustness of the downlink process. Packets include a checksum to protect against lost or corrupted data during downlink.

7.5.4.1 S-Band

S-band data packet structure can be seen in Figure FSW-3. The packet "page" size will be 512 or 1024 bytes (still TBD). Packets are placed in VCDUs (Virtual Channel Data Units), fixed-length 2048-byte frames that contain some non-integer number of CCSDS packets, where empty fractions of frames get packed with a fill packet. VCDUs help the radio stay locked on the downlink, add robustness to the downlinked data, and reduce drops. They also have a VCID that distinguishes between playback and real-time data. The format adds a 14-byte overhead to each VCDU.

7.5.4.2 UHF

The UHF is not as far along in development, with some decisions needing to be made regarding both commanding and downlink. More information about the state of UHF development can be found in the Comms section.

UHF downlink format is required to follow the AX.25 protocol for amateur band communications and will consist of framed CCSDS data packets. At present, the protocols for commanding and packet structure itself are under development.

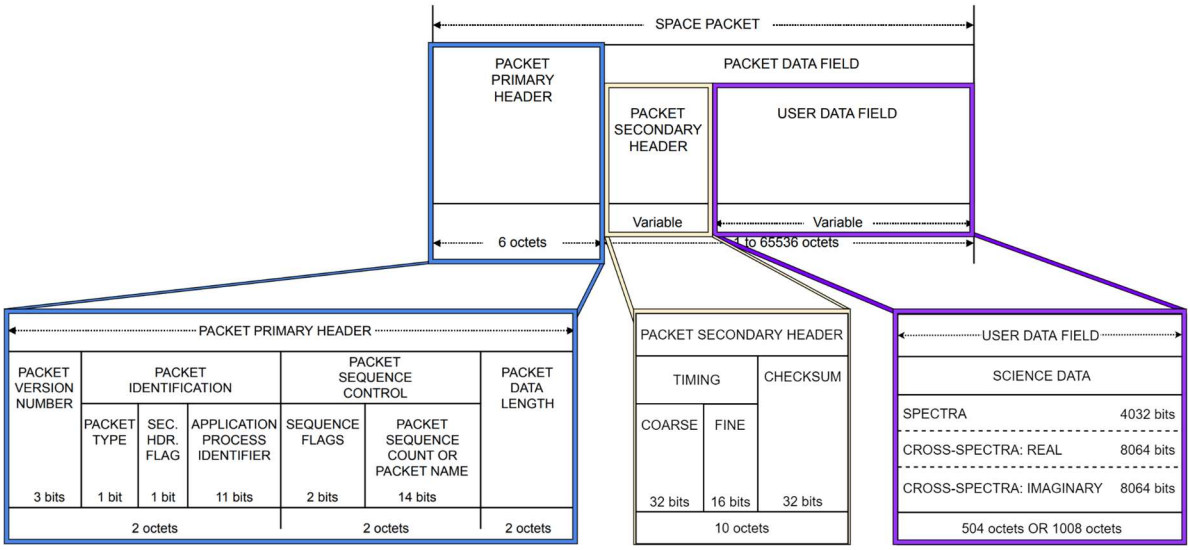

Figure FSW-3. S-Band Data Packet Structure

7.5.5 FSW STATUS

7.5.5.1 Background

At the start of the Spring 2021 semester, CANVAS was without a dedicated flight software lead and the decision was made at mid-semester to transition the existing MAXWELL architecture to a Common Code framework – and to transition the code development from the CANVAS team to the LASP Flight Software group. As peripheral components and various CANVAS subsystems come online, the LASP FSW team interfaces and integrates those components into their code base to ensure interoperability and functionality. This work has been taking place throughout the Fall 2021 semester.

7.5.5.2 Flat Sat Test Setup

At the conclusion of the Fall 2021 semester, the CANVAS and LASP teams were prepared to move forward with setting up the Flat Sat engineering and test model. Currently, the Flat Sat is being set up at the LASP lab space in LSTB 101, but eventually will be moved to a dedicated CubeSat assembly space in the ARL building, which is currently under construction.

Figure FSW-4 shows the conceptual setup for software image testing. A development machine interfaces with the PIC controller on the CDH board via the Hydra language. Hydra is a command and telemetry system that enables image testing in a way consistent with the eventual operations procedures. **Telemetry packets** are sent from the software running on the PIC processor to the development machine, where Hydra decomposes the packet into individual items. Then **command packets** are formatted by Hydra before being sent to the PIC, where they are easily understood by the flight software and processed.

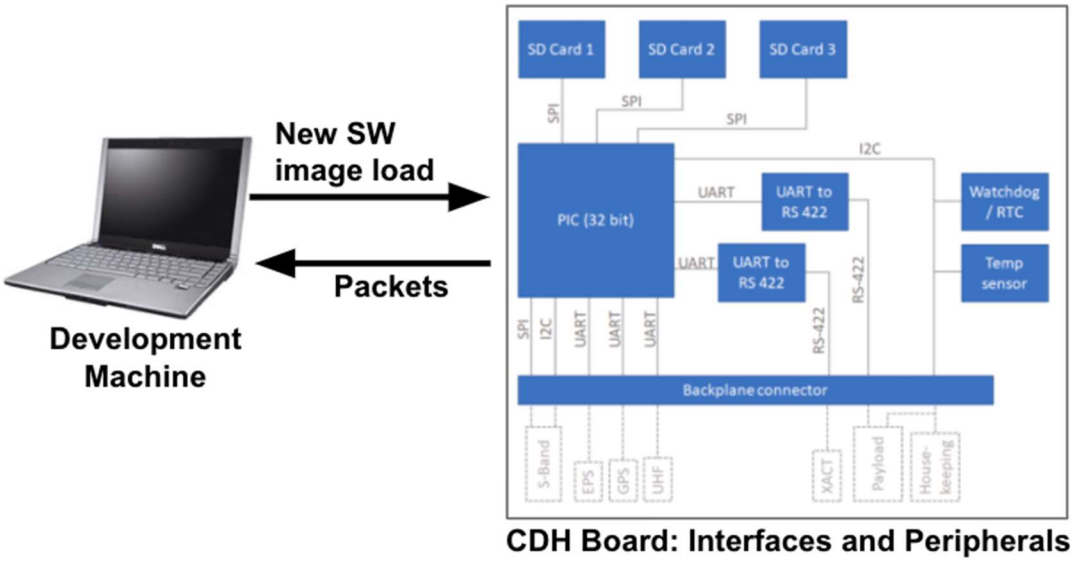

Figure FSW-4. Image testing diagram

7.5.5.3 Spring 2022 Test Plan

A high-level test plan for FSW and adjacent subsystems has been developed and planned for implementation in the spring and summer. Since module and component testing has been occurring throughout the development process, this test plan focuses on comprehensive functional testing, many of which will necessarily occur after integration but before environmental testing. The FSW test plan can be found here.

7.5.6 FSW NEXT STEPS

Software design often follows a design, implement, and test development flow, and this flight software is no different. Design work for the CDH software is still necessary to specify the data downlink and command uplink packet contents, select the housekeeping data for the real-time and full housekeeping packets, and to define the SD card store and fetch operations for all packet types. The latter task is occurring with LASP.

With ongoing module/component testing underway, only a handful of peripherals still need to be interfaced. The greatest upcoming development challenges will involve the remaining CANVAS-specific modules with little Common Code heritage: SD cards, GPS, and instrument payload. The anticipated FSW delivery schedule for the spring 2022 semester can be seen in Figure FSW-5. These three components have long lead times and dependencies associated with the development of the actual subsystems, including personnel availability. The implementation of this timeline is expected to serve as a tool for organizing work across both the CANVAS and LASP teams, with an expected final delivery of the FSW system by mid-April.

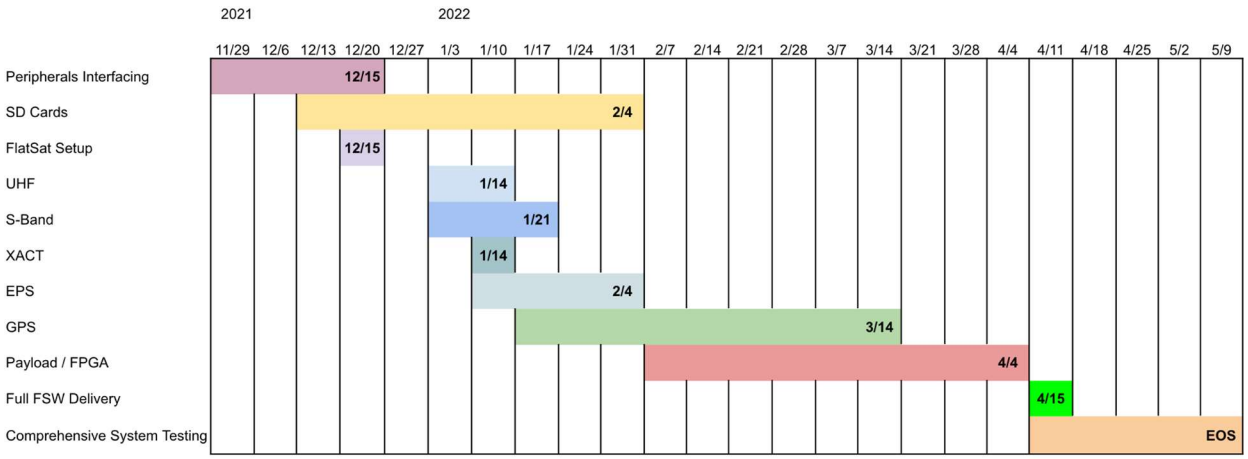

Figure FSW-5. FSW Delivery Schedule Gantt Chart

7.6. Structure Subsystem

7.6.1. STRUCTURES OVERVIEW

The structures subsystem's major responsibilities this fall included final component design changes, component manufacturing, and where applicable, component testing. During the fall, design changes have been made to the bus panels, stoppers/standoffs, battery enclosure, UHF antenna housing, and fasteners. Manufacturing consisted of machining the flight UHF housing and flight bus panels. Already machined components include the E-field crown, battery enclosure, and E-field housings. No physical fatigue or deployment testing was done this fall in addition to what was completed during the Spring 2021 semester and over the Summer, although SolidWorks was used to update the CG/mass analysis.

7.6.2. STRUCTURES KEY REQUIREMENTS

The driving requirements for the CANVAS structural work completed during the semester are shown below in Table STR-1.

Table STR-1. STR and THR Key Driving Requirements

Req.	Description
STR-1	CANVAS shall conform to a 1x4U (4U) configuration.
STR-2	CANVAS shall not exceed 6.0 kg in mass.
STR-4	The subsystem shall have rails that adhere to NRCSD requirements.
STR-7	CANVAS deployable systems shall have independent restraint mechanisms that do not rely on the NRCSD.
STR-17	The subsystem shall use threaded fasteners, where fasteners are needed, with 2 methods of back-out protection for joining components and assemblies.
STR-3	The subsystem shall be designed to withstand the launch and on-orbit environments of without failure, leaking fluids, or releasing anything (NanoRacks load requirements detailed below in the 'Analyses' section)

The structural subsystem requirements were derived from the NanoRacks requirements provided by the NanoRacks ICD document for a 4U CubeSat structure.

7.6.3. STRUCTURE STATUS

Overview: The structures subsystem is currently finishing manufacturing and beginning

preparations for integration. Having completed the final UHF Housing and bus panel redesigns, only manufacturing of flight solar panel hinges, E-field housings, L-shaped heat sink, and body mounted solar panel bumpers remains before structures is ready to integrate. The coming sections will briefly summarize design, manufacturing, and testing updates on a component level.

Mass budget

Table STR-2 shows the most recently updated mass budget as of PIR design changes. We have a total of 1026 grams to spare and stay within the requirement.

Table STR-2: Mass Budget

Component	Total Mass of component, including buffer (g)
Structure	1865.43
Comms	268.97
ADCS	929.75
EPS	687.47
CDH	107
Electronics (Wires, etc)	146.44
Payload	967.96
Total	4973.02
Total Mass Allowed	6000.00
Mass remaining	1026.98
Mass remaining %	17%
Goal Margin %	10%

Hinge design: The hinge design was considered completed as of Spring 2021, but to simplify integration, the decision was made to shift from a screw-and-nut attachment method to a threaded hole in the hinge.

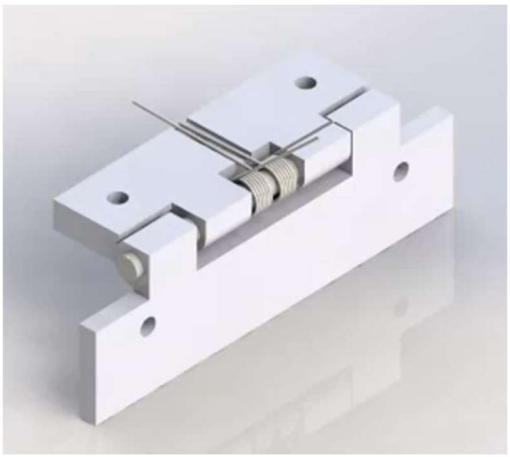

Figure STR-1: CAD Model of the Hinge Design

The design makes use of two torsional screws, a threaded hinge pin, through holes for solar panel mounting and threaded holes for bus panels.

This design successfully passes the fit check, hinge deployment test, fatigue test, and solar panel deployment test.

Status: As of the end of Fall 2021, the design is considered flight ready and five flight assemblies are in progress at the aerospace machine shop.

Bus Panels: The four bus panels underwent moderate changes throughout the course of the last semester. They are discussed individually below.

The top (+Y) bus panel underwent the following changes: number of battery assembly fasteners was reduced from 4 to 3, a mounting point was added in the rail for an RBF switch and corresponding trigger screw, bus panel mounting holes were increased to accommodate larger screws, and two additional mounting holes were added for the body-mounted solar panel.

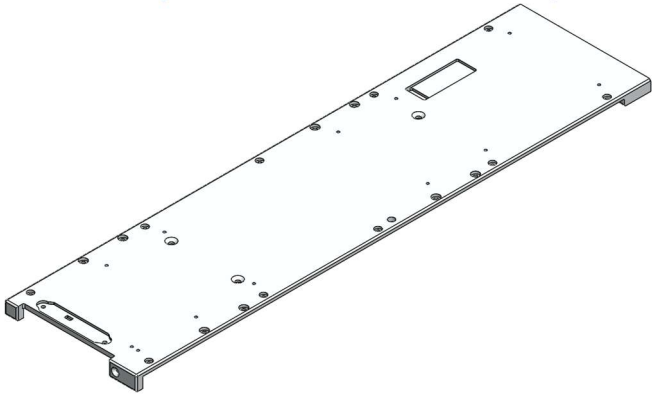

Figure STR-3: +Y Bus Panel

The bottom (-Y) bus panel has not undergone any major changes since Summer 2021, but the UHF carrier board mounting holes were slightly repositioned.

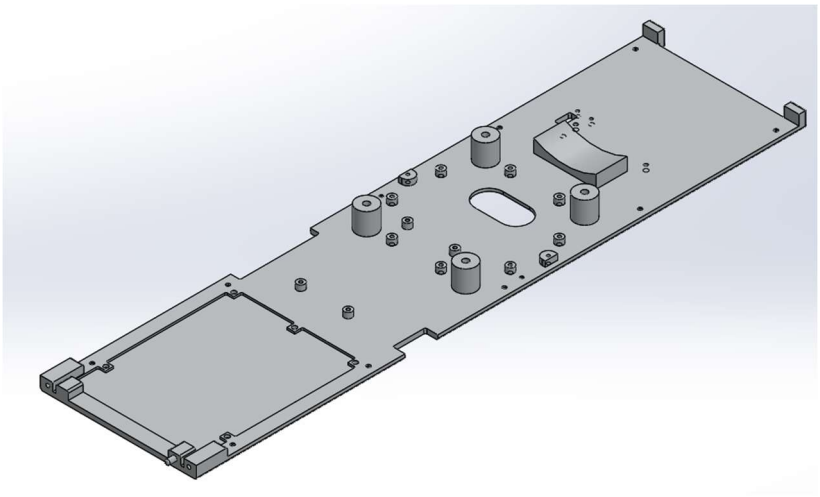

Figure STR-4: -Y Bus Panel

The +X bus panel underwent minor changes since Summer 2021, including adding a cutout for the Boom box to fit, and adjusting the locations of the S-band mounting holes to ease integration.

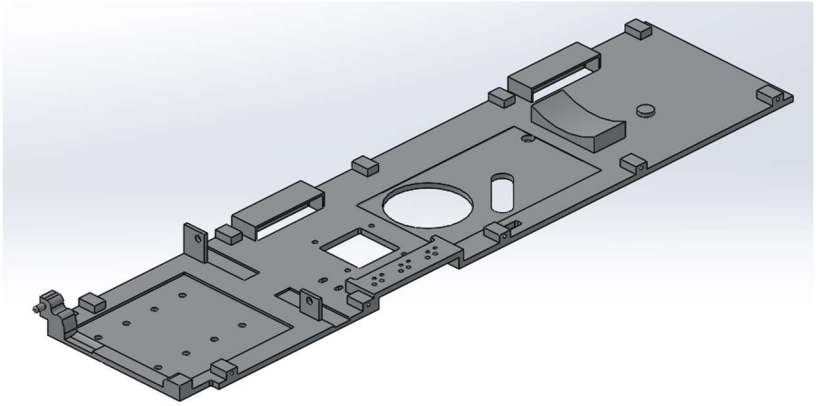

Figure STR-5: +X Bus Panel

The +X bus panel underwent larger changes, with a cutout being added for the UHF housing, and S-band mounting holes being adjusted.

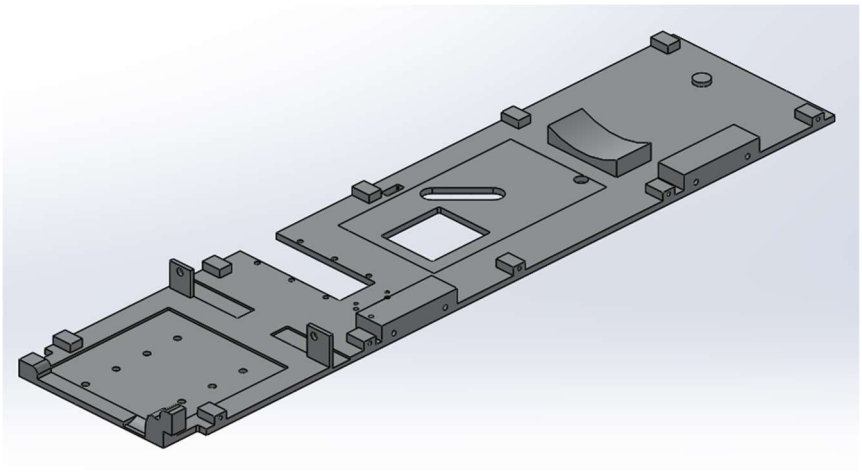

Figure STR-6: -X Bus Panel

Status: The bus panel designs were finally finalized this semester, and were ordered from RapidCut. They have been delivered, gone through a preliminary cleaning, and been fit checked with other flight hardware. As a result, we found that all components fit perfectly except one, which should be easily fixed next semester.

Standoffs: No changes to the E-field antenna bumpers on the +/-X panel and -Y panel. The design of the body-mounted solar panel bumpers was updated to include a guide for the E-field antenna and be mounted using the same mounting holes as the solar panel itself.

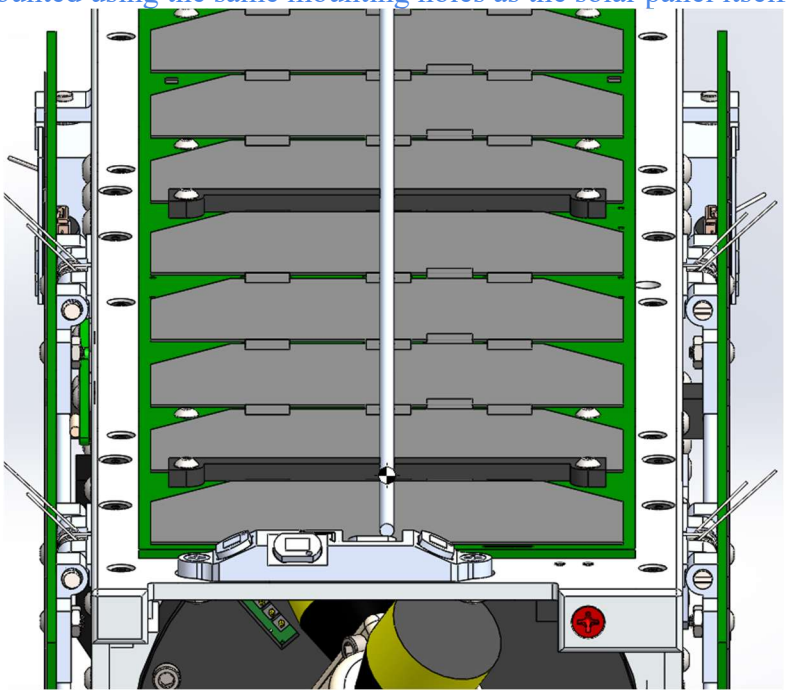

Figure STR-6: Body-Mounted Solar Panel Bumpers

Status: E-field standoffs were machined and are on hand. Body-mounted solar panel bumper design is finalized and currently being machined by the aerospace machine shop.

Deployment Mechanisms: One of the new additions to the CAD assembly back in the Spring 2021 semester were deployment mechanisms. These consist of burn wire routing, fastener placement for securing the wires, and resistor placement on PCBs for severing the wire when current is passed to it. These mechanisms are required for all the deployable components onboard CANVAS.

The two deployable solar panels are tied down through the use of channeling and a fastener on the bottom of the -Y bus panel. This is seen in Figure STR-7, where the wire is wrapped and tied around the resistor on the PCB and fed through the slot and channel to a threaded fastener. This design has been slightly modified during Summer 2021, mostly shifting its location along the z-axis and also changing the threaded fastener hole from a through hole to a counterbore hole.

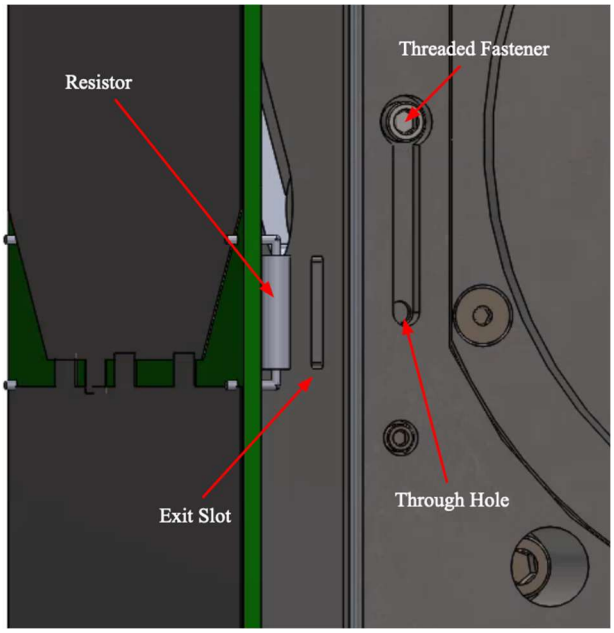

Figure STR-7: Deployable Solar Panel Mechanism

Burn wires are also needed to secure the top and bottom E-field antennas in the stowed position. For the top antenna laying on the body mounted solar panel, a resistor is placed on one side of the panel PCB, in between two through holes. The burn wire is wrapped around the resistor and through these holes, then tied. The loose end is fed over the antenna, pulled tight, then wrapped around a threaded fastener and secured. This is drawn out in Figure STR-8. The E-field antenna on the bottom bus panel is planning to use a replica of the UHF antenna PCB to hold the resistor. Figure STR-9 shows the location for this PCB that features three screw holes. The burn wire would wrap around one of them, then around the resistor, over the antenna, and wrap around another screw that sinks into the bus panel itself. The design for the E-field antenna on the -Y bus panel was finalized during Summer 2021, as fasteners and washers were added and the location was nailed down.

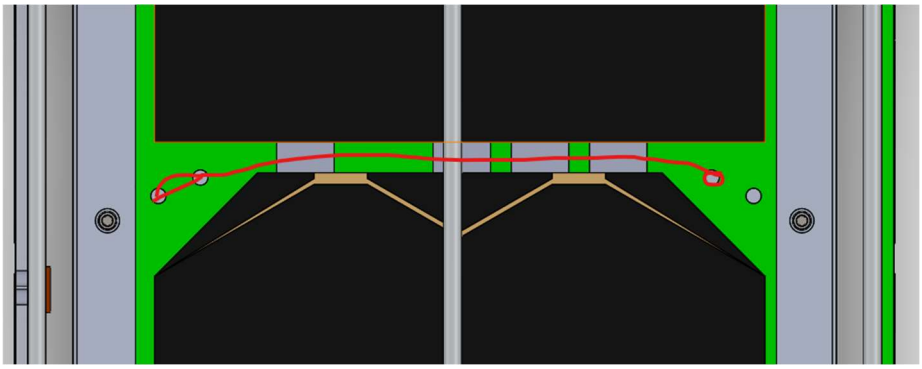

Figure STR-8: E-field Antenna Burn Wire Plan on Body Mounted Solar Panel

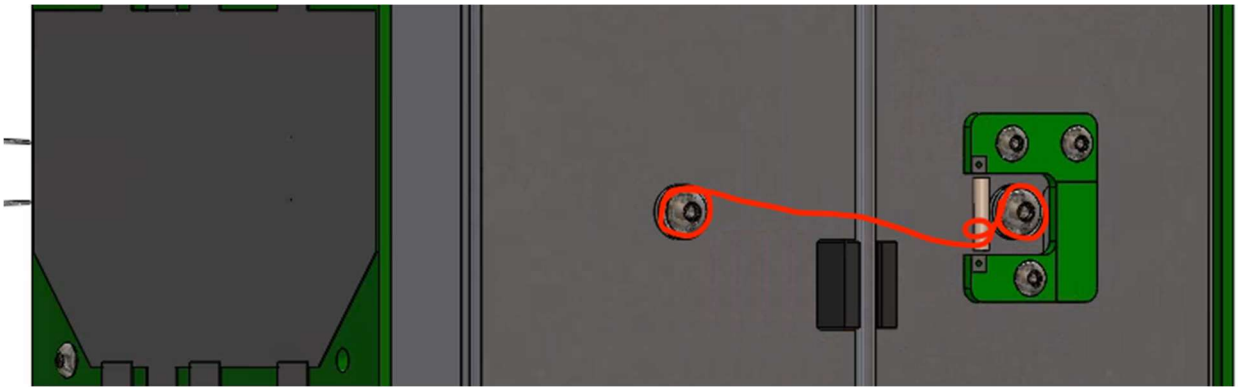

Figure STR-9: E-field Antenna Burn Wire Plan on -Y Bus Panel

The burn wire routing and deployment mechanism for the UHF antenna has not changed this summer, as the plan is still to take advantage of the component's flight heritage.

Status: All required fasteners for the deployment mechanisms were added to the CAD assembly during Summer 2021. As of August 17, 2021, it is believed that no further CAD work needs to be done regarding these designs.

Fasteners: All fastener selections have been finalized and procured. All component interfaces are tracked through the Master Assembly Matrix, while the corresponding fastener types and quantities are tracked through the Fasteners spreadsheet. However, please reference the assembly plan for most accurate information.

Status: As of the end of Fall 2021, all fasteners have been selected, purchased, and organized in the BASIL Lab.

Documentation: As it relates to structures, the assembly document is the critical reference document from this semester. This document has the step-by-step plan for assembling the CubeSat. The current document lays out a sequence of assembly with images and tables with specified fasteners and cables. It also includes systematic labeling for all parts, including fasteners and tools. For past work on structural analysis, see Nathan's document from the end of the Summer.

Table STR-3: Reference Documents

Document No.	Title	Author(s)
1	Assembly Plan	Andy Starr, Andrew Sabovik
2	Structural Analysis	Nathan Sunnarborg

Analyses

Table STR-4 presents the results for the four SolidWorks analyses used for preliminary checks of the NanoRacks launch load requirements. Each of the four analyses were simulated with the full-detail spacecraft assembly, with the exception of fasteners and other mechanical hardware. At this point in time, the results of the simulations cannot be used for requirement verification, this will come after spacecraft integration and physical testing in the Spring 2022 semester. The static load analysis, acceleration analysis, and vibration analysis underwent significant changes from the Summer, to account for a 1320N load instead of a 1200N load, and to look at the effect of new bus panel geometry on dynamic loads of greater concern.

Table STR-4: Structural Analysis Results

Analysis	Critical Results Value	Requirement Value	Comments
1320N Load	7.05 N/m^2	2.55e8 N/m^2	Factor of safety 3.62 - Not a concern
Acceleration Loads	2.79e7 N/m^2	2.55e8 N/m^2	Factor of safety 9.14 - Not a concern
Random Vibration	2.22e7 N/m^2	2.55e8 N/m^2	Factor of safety 11.5 - Not a concern
Natural Frequency	1,163 Hz	10-35 Hz	Factor of safety 33 - Not a concern

Table STR-4 presents results for the structural analyses. First, we need to ensure that the CubeSat is able to withstand 1320 N load on the rails in the Z-axis. The criteria is a 2.0 factor of safety compared to the yield strength of the material - 6061-T6 aluminum in this case. The yield strength of this material is 255 MPa, or 2.55e8 N/m^2. The maximum stress seen in this simulation is 7.05e7 N/m^2 which is a factor of 3.62. Hence the criteria is currently fulfilled, but not yet verified/validated.

The second row of Table STR-4 shows the results for the acceleration load requirement (NRCSD 4.3.1). We need to ensure that the CubeSat is able to withstand at least a 4g load in the Y and Z axes and a 7g load in the X-axis. NanoRacks section 4.3.1 presents the g loads our CubeSat needs to withstand. The criteria is a 2.0 factor of safety compared to the yield strength of the material - 6061-T6 aluminum in this case. The yield strength of this material is 255 MPa, or 2.55e8 N/m^2. The maximum stress seen in this simulation is 2.79e7 N/m^2 which is a factor of safety of 9.14. Hence the criteria is fulfilled, but not yet verified/validated.

The third row of Table STR-4 shows the results for the random vibration requirement (NRCSD 4.3.2-1). We need to ensure that the CubeSat is able to withstand random vibration during flight. NanoRacks Section 4.3.2 presents the mounting inputs for the CubeSat. We ran this analysis on a soft-mount input because the document specifies that spacecraft within the dispenser are subjected to a soft-mount environment. The criteria is a 2.0 factor of safety compared to the yield strength of the material - 6061-T6 aluminum. The yield strength of this material is 255 MPa, or 2.55e8 N/m^2. The maximum stress seen in this simulation is 2.22e7 N/m^2 which is a factor of safety of 11.5. Hence the criteria is currently fulfilled, but not yet verified/validated.

Finally, the last row of Table STR-4 shows the results for the natural frequency analysis which is not a strong requirement but is important to check if the natural frequency resonates with the launch vehicle frequency. If the determined frequency of the modes matches the expected 10-35 Hz of the launch vehicle, the spacecraft is likely to experience mechanical failure. After running the simulation, the first and lowest mode has a frequency of 1,163 Hz. This is 33 times higher than the upper bound of the launch frequency range, leading to the assumption that the criteria is fulfilled, but not yet verified/validated.

As an important note, it should be noted that these factors of safety are likely conservative, as SolidWorks is not a very high-fidelity structural analysis program, and many localized high stresses are likely a result of ill-conditioned meshes.

7.6.4. STRUCTURES PATH TO PER

As we move forward to the Pre-Environmental phase, a lot of tasks need to be completed. Table STR-5 summarizes the tasks for the structures team moving forward throughout the Spring 2022 semester.

Table STR-5: Structures Path Forward to PIR

	Name	Description	Duration (days)	Estimated Completion Date	Required Step to PER?
Manufacture	Anodize bus panels	6061-T6 aluminum (anodized)	10	02/15	**YES**
	L-shaped heat sink	6061-T6 aluminum	42	01/24	**YES**
	5x hinge assembles	6061-T6 aluminum	42	01/24	**YES**
	BMSP Bumpers	Delrin	42	01/24	**YES**
Test	UHF antenna	Deployment w/ burn wire and electronics	2	02/15	**YES**
	Hinges	Deployment w/ burn wire and	2	02/15	**YES**

		electronics			

7.7. Thermal Subsystem

7.7.1. THERMAL OVERVIEW

The CANVAS thermal subsystem protects the spacecraft, science instruments, and internal hardware from the harsh and unforgiving thermal environments of space. It functions to ensure that each component within the spacecraft remains within its allowable temperature limits throughout all phases of the mission. The spacecraft will use both passive and active thermal control elements to maintain components within their operational temperatures. Figure THR-1 presents the thermal subsystem block diagram, which illustrates, at a high level, how this subsystem works to protect the spacecraft. The satellite's passive control elements include thermally protective and radiative surface coatings, certain component thermal isolation, a hot to cold bus structure design, and optimized conductive heat paths. The active protection elements include battery heaters, which are helpful for the batteries' sensitive temperature limits. Overall, the thermal subsystem is essential to the success and survival of the CANVAS mission because it ensures that all subsystems can withstand extreme temperature ranges, electronic and environmental heat fluxes, and temperature gradients during the mission.

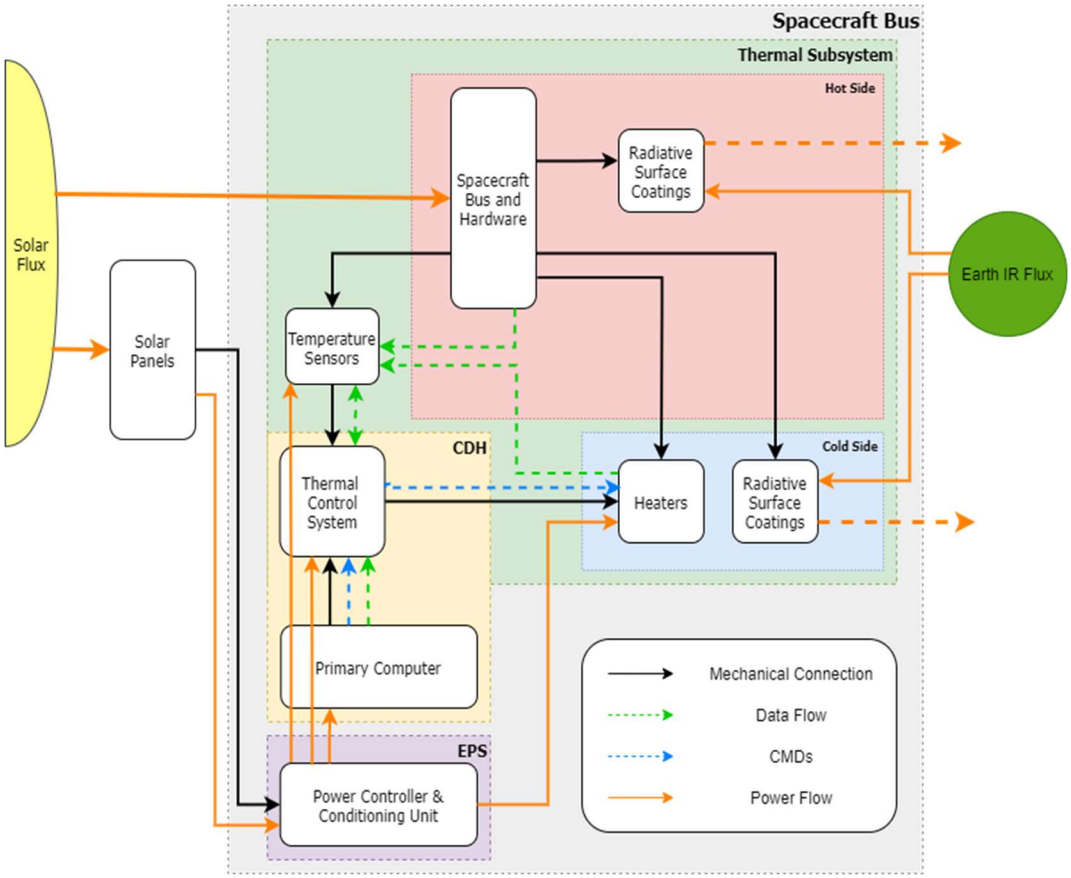

Figure THR-1: Thermal Subsystem Block Diagram

7.7.2. THERMAL KEY REQUIREMENTS

The purpose of the thermal subsystem is to maintain the spacecraft and its components within their allowable temperature ranges throughout the entire mission. The key driving requirements of the thermal subsystem are presented in Table THR-1. The first two requirements are similar; they state that the thermal subsystem shall maintain all components within their temperature limits during nominal operations and during survival mode. These requirements will be verified through Thermal Desktop simulations and TVAC testing. The third requirement is that the thermal subsystem shall be controlled by the CDH. This requirement includes monitoring temperatures and controlling heaters to maintain temperature ranges, and it will be verified through component testing.

Table THR-1. THR Key Driving Requirements

KDR	Description	Reasoning	Verification
THR-1	The subsystem shall maintain all components	Due to the harsh temperature environments of space, the	Simulation and TVAC

	within operational temperature limits during Normal Operations Mode.	spacecraft must withstand large temperature ranges to operate successfully.	testing.
THR-2	The subsystem shall maintain all components within survivable temperature limits for mission duration.	Due to the harsh temperature environments of space, the TCS must maintain all spacecraft components within their allowable temperature ranges.	Simulation and TVAC testing.
THR-3	The subsystem shall be controlled by the CDH.	CDH is needed to control and maintain (heaters) spacecraft temperatures as measured by the TCS.	Testing.

7.7.3. THERMAL STATUS

Thermal Model and Analysis Status

The CANVAS thermal model contains the spacecraft's current geometry, materials, radiative optical properties, component heat loads for each mission mode, and worst-case orbital scenarios. At the beginning of the semester, the initial plan was to update the existing thermal model; however, a new model was built due to major changes that took place after Spring 2020. The previous thermal model was helpful for predicting general on-orbit temperature ranges before the mature design of the spacecraft and orbital modes was updated. Rather than updating the existing model, a new one was developed to ensure that all changes were reflected and that any outdated information was not left accidentally in the model. CANVAS's current thermal model mesh is presented in Figure THR-2.

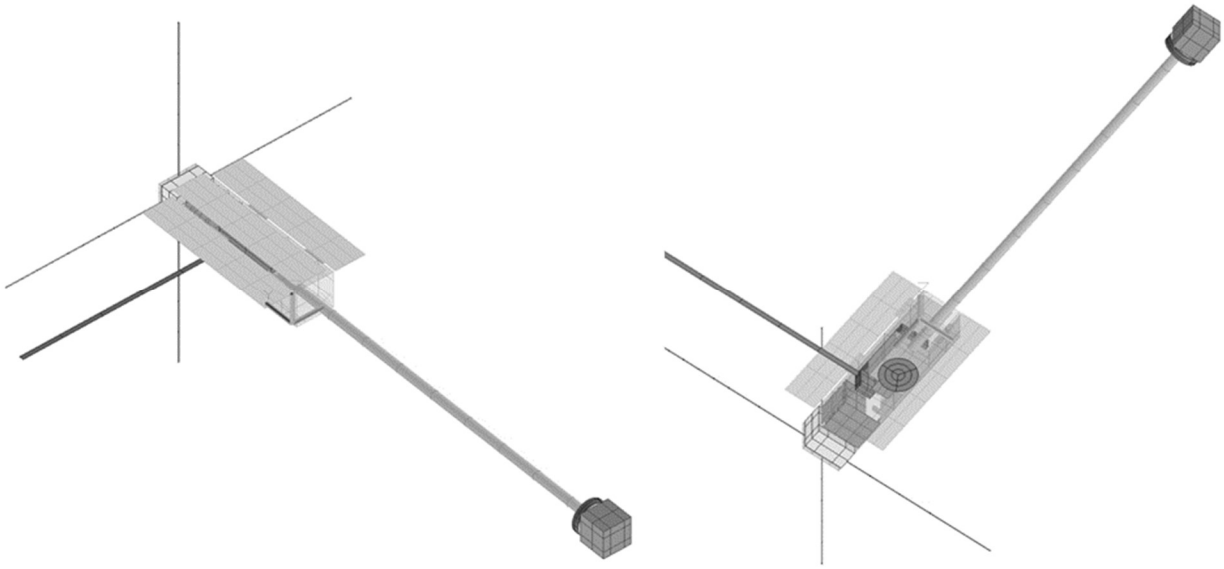

Figure THR-2: Thermal Model Finite Element Mesh

CANVAS's thermal analysis is also up to date, and the results indicate that all components will remain within their allowable temperature limits except for the batteries. Additional physical thermal testing is required to validate the batteries' and heaters' operation during the mission. Since the development of the previous thermal model, many updates have been made to the current one to reflect changes to all spacecraft subsystems. These changes include updated component heat loads based on the results from physical testing, updated worst-case hot and cold orbital scenarios based on refined mission analyses and STK models, an updated spacecraft component layout, and new conductions paths from the hot to cold side of the spacecraft.

The spacecraft's internal and external environments were modeled using applied component heat loads as well as external environmental heat fluxes from the Sun, Earth IR, and Albedo. The component heat dissipation values and environmental heat fluxes were derived from the mission ConOps and power budget per mission mode and are shown in Figure THR-3. Bounding, or worst-case, thermal scenarios were developed from these mission modes and analyzed using the thermal model. The worst-case hot scenario models the spacecraft in a fully-sunlit orbit with its solar panels and bus angled 52 degrees away from the sun during downlinking. The worst-case cold scenario models the spacecraft in a 63% sunlit orbit in Phoenix (lowest component power) mode. Overall, component heat dissipation and environmental heat fluxes during the mission are the main drivers of temperature change within the spacecraft; therefore, it is vital to accurately model and analyze each scenario to ensure all components remain within their thermal limits. A full and detailed description of the thermal model is provided in the CANVAS Thermal Analysis Results report.

Component Heat Loads		
Submodel	Worst-Case Hot (W)	Worst-Case Cold (W)
CDH Card	0.1	0.1
UHF Radio	0.89	0.28
Sband Radio	5.88	0
XACT	3.22	0
EPS Card	0.08	0.08
Efield Board	0.26	0
Bfield Board	0.03	0
Analog Card	3.96	0
Digital Card	0.72	0
GPS Receiver	1.22	0
Battery	0.46	0.46
TOTAL	16.82	0.92

Battery Heater Parameters	
Parameter	Value
Power (each)	1.04 W
On Temp	6 C
Off Temp	12 C

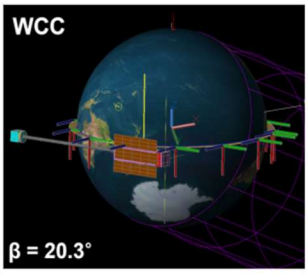

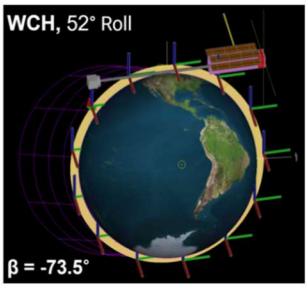

Orbital Parameters			
Parameter	Worst-Case Hot (W)	Worst-Case Cold (W)	Units
Solar Flux	1354		W/m^2
Albedo	0.35		
Inclination	51.6		degrees
Pressure	10e-07		
Altitude	600	500	km
Argument of Periapsis	30	35	degrees
RAAN	202	15.1	degrees
No. of Orbits	3	3	
Period	5801.23	5676.98	seconds
Start Date	01/06/21, 18:00 GMT	12/01/21, 00:00 GMT	date, time
Orbit Plane Beta Angle	-73.5	20.3	degrees
Spacecraft Beta Angle	38	90	degrees
% of Orbit in Eclipse	0%	37%	

Figure THR-3: Thermal Environments

The results from the worst-case hot and worst-case cold scenarios were combined and analyzed to provide two time-independent bounding temperature sets for the spacecraft. They show the maximum and minimum temperatures achieved between all scenarios. Figure THR-4 presents the minimum and maximum temperatures achieved on the spacecraft as well as the required heater power and duty cycle. As stated previously, all components remain within their temperature limits during the worst-case hot and cold mission modes except for the batteries.

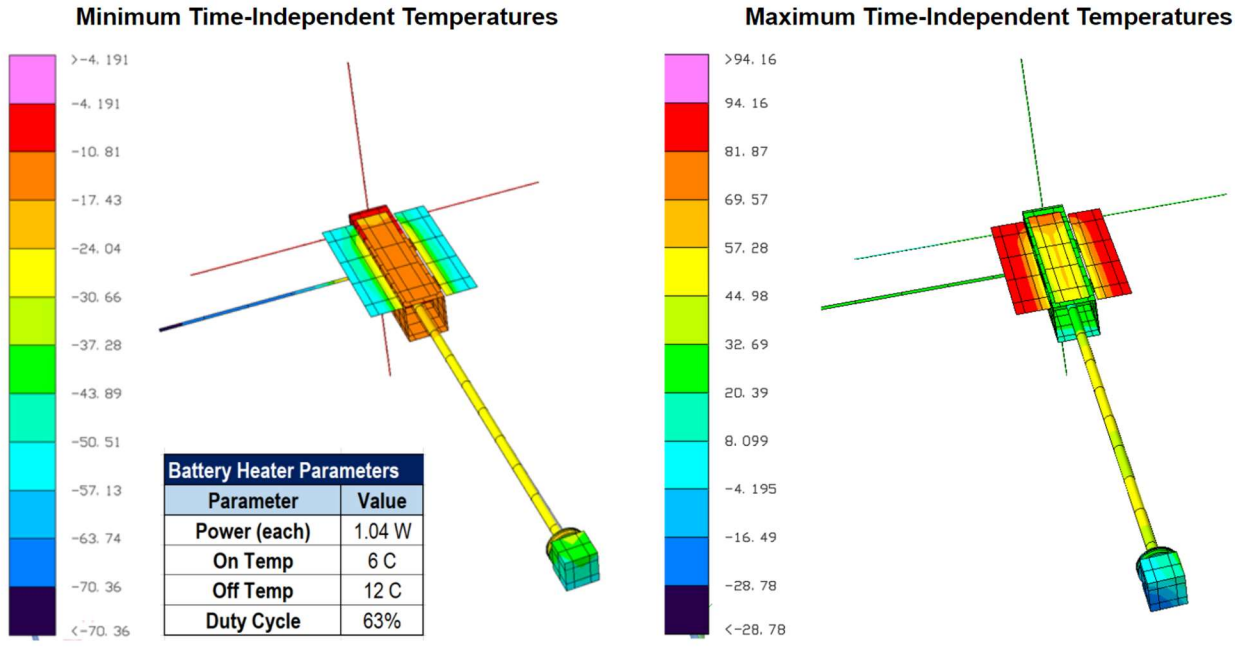

Figure THR-4: Thermal Analysis Results Temperature Maps

The batteries' allowable temperature range is from 0 C to 40 C. During the worst-case cold scenario, however, the batteries fail to reach their minimum allowable temperature. Figure THR-5 presents the minimum time-independent and transient temperature results of the batteries with heaters modeled. As shown, the top surface of the battery is within its thermal limits; however, the bottom surface reaches temperatures below 0 C because it is connected to the boom box, which is not actively heated and can radiate heat easily to space. This connection is vital to maintain the battery within temperature limits during the worst-case hot orbital scenario. While these temperature results are not ideal, these thermal issues may be mitigated through battery and heater tests in a thermal chamber.

The spacecraft's thermal model is useful for predicting general on-orbit temperatures; however, it is limited by its level of fidelity. The batteries are modeled as a solid meshed block with bulk thermophysical properties of lithium-ion batteries. The specific geometries and material properties of the individual battery cells are not modeled; therefore, physical testing is needed to determine if the batteries can operate in environments below their operational temperature limits with heaters. This testing procedure may be found in the Battery and Heater Worst-Case Cold Test document.

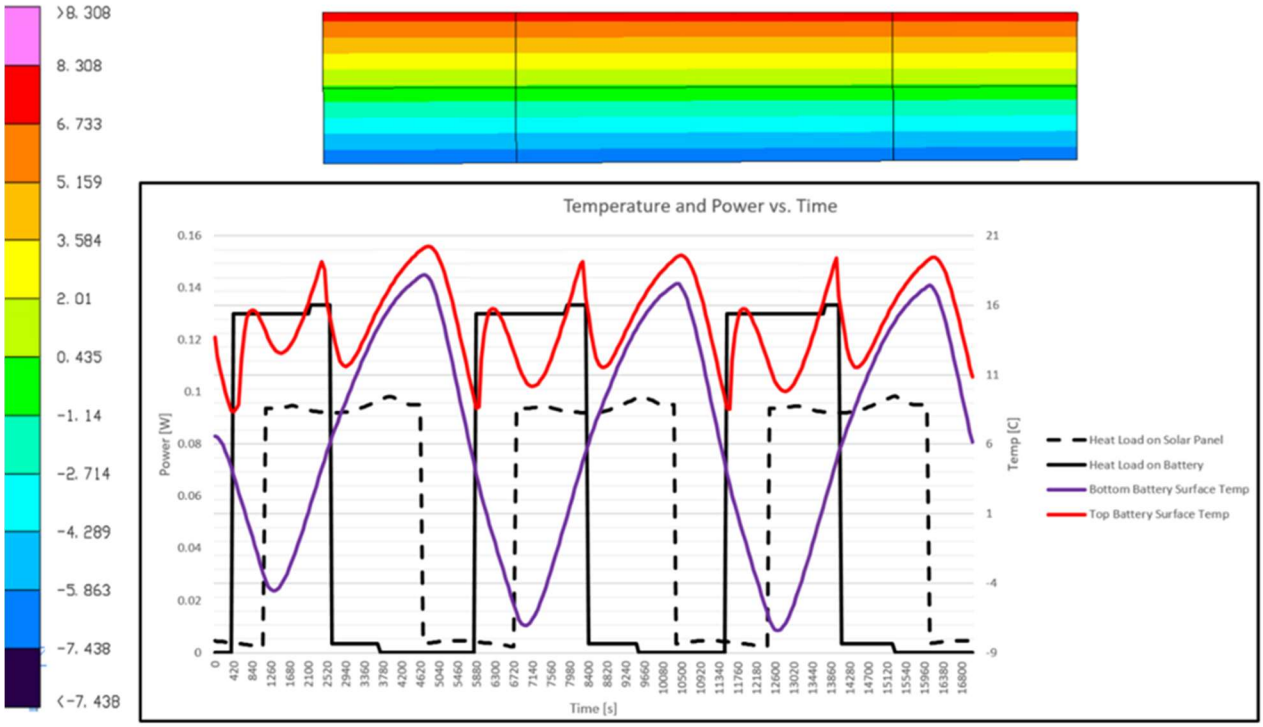

Figure THR-5: Battery Temperature Profile with Heaters

Lastly, the final thermal model margined temperature results are presented in Table THR-2. Based on NASA's thermal margin standards for flight electronics, a 5 C temperature margin was applied to all results. Overall, the results of this thermal analysis provide insight into the temperatures that may be seen on orbit. Thermal testing must be performed in addition to the

results of this thermal analysis to validate component operation.

Updated Model Temperature Results with Margin				
Label	**Submodel**	**Min (C)**	**Max (C)**	**Allowable Range (C)**
1	BATTERY_BOARD	3	34	-30 to 70
2	BATTERY_BOX	-13	32	-250 to 250
3	**BATTERY_LI**	**-12**	34	**0 to 40**
4	BFIELD_PREAMP_BOARD	-38	2	-40 to 85
5	BFIELD_PREAMP_HOLDER	-54	36	-250 to 250
6	BFIELD_SEARCH_COILS	-62	29	-250 to 250
7	BOOM	-38	51	-250 to 250
8	BOOM_BOX	-13	31	-250 to 250
9	BUS	-20	37	-250 to 250
10	CROWN	-11	36	-250 to 250
11	EFIELD_ANTENNAS	-14	35	-250 to 250
12	EFIELD_PREAMP_BOARD	-11	37	-25 to 85
13	GPS	-17	33	-45 to 85
14	GPS_REC	-15	44	-40 to 85
15	HEAT_SINK	-15	44	-250 to 250
16	KOOHLER_RAILS_NEG_X	-17	33	-250 to 250
17	KOOHLER_RAILS_POS_X	-16	36	-250 to 250
18	SBAND_ANTENNA	-15	32	-250 to 250
19	SBAND_BACKPLANE	-16	43	-30 to 70
20	CARD_1_RADIO	-16	45	-25 to 85
21	CARD_2_SDB	-16	44	-25 to 85
22	CARD_3_ANALOG	-16	64	-25 to 85
23	CARD_4_DIGITAL	-16	45	-25 to 85
24	CARD_5_CDH	-15	37	-25 to 85
25	CARD_6_EPS	-15	36	-30 to 70
26	SBAND_RADIO	-15	47	-25 to 61
27	SP_BODY	-23	89	-75 to 100

28	SP_HINGES_NEG_X	-22	35	-250 to 250
29	SP_HINGES_POS_X	-21	37	-250 to 250
30	SP_NEG_X	-63	99	-75 to 100
31	SP_POS_X	-62	96	-75 to 100
32	UHF_BOARD	-15	32	-250 to 250
33	UHF_BOOM	-76	37	-250 to 250
34	UHF_HOUSING	-19	32	-250 to 250
35	UHF_RADIO	-14	34	-30 to 70
36	XACT	-11	36	-20 to 60

Table THR-2: Thermal Model Results Summary

Manufacturing Status

All thermal subsystem components except for the silver-coated teflon tape have been received, and some of these components have been tested. Table THR-3 presents a summary of the manufacturing status. The silver-coated teflon tape is delayed due to the initial possibility of using Kapton tape instead, which CANVAS already has, budget concerns, and the possibility of buying the tape from LASP next semester. Additional thermal analyses indicated that the Kapton tape causes the satellite to overheat in its worst-case hot orbital scenario because its solar absorptivity is four times greater than the absorptivity of the silver-coated teflon tape. Conversations have been started with LASP engineers about buying the silver-teflon tape from them during Spring 2022.

Component Name	Model	Specifications	Image	Status
Resistive Thermal Detectors (RTD)	Littelfuse PPG102A6	-50°C ~ 500°C ±0.15°C		Procured, tested
Battery Heaters	BK3522-55-L24-E03	3.8W Peak		Procured, tested
Silver-Teflon Tape	G427450-146656	5 mil, e = 0.81, a = 0.08		Need to order

Thermal Gap Filler 1mm	926-A18213-04-ND	k = 10 W/m^2K, 229x299x1mm		Procured
Thermal Gap Filler 3mm	926-A18213-12-ND	k = 10 W/m^2K, 229x299x3mm		Procured

Table THR-3: Thermal Manufacturing Status

Testing and Integration Status

None of the thermal subsystem components have been integrated yet. The two main thermal-related integration components are the battery box assembly and the battery box to boom box connection. These components are shown in Figure THR-6. The battery box subassembly has yet to be integrated because the battery PCB has not been manufactured yet. All other components have been gathered. The battery box to boom box connection cannot occur until the battery box subassembly is complete. This integration step is likely to occur at the end of the satellite's assembly. Lastly, the thermistors will be integrated into the components they are on during assembly of each's component.

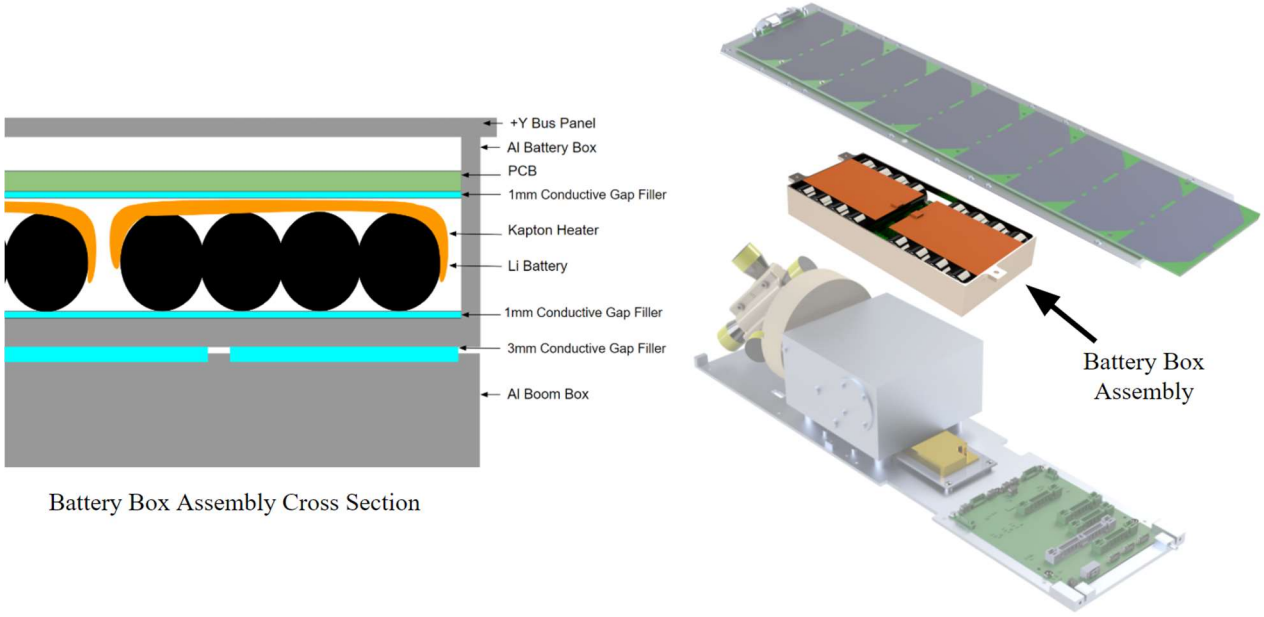

Figure THR-6: Battery Box Assembly Integration

In order to verify the thermal KDRs used to make the mission successful, various tests must be completed for components and assemblies. The thermal subsystem testing status is shown in Table THR-4. The Kapton heaters have been tested to validate successful operation during their nominal operation mode. The heater specification sheet states that they should consume 3.8 W each, and testing proved that they use 3.76W with a constant temperature between 93F and 102F throughout the pads. This test indicates that the heater performs nominally. Additionally, the thermistors were also tested using the battery temperatures. To

characterize the thermistor, a linear model was developed to translate voltages to temperatures. Overall, measurement errors were quantified and found to be within the EPS team's margin of safety, which proves successful operation of the thermistors.

Four tests are planned to occur next semester, which include the battery and heater operational test, component and subassembly bakeouts, full system bakeout, and full system TVAC test. To understand whether the batteries and heaters can operate in an environment where surrounding temperatures are below the minimum allowable battery temperature, a thermal test plan was created. Passing this stressing-scenario test should be sufficient to prove that the batteries can withstand the worst-case cold environmental temperatures during mission eclipse periods. This test must be completed before full system integration and TVAC testing to ensure the batteries will be operational during the spacecraft's worst-cold case. In terms of bakeout and TVAC test plans, some work has been started, but these plans will continue into next semester. Researching TVAC test procedures, conversations with LASP, and some planning for bakeout and TVAC have been started but are not complete due to the delays in the completion of the thermal analysis.

Test #	Description	Components Needed	Expected Date	Status
THR 1-1	Kapton Heater Power Test	EPS, CDH	10/7/2021	Complete
THR 2-1	Thermistor Test and Characterization	EPS, CDH	10/7/2021	Complete
THR 3-1	**Battery and Heater Operational Test**	**EPS, CDH, STR**	**2/15/2022**	**Planned**
THR 4-1.1	Component/Subassembly Bakeouts	EPS, CDH, STR, INSTR	4/1/2022	Planned
THR 4-1.2	Full System Bakeout	All	4/20/2022	Planned
THR 5-1	Full System TVAC	All	5/12/2022	Planned

Table THR-4: Thermal Testing Status

7.7.4. THERMAL NEXT STEPS AND PATH TO PER

As CANVAS moves forward to the Pre-Environmental Review and full system testing, various tasks are planned to be completed next semester. Table THR-5 summarizes the necessary tasks to be completed for the thermal subsystem. It is important to note that the battery and

heater operational test must be completed before full system integration and TVAC testing to ensure the battery will be operational during the worst-case cold orbital scenario.

	NAME	DESCRIPTION	DURATION	Estimated COMPLETION DATE
Manufacturing	Silver-Teflon Tape	Procure silver-teflon tape.	4 weeks	03/01/2022
Testing	Battery and Heater Operational Test	Plan and complete test.	1 week	02/20/2022
	Component/ Subassembly Bakeouts	Plan and complete tests.	4 weeks	03/30/2022
	Full System Bakeout	Plan and complete test.	4 weeks	04/30/2022
	Full System TVAC	Plan and complete test.	4 weeks	06/10/2022
Documentation	Battery and Heater Operational Test	Finalize test plans.	1 week	01/20/2022
	Component/Subassembly Bakeouts	Write test plans.	3 weeks	02/20/2022
	Full System Bakeout	Write test plans.	3 weeks	01/20/2022
	Full System TVAC	Write test plans.	3 weeks	03/20/2022

Table THR-5: Thermal Next Steps

8. Risk Analysis

This section includes a detailed view of the risks the CANVAS team has been tracking as development on the spacecraft continues, the hardware budget, and the project schedule as the team continues into the summer. Most of the systems engineering documentation is contained in the separate ConOps, Deployment & Commissioning Sequence, Spacecraft ICD, Payload ICD, Test Plan documents, as well as the living power budget, data budget, and link budget.

Below, Table Risk Analysis-1 describes our top identified risks. A prioritization score has been assigned to each risk, taking into account likelihood, consequence, and the earliest the risk is likely to occur. A higher score indicates more resources should be devoted to that particular risk in either development or mitigation strategies.

Figure Risk Analysis-1 below the table organizes our risks based on the assigned likelihood and consequence. The risk analysis table is a living document and should be continually reassessed during the semester to identify what the team should be focusing development on (i.e. it is unlikely the table will be the same by the end of next semester).

It should be noted that several new risks were added for the FA2021 semester. Namely, the team is now tracking the risk of the battery temperature exceeding the operational limits (RI 7), the risk of an ADC latch up as a result of a SEL (RI 11), the risk of an outdated ADCS control law due to the XACT MOI mismatch (RI 12), the risk of momentarily losing onboard time keeping due to the lack of timekeeping redundancy (RI 13), and the risk of lacking engineering design units (RI 20). Please see the CANVAS Risk Analysis (link below) for more detail on these risks and those retired this semester.

Please refer to the Risk Analysis Template and CANVAS Risk Analysis Document for more information on how we approached, analysed, and assessed the mission risks.

Table Risk Analysis-1: CANVAS Top Risks

Risk Index	Risk Type	Risk Description	Prioritization Score
1	Safety (Asset)	Solar panel deployment failure Given solar panel deployment, there is a possibility of a burn wire malfunction adversely impacting the solar panels, thereby leading to a failure in power generation.	12

2	Safety (Asset)	UHF antenna deployment failure Given current UHF antenna housing design, there is a possibility of the housing design adversely impacting the UHF antenna, thereby leading to a failure of our communication system.	24
3	Safety (Asset)	E-field antenna deployment failure Given E-Field antenna deployment, there is a possibility of a burn wire malfunction adversely impacting the E-Field antennas, thereby leading to a failure taking electrical field data.	12
4	Safety (Asset)	CTD Boom deployment failure Given the CTD boom, there is a possibility of an electrical or mechanical failure of the deployment mechanism, thereby leading to a failure taking magnetic field data.	17
5	Safety (Asset)	Solder and assembly quality when in house. Given in-house PCB assembly, there is a possibility of a component failing due to improper soldering adversely impacting the performance of the PCB, thereby leading to failure or poor performance of the board.	18
6	Safety (Asset)	Single Event Upset (SEU) Corruptions. Given that there is a lack of radiation tolerance on the board components, there is possibility of TID or a SEU adversely impacting a board or board component, thereby leading to component or total board failure	22
7	Safety (Asset)	Battery temperature exceeds operational limit (for WCH) Modeling in Thermal Desktop predicts the temperature of the batteries approaching their upper operational limit for the worst case hot scenario	20

8	Safety (Asset)	Given that CANVAS is in its orbit and the power generation of the analog board, there is a possibility of exceeding the acceptable operational temperature adversely impacting the analog board, thereby leading to partial or total failure of the board	17
9	Performance	E-field antennas malfunction Given the E-Field antennas lack of heritage, there is a possibility of a mechanical failure of the antennas adversely impacting the antenna, thereby leading to a failure to take electrical field data.	16
10	Performance	Magnetic search coils malfunction Given the magnetic search coils have low heritage, there is a possibility of an electrical or mechanical failure of the magnetic search coils, thereby leading to a failure to take proper magnetic field data.	16
11	Performance	ADC Latch Up as a result of SEU The ADC has a certain tendency to get latched up through to single event effects.	16
12	Performance	Outdated ADCS Control Law due to XACT MOI mismatch	22
13	Performance	Potential to momentarily lose onboard time keeping due to lack of redundancy	17

14	Performance	Power budget exceeded Given the fidelity of the power budget, there is a possibility of exceeding the power budget once in orbit adversely impacting the power capabilities of CANVAS, thereby leading failing to complete one or all of our mission objectives.	14
15	Performance	Data downlink capabilities exceeded Given the high data production rate of CANVAS, there is a possibility of CANVAS exceeding our ground station's data downlink capabilities adversely impacting the science data we can receive, thereby leading to a lower return of science data	23
16	Cost	Almost all funding has been allocated as of PIR Risk of exceeding budget if we need to rebuild/re-purchase anything costly. No budget for replacements	14
17	Schedule	Short path to flight and long lead time of components Given our development cycle and the nature of cubesats, there is a possibility of schedule creep adversely impacting CANVAS, thereby leading to not being able to perform the tasks at the end of the schedule (i.e. testing).	14
18	Schedule	Given that we are outsourcing FSW development to LASP, there is a possibility of not having the necessary flight software available adversely impacting the hardware testing schedule, thereby leading to a delay in the overall project schedule	23
19	Schedule	Given that there is a lack of availability of silicon components throughout the world, there is a possibility of not being able to procure a component adversely impacting the schedule to Pre-Integration Review, thereby leading to a	23

		delay in PIR	
20	Schedule	Lack of engineering design units (EDUs) Several flight components do not have engineering models. If one of the flight components were damaged during testing, the schedule and budget would be impacted severely.	18

Risk Map						
Likelihood	5	0	0	1	0	0
	4	0	0	0	0	0
	3	0	2	1	4	1
	2	0	0	1	7	1
	1	0	0	0	2	0
		1	2	3	4	5
		Consequence				

Figure Risk Analysis-1: CANVAS Risk Matrix

9. Hardware Budget

In Fall 2021, The Hardware Budget was overhauled so that all purchases to date are included. There was a discrepancy between purchases in the budget and what was accounted for in P-Card summary sheets. To account for this, the budget was updated with all expenditures included in the P-Card transactions, so that it shows a true representation of CANVAS's hardware budget. The biggest alteration made to the budget was for avionics boards and components. Separate sheets have been added to the financial budget to account for these procurements. An extensive effort would be required to separate the electrical components by board so for simplicity, components have been budgeted in a general avionics category. In addition to including missing purchases, the expected costs remaining have been updated to only include items that still have expenditures remaining. This is reflected in a "Closed Out" column

which will change the expected costs to the amount spent if "Yes" is typed. Instead of including contingency on a per item basis, the current budget has contingency removed to allow a better understanding of the total margin.

In addition to the changes to the sheet, major purchases were made. The summary is shown in the table below.

BGT-Table 1: Summary of purchases Fall 2021 semester

Items	Vendor	Cost	Dates purchased
Bus Panels	Rapid Cut	$1,860	11/4/2021
Fasteners	McMaster-Carr	$15.24	11/4/2021
Fasteners	McMaster-Carr	$86.99	11/16/2021
Thermal Pads	Sager/Mouser	$598.21	11/19/2021
Fastener Organizer	Home Depot	$14.80	11/28/2021
Total		**$2575.40**	

In the Spring semester there are some anticipated purchases that will be required for flight hardware and testing. Major anticipated purchases are summarized in the table below:

BGT-Table 2: Anticipated purchases Spring 2022 semester

Items	Expected Cost	Justification
Conformal Coating	$500	Rough Estimate
TVAC Testing	$780	2 Days of Chambers from LASP
Thermal Pads	$598.21	Already ordered Rev 0
Vibe Testing	$2400	Quote from David Malaspina 2019
Flight Components	$1000	Estimate from Sebastian
Flight Boards	$1527	Based on previously ordered boards
Flight GPS Receiver	$900	Estimated in previous semester
Total	**$7705.21**	

In order to finish development on the satellite the team will likely need to transfer some money from the CANVAS labor budget over to the hardware budget. The expected purchases included in Table Budget-2 exceed the hardware budget by $1,796.93. To correct for this negative margin, some of the labor budget may need to be transferred to hardware in order to

facilitate the completion of the satellite. According to the agreement with NSF, up to 15% of the labor budget can be transferred without a request for approval. However, this option should be used sparingly so that the majority of the remaining labor budget can be allocated for satellite operations.

10. Path to PER and Summary

As of Fall 2021 there are currently two forms of the CANVAS schedule. There is a Master Schedule on Google Drive so that the team has access to the current schedule and can collaborate as needed. Additionally, there is a Microsoft Project acting as the primary WBS to help identify the critical path and key tasks. In the Fall 2021 semester the team completed the PIR and began subsystem testing and integration. The Spring 2022 semester shall be focused on completing subsystem level testing and preparing the satellite for full integration, so that the PER can be presented by the end of April. If the team can stick to this schedule CANVAS should be prepared for launch by October 2022 with margin for extra testing if needed. Due to the complexity of inter-system dependencies the schedule is presented in the form of tables rather than a GANTT chart.

Due to the project being funded by the NSF, the project is slated to be funded by their standard 4-year policy. With a one year on-orbit mission, the spacecraft will need to be ready for launch by the end of 2021.

10.1 Subsystem Summary and Schedule

10.1.1 Structures

Throughout Summer 2021, the primary focus for the structures team was to entirely finish the CAD design of the spacecraft assembly and to manufacture as many flight-version components as possible. These goals were successfully completed as the SolidWorks assembly has all components modeled and placed, all fasteners are included, all components have defined materials and masses (if their flight versions have been weighed), and results have been updated for CG/mass analysis and structural analysis. As for manufacturing, flight versions of the solar panel hinges, battery enclosure, E-field crown, and E-field antenna housings have all been completed. Flight versions for both types of E-field stoppers/standoffs are currently in progress as of August 17, 2021.

In the Fall 2021 semester the structures team completed the design of all spacecraft components and manufactured the UHF housing and all 4 bus panels. Once manufacturing was completed the structures team weighed components and performed fit checks to verify the expected mass and structural interfaces. The only error found through fit checks was a discrepancy in mounting holes for one of the Kooler Rails. However, this flaw is easily mitigated as explained in the structures section of this document. Once the structural design was finalized, structures members began preparing assembly and integration plans. This work is expected to continue into the Spring 2022 semester as shown on Table SCH-1:

Task #	Description	Dependencies	Expected Completion
STR-33	Anodize bus panels	STR-27	2/15/2022
STR-34	L-shaped heat sink		1/24/2021

STR-35	5x hinge assembles		1/24/2021
STR-36	BMSP Bumpers		1/24/2021
STR-32	UHF antenna deployment test with housing, burn wire, electronics	STR-24, STR-28	1/20/2021
STR-30	Flight Hardware Fit Checks	EF-2, BF-4, SP-4, BP-6	2/12/2022
STR-29	UHF Storage Test	UHF-8	2/15/2022

Table SCH-1: Structures Schedule for Spring 2022

10.1.2 Thermal

In the Fall 2021 semester a new thermal model was developed in order to remove all outdated information in the previous model. This new model provided more accurate analysis that informed the team of potential issues the satellite may encounter. The largest potential fault discovered is overheating of the batteries during the worst case hot scenario. In order to mitigate this risk, the battery box was reconfigured and a new mode has been added that will tilt the satellite away from the sun in no eclipse orbits. In the Spring 2022 semester the thermal team will focus on battery temperature testing and preparing for environmental tests. A summary of expected tasks can be seen on Table SCH-2:

Task #	Description	Dependencies	Expected Completion
THR-4	Procure silver teflon tape and heat transfer tape		3/1/2022
THR-5	Battery and Heater Operational Test		2/20/2022
Doc-8	Write test plan for TVAC testing in the spring		2/14/2022

Table SCH-2: Thermal Schedule for Spring 2022

10.1.3 Instrumentation

In the Fall 2021 semester the instrumentation team made significant progress on component level testing and subsystem integration. The analog system performed full signal chain testing on the current revision of E-Field and B-Field Preamps in conjunction with the Analog Board. Initial results are promising and only slight adjustments are expected for the flight analog boards. The digital system had significant delays due to the FPGA code. It is expected that this code shall be provided in the month of December so that digital algorithm testing can be conducted at the beginning of the Spring 2022 semester. Barring significant failure, the Digital Board is at its flight revision and further development will only pertain to software. Additionally, the flight version of analog hardware is expected to be completed towards the beginning of the

Spring semester so that it can be tested before full spacecraft integration. A summary of instrumentation tasks can be seen on Table SCH-3:

Task #	Description	Dependencies	Expected Completion
E-Field			
EF-1	Remachine Brass and Delrin Pieces		1/17/2022
EF-2	Finish Antenna Assembly with Crown	EF-1	1/24/20222
EF-3	Manufacture/Populate Flight Preamp	EF-6	12/31/2022
EF-4	SFDR Testing	EF-3	1/10/20222
EF-5	Capacitance Test		1/26/20222
EF-7	Integration Fit Check	EF-2,EF-3	2/7/2022
EF-8	Antenna Deployment	EF-7, SP-5	2/2/2022
B-Field			
BF-1	B-Field Pre Amp Redesign		12/30/2021
BF-2	B-Field Pre Amp Manufacturing/Assembly	BF-1	1/10/2022
BF-3	B-Field Holder Modifications	BF-2	Completed
BF-4	B-Field Holder Reprint	BF-3	12/31/2021
BF-6	Test functionality of Boom deployment	Doc-6	3/15/2022
BF-7	Flight Signal Testing	BF-2, AB-3	1/14/2022
BF-8	Instrument Subassembly	BF-4, BF-7	3/20/2022
BF-9	Integration Fit Check	BF-4, STR-27	3/22/2022
Doc-6	CTD Boom Test Preparation		3/1/2022
Analog Board			
AB-1	Schematic Changes	FSW-2,EF-5,BF-5	12/19/2022
AB-2	PCB Layout	AB-1	12/20/2022
AB-3	Manufacturing/Assembly	AB-2	1/10/2022

AB-4	ADC Interface Test		12/15/2021
AB-5	Analog Signal Chain Testing	AB-3,EF-6, BF-7	1/21/2022
AB-7	Payload testing		12/4/2021
AB-8	CDH HK testing		12/15/2021
Digital Board			
DB-1	Memory test		11/21/2021
DB-3	CDH communication and HK testing	FSW-2	12/15/2021
DB-4	Algorithm Testing		2/11/2022
DB-5	Signal chain testing	DB-4	2/25/2022
DB-6	Finish FPGA Code	DB-4, DB-5	4/10/2022

Table SCH-3: Instrumentation Schedule for Spring 2022

10.1.4 CDH and Backplane

Over Summer 2021, initial revisions of the GSE and CDH were procured and populated. In Fall 2021 the boards were successfully brought up and hardware integrated with all avionics components. In December the team is hoping to complete initial flat sat integration and verify all software connections. Once these interfaces have been verified, development can begin on the flight version of the CDH and the GSE schematic can be transferred to the backplane layout. Almost all functionality of the backplane should be identical to the GSE, so this should also be a flight board once developed. Further CDH testing is mostly reliant on FSW, but all of the remaining hardware tasks can be seen on Table SCH-4:

Task #	Description	Dependencies	Expected Completion
CDH			
CDH-1	Design Rev 1	FSW-2	1/5/2022
CDH-2	Manufacture Rev 1	CDH-1	1/15/2022
CDH-3	Assemble Rev 1	CDH-2	1/20/2022
Backplane			

BP-3	Finalize Schematic	FSW-2	1/15/2022
BP-4	Layout PCB	BP-1,BP-2	1/31/2022
BP-5	Manufacturing, procurement and assembly	BP-4	2/10/2022
BP-6	Board bring up and initial testing	BP-5	2/12/2022

Table SCH-4: CDH & Backplane Schedule for Spring 2022

10.1.5 EPS

This semester the team tested the EPS board with the GSE board. The team also did a solar panel efficiency curve test and the plan is to procure the EPS next revision in mid May. Quite a lot of change was done in the solar panel design, especially finalizing the connector and resistor position. Most of next semester will focus on getting the solar panels manufactured and tested as well as getting the EPS board tested.

Sebastian is currently figuring out the number of hours and personnel at hand, but based on the recruitment event, at least 3 people were interested in working on electronics.

Over Summer 2021 procurement and population of the EPS Rev 1 was completed and software development was started. In Fall 2021 there was significant progress in EPS testing and software. This included bring up testing, battery characterization testing, component interfaces and the CDH-EPS FSW interface was constructed. Development has begun on the peak power tracking algorithm and this work shall continue into the Spring 2022 semester. Additionally, the solar panel design has been finalized and flight boards shall be procured and populated towards the beginning of the Spring semester. The EPS tasks, including EPS specific FSW can be seen on Table SCH-5:

Task #	Description	Dependencies	Expected Completion
Power Management Board			
EPS-1	Design Rev 2	FSW-2, EPS-7	1/28/2022
EPS-2	Manufacture Rev 2	EPS-1	2/4/2022
EPS-3	Assemble Rev 2	EPS-2	2/18/2022
EPS-4	Testing of Battery SOC estimation algorithm		2/15/2022
EPS-5	Development and Testing of PPT algorithm	SP-6	3/15/2022
EPS-6	Test EPS-CDH FSW Communication	FSW-6	11/10/2021
EPS-7	Reconfiguration of the watchdog astable circuit		1/1/2022
EPS-8	Fault Tolerance Testing		2/28/2022
EPS-9	Perform Nanoracks battery tests	EPS-4	3/1/2022

Solar Panels			
SP-3	Manufacture boards	SP-2	2/1/2022
SP-4	Mechanical test boards with hinges, burn wire tie-down, deploy	SP-4	12/30/2022
SP-5	Electrical test burn-wires	SP-4	2/2/2022
SP-6	Full assembly with solar cells	SP-5	2/14/2022

Table SCH-5: EPS Schedule for Spring 2022

10.1.6 ADCS

In Fall 2021, Nathan Sunnarborg was able to continue the testing on ADCS started by the team in the Spring. This primarily involved running simulations on the ADCS with an updated moment of inertia caused by structural changes since the Spring semester. A major concern with the ADCS moving forward is the discrepancy in MOI assigned to the XACT compared to the one programmed in the firmware. An update from Blue Canyon would cost $15,000, so other mitigation strategies such as adding ballast are recommended. Upcoming ADCS tests can be seen on Table SCH-6:

Task #	Description	Dependencies	Expected Completion
ADCS-3	Command, housekeeping & telemetry exchange	FSW-4	1/14/2021
ADCS-4	Diodes can track flashlight vector		1/31/2022

Table SCH-6: ADCS Schedule for Spring 2022

10.1.7 COMMs

In the Fall 2021 semester, there was extensive work performed to get the COMMs subsystem up to speed and unit tested for PIR. Unit testing has been completed for the UHF radio and similar tests are scheduled to be performed on the S-Band transmitter. After unit testing is complete, the major focus of the COMMs subsystem will be radio licensing and full transmission and receive testing. Licensing is required before non attenuated signals can be sent so this shall be a priority in the Spring 2022 semester as shown on Table SCH-7:

Task #	Description	Dependencies	Expected Completion
S-Band			
SB-1	Configure S-Band		12/15/2021
SB-2	Test for S-Band Power		12/16/2021
SB-3	S-Band Spectrum		12/17/2021
SB-4	S-Band max Bandwidth		12/18/2021
SB-5	S-Band functional transmit	SB-4,LISC-1	3/15/2022
UHF			
LISC-1	Obtain Radio License		3/15/2022
UHF-8	Test UHF radio interfaces and functionality		12/17/2021
UHF-9	UHF Functional Transmit/Receive	UHF-8,LISC-1	3/20/2022

Table SCH-7: COMMs Schedule for Spring 2022

10.1.8 FSW

FSW has been altered significantly since the Spring 2021 semester. Over the summer the group began working with LASP to develop our FSW from their common code. The LASP team is now in charge of the development of all FSW excluding the EPS. As of Fall 2021, initial contact has been made with most of the spacecraft components. As stated for the hardware, the team is hoping to get initial communication between all components in the month of December. The team will continue to work with LASP in the spring semester to finish developing and validating the FSW before integration. A summary of anticipated FSW tasks can be seen on Table SCH-8:

Task #	Description	Dependencies	Expected Completion
FSW-1	Peripherals Interfacing		12/15/2021
FSW-2	FlatSat Setup		12/15/2021
FSW-3	UHF		1/14/2022
FSW-4	XACT		1/14/2022

FSW-5	S-Band	SB-1	1/21/2022
FSW-6	EPS	EPS-6	2/4/2022
FSW-7	SD Cards		2/4/2022
FSW-8	GPS	Doc-9	3/14/2022
FSW-9	Payload / FPGA	DB-6	4/10/2022
FSW-10	Full FSW Delivery		4/15/2022

Table SCH-8: FSW Schedule for Spring 2022

10.2 Environmental Testing Summary and Schedule

In the Fall 2021 semester the team began preparing for full flight integration and environmental testing. As the team gets closer to PER at the end of the Spring 2022 semester the fidelity of these test plans and schedule will need to be increased. The current testing plan can be found here and the current integration document is detailed here. The preliminary dates selected for environmental testing are summarized on Table SCH-9:

Task #	Description	Dependencies	Expected Completion
INT-1	Flight Flat Sat Testing	BF-2, EF-3, AB-3, CDH-3,EPS-3, UHF-1,UHF-5, FSW-3, FSW-4, FSW-5, FSW-6, FSW-8	3/17/2022
INT-2	Flight Integration	INT-1 BP-6, SP-6, UHF-9, SB-5, STR-30	3/31/2022
EVR-1	Pre Vibe Functional Tests	INT-2, FSW-10	4/25/2022
EVR-2	Full System Vibe	EVR-1	4/25/2022
EVR-3	Post Vibe Pre TVAC Functional Tests	EVR-2	5/6/2022
EVR-4	Full System Bakeout	EVR-3	6/2/2022
EVR-5	Full System TVAC	EVR-4, Doc 11	6/3/2022

Table SCH-9: Environmental Testing Schedule for Spring 2022